uOttawa

L'Université canadienne
Canada's university

FACULTÉ DES ÉTUDES SUPÉRIEURES ET POSTOCTORALES

uOttawa

L'Université canadienne
Canada's university

FACULTY OF GRADUATE AND POSDOCTORAL STUDIES

Libardo Enrique Orejarena
AUTEUR DE LA THÈSE / AUTHOR OF THESIS

M.A.Sc. (Civil Engineering)
GRADE / DEGREE

Department of Civil Engineering
FACULTÉ, ÉCOLE, DÉPARTEMENT / FACULTY, SCHOOL, DEPARTMENT

Modeling the Effects of Sulphate and Curing Temperature on the Strength of Cemented Paste Backfill Using Artificial Neural Networks

TITRE DE LA THÈSE / TITLE OF THESIS

Mamadou Fall
DIRECTEUR (DIRECTRICE) DE LA THÈSE / THESIS SUPERVISOR

CO-DIRECTEUR (CO-DIRECTRICE) DE LA THÈSE / THESIS CO-SUPERVISOR

Paul Simms

Ousame Seidou

Jules Ange Infunte Seano

Gary W. Slater
Le Doyen de la Faculté des études supérieures et postdoctorales / Dean of the Faculty of Graduate and Postdoctoral Studies

MODELING THE EFFECTS OF SULPHATE AND CURING TEMPERATURE ON THE STRENGTH OF CEMENTED PASTE BACKFILL USING ARTIFICIAL NEURAL NETWORKS

By

Libardo Enrique Orejarena

Thesis submitted to the Faculty of the Graduate and Postdoctoral Studies in partial fulfillment of the requirements for the M.A.Sc. degree in Civil Engineering

Department of Civil Engineering
Faculty of Engineering
University of Ottawa

Your file Votre référence
ISBN: 978-0-494-65530-6
Our file Notre référence
ISBN: 978-0-494-65530-6

Thesis: MODELING THE EFFECTS OF SULPHATE AND CURING TEMPERATURE ON THE STRENGTH OF CEMENTED PASTE BACKFILL USING ARTIFICIAL NEURAL NETWORKS

Abstract:

The effects of sulphate and curing temperature play an important role on the strength development and durability of Cemented Paste Backfill (CPBs). Depending on the application of the CPB, different strength values, measured as unconfined compressive strength (UCS), are targeted. There is a lack of proven theory to predict the UCS for a specific CPB mix due to the complexity of the interactions between the variables that affect the CPB strength.

This thesis presents an approach to use the artificial neural network (ANN) methodology in order to develop two models that can predict the effects of sulphate and curing temperature on the UCS of CPBs. The ANN models here developed illustrate an outstanding accuracy in the UCS prediction for the simulation of sulphate and its coupled effect with curing temperature. The ANN models provide a better understanding of the effects of sulphate and/or temperature on the strength of CPBs.

Dedicated to my wife and daughter

Abstract

A worldwide increase in mining operations and awareness of the importance of environmentally friendly methods for the disposal of mine waste have contributed to the development and application of cemented paste backfill (CPB) technology in the last few decades. Due to its nature as a cement-based material, the effects of sulphate and curing temperature on CPBs play an important role in their strength development and durability. Depending on the application of the CPB structure, different strength values, usually measured as unconfined compressive strength (UCS), are targeted in the mix design. However, the prediction of a specific UCS value is not an easy task for an engineer since it requires a broad understanding of the different variables that affect CPB strength. On the other hand, in order to attain the desired strength, the complexity of the interactions of such variables has made it very challenging to develop a proven theory that can predict the UCS for a specific dosage of CPB. In this regard, this thesis presents to the reader, an approach on ways to use the artificial neural network (ANN) methodology in order to develop two models that can predict the effects of sulphate and curing temperature on the UCS of CPBs. The ANN models that will be developed and validated in this study illustrate an outstanding accuracy in the prediction of the UCS for the simulation of sulphate and the coupled effect of sulphate and curing temperature on CPB strength. The ANN models provide a better understanding of the effects of sulphate and/or temperature on the strength of CPBs.

Acknowledgments

I would like to thank my supervisor, Professor Mamadou Fall, who encouraged me during my studies and Master's thesis, and provided me with all his sound knowledge and expertise on the subject of CPBs. A special mention goes to my colleagues, Mukesh Pokharel and Jean Claude Celestin, whose experiments constitute the main source of the database used in the model development. A special recognition goes to Joel Mateo for his valuable teamwork during the completion of different courses under the Master's program. Also, I would like to thank Michael Lelacheur at EllisDon for his understanding and sensible guidance during the Montfort Hospital redevelopment project which allowed me to overcome the challenging task of combining work and studies. A special appreciation is also due to my friend, Nicolas Pinson and his family, for being there during the most difficult moments when I started a new life in a new country.

Finally, but most significantly, I want to acknowledge my wife, Ginna Paola Sanchez, who is also a graduate student at the University of Ottawa, and has always been there since day one of our joint lives; supporting and encouraging me in every single task that I carry out.

TABLE OF CONTENTS

LIST OF FIGURES

LIST OF TABLES

1. Chapter 1 - Introduction

1.1 Problem statement

The mining industry in Canada accounts for approximately 19% of its total exports as well as more than 363,000 direct employment positions. The industry paid $8 billion to the Canadian government in 2006 and Canada is internationally recognized as the first worldwide producer of potash and uranium, second in nickel, third in platinum and aluminum, and fifth in zinc. In Canada, 222 mines are currently in production [1,2]. However, all of these important figures also come with a disadvantage: the mining industry is responsible for almost 95% of all solid waste generated in Canada each year, which is estimated at about 650 million tons of annual waste [3]. This issue is not exclusive to Canada since mining procedures around the world are based on the same principle: extract valuable minerals and dispose the rest. Therefore, the concern about mine waste is global and research is carried out in the same manner in order to minimize the effects of such waste on the environment. One of the most commonly used methods to dispose mine waste in a safe way is the utilization of cemented paste backfill (CPB) which has taken importance during the last few decades. This method not only allows an environmentally friendly approach to dispose waste, but also entitles the operators to increase the potential of extraction of minerals [4]. In addition, underground disposal of tailings eliminates the safety concerns about construction of tailings dams that can present problems, such as leakage, ground water contamination and catastrophic failure, as noted by some authors [5, 6].

CPB is primarily made of mine tailings that come from mineral extraction mixed with a binder, usually Portland cement (PC) and water, which can be fresh water or those that originate from the processing of ores. The addition of binder contributes to the strength development in the CPB mass so that the CPB constitutes a self-supporting structure that enhances the ability of the mine operator to maximize ore extraction [7]. One of the most important quality criteria for a hardened CPB is mechanical stability. One of the most important parameters used in practice to judge the mechanical stability of a CPB structure is uniaxial compressive strength (UCS). This is because the UCS test is relatively inexpensive and quick, and can be easily incorporated into routine quality control programs at the mine [4]. On the other hand, CPB costs must be effective and the best way to achieve to attain this goal is to obtain an optimal dosage of the binder. In this regard, alternative binders such as pozzolanic materials (fly ash (FA) or ground blast furnace slag), are usually combined with PC in order to reduce its cost. It has been noted that the binder represents up to 75% of the cost of the CPB [8].

It was experimentally demonstrated that the UCS, i.e., the mechanical stability of a CPB can be affected by sulphate content and curing temperature [9,10,11,12,13]. The sulphate, curing temperature, and their interaction can positively (increase of UCS) or negatively (decrease of UCS) affect the strength of the CPB [11,12,13]. Despite the tremendous progress that has been made by the aforementioned studies in understanding the effects of sulphate, temperature and their interaction on the strength of CPBs, a fundamental understanding of the effects of such

influencing factors on the UCS of CPBs is still far from complete. Most of the previous research have only been experimental, centered on limited CPB mixes, and did not take into account, the simultaneous coupled effect of sulphate and temperature on the strength of CPBs. Furthermore, the mathematical approach for the analysis and modeling of the coupled effect of sulphate and temperature on the UCS of CPBs has not been considered in this type of study until now, nor has a prediction been done on the mechanical strength of the CPB under sulphate attacks and various thermal loading conditions.

For the reasons mentioned above, the present thesis will deal with the development of mathematical models based on artificial neural networks (ANNs) for the prediction and analysis of the effects of sulphate as well as the coupled effects of sulphate and temperature on the strength of different types (mixes) of hardened CPBs. To the best of the author's knowledge, this thesis is the first attempt to apply ANN methodology to the subject of strength development in CPBs subjected to chemical (sulphate) and/or thermal loads.

Since a CPB mix is designed for an intended UCS value which must be maintained during the lifespan of the structure, two main processes will be addressed through the application of ANNs in this thesis, which are:

- the long term strength due to the presence of sulphate in the CPB cured at room temperature, and
- the long term strength when the CPB is subjected to different thermal (curing temperatures) and chemical (sulphate) loading conditions.

1.2 Thesis objectives

The main objective of this thesis is to develop two ANN models that will allow:

- the prediction and analysis of the effects of sulphate on the UCS of mature CPBs cured at room temperature,
- the prediction and analysis of the coupled effects of sulphate and temperature on the strength of mature CPBs, and
- the gaining of a better understanding of the resistance of CPBs to sulphate attack under various thermal curing conditions.

1.3 Organization of the thesis

The thesis is organized in the form of technical papers. Chapter 1 presents an introduction and statement of the problem to the reader. Chapter 2 provides the technical background on CPB technology, ANN and cement hydration. Chapter 3 presents the first technical paper (Technical paper I). In this paper, the development of an ANN model for the prediction and analysis of the effects of sulphate on CPB strength, and the modelling results, are presented and discussed. Chapter 4 provides the second technical paper (Technical paper II). This paper shows the modeling approach and results of the ANN model developed to predict and assess the strength of a CPB subjected to the coupled effect of sulphate and

curing temperatures. Finally, Chapter 5 includes a summary of the main findings and results obtained through the present research, and provide recommendations for further studies. It should be mentioned that because the main results of the thesis are presented as technical papers, therefore, some information is repeated. This is because each paper is written independently (i.e., without taking into account the content of other papers or the rest of the document), and in accordance to the manuscript preparation instructions of the corresponding journal.

1.5 References

1. Contribution of the Mining Industry: A Positive Message to Canadians. Presentation Material for Use by the Canadian Mining Industry, Canadian Mining Association, February 2009.
http://www.mining.ca/www/Resource_Center/Presentations.php

2. General information, Potash One Inc., http://www.potash1.ca/s/Production.asp

3. Muldoon Paul, CELA and Mark Winfield, CIELAP. Brief to the House of Commons standing committee on Natural Resources regarding Mining and the Environment. 1996. Included in report: "The Boreal Below". Mining Watch Canada. 2001.

4. Fall M., Benzaazoua M., Saa E.G., Mix proportioning of underground cemented tailings backfill, Tunneling and Underground Space Technology 23 (2008) 80–90.

5. Zou DH, Sahito W. Suitability of mine tailings for shotcrete as a ground support. Can.J.Civ. Eng. 31 4 (2004) 632-636

6. Rico M, Benito G, Salgueiro AR, Diez-Herrero A, Pereira HG, Reported tailings dam failures. A review of the European incidents in the worldwide context. J Hazardous Materials 152 (2008) 846-852

7. Belem T., Benzaazoua M., Design and Application of Underground Mine Paste Backfill Technology, Geotech Geol Eng (2008) 26:147–174. DOI 10.1007/s10706-007-9154-3

8. Grice, T., 1998. Underground mining with backfill. In: Proceedings of 2nd Annual Summit, Mine Tailings Disposal Systems. Brisbane, Australian, Australasian Institute of Mining and Metallurgy, Carlton South,Australia 1998, p. 14.

9. Benzaazoua M., Ouellet J., S. Servant, P. Newman, R. Verburg, Cementitious backfill with high sulfur content: physical, chemical and mineralogical characterization, Cem. Concr. Res. 29 (1999) 719–725.

10. Kesimal A. et al., Effect of properties of tailings and binder on the short-and long-term strength and stability of cemented paste backfill, Materials Letters 59 (2005) 3703 – 3709.

11. Fall M., Benzaazoua M., Modeling the effect of sulphate on strength development of paste backfill and binder mixture optimization, Cement and Concrete Research 35 (2005) 301–314.

12. M. Benzaazoua M.,Fall M., Belem T., A contribution to understanding the hardening process of cemented pastefill, Minerals Engineering 17 (2004) 141–152.

13. Pokharel M., Geotechnical and Environmental responses of paste tailings systems to coupled thermo-chemical loadings. Masters Thesis, Department of Civil Engineering, Faculty of Engineering, University of Ottawa, 2008

2. Chapter 2: Technical Background

2.1 Background on cemented paste backfill

2.1.1. Introduction

The use of CPB technology in mining operations is considered to be beneficial from both economic and environmental points of view and it is currently used in Canada and several other countries [1,2]. Used as support for the overlying ground, the paste backfill or "paste fill' as referred by other authors, can contribute to the substantial reduction of the amount of tailings to be disposed on the surface and thus reduce the environmental impact of mining operations [3]. CPB technology can allow a return of up to 60% of the tailings that are generated by the mine underground [4]. In addition, the use of CPB allows the mine operator to obtain a greater recovery of ores and therefore, a better profitability of the mine [4]. Since its first use in the Bad Grund Mine in Germany in the late 1970s, CPBs have been extensively and increasingly used in underground mines worldwide. The use of this technology can be very attractive for any country when taken into consideration that the Canadian mining industry is responsible for the generation of approximately 650 million tons of waste per year and over 95% of all the solid waste generated in Canada each year [5].

CPB is basically made of dewatered tailings combined with a hydraulic binder and water. The binder is usually PC, used alone or blended with FA or blast furnace

slag (Slag) [4]. The concentration of binder and tailings in the mix are usually between 3% to 7%, and 70% to 85% by weight, respectively [6]. However, as noted below, the composition of the mix can vary, depending on the strength requirements and different internal factors in the mix itself. These components are combined and mixed in a plant usually located on the surface and transported (by gravity and/or pumping) to the underground mine, where the CPB is used for underground mine support and/or tailings storage. Figure 2.1 shows the main components and phases of CPB technology. Further relevant technical information on CPBs is given in the coming paragraphs. The scope of these paragraphs is limited to the following aspects:

- a review of the main advantages and disadvantages of CPB technology will be presented,
- a brief description on the process of production of CPBs will be provided,
- the strength requirements of CPBs according to their use will be presented,
- the main factors that affect the strength of CPBs will be presented and discussed, and
- some conclusions will be outlined.

Additional background information, such as sulphate attack mechanisms and sources of sulphate and temperature in CPB operations are given in the technical papers.

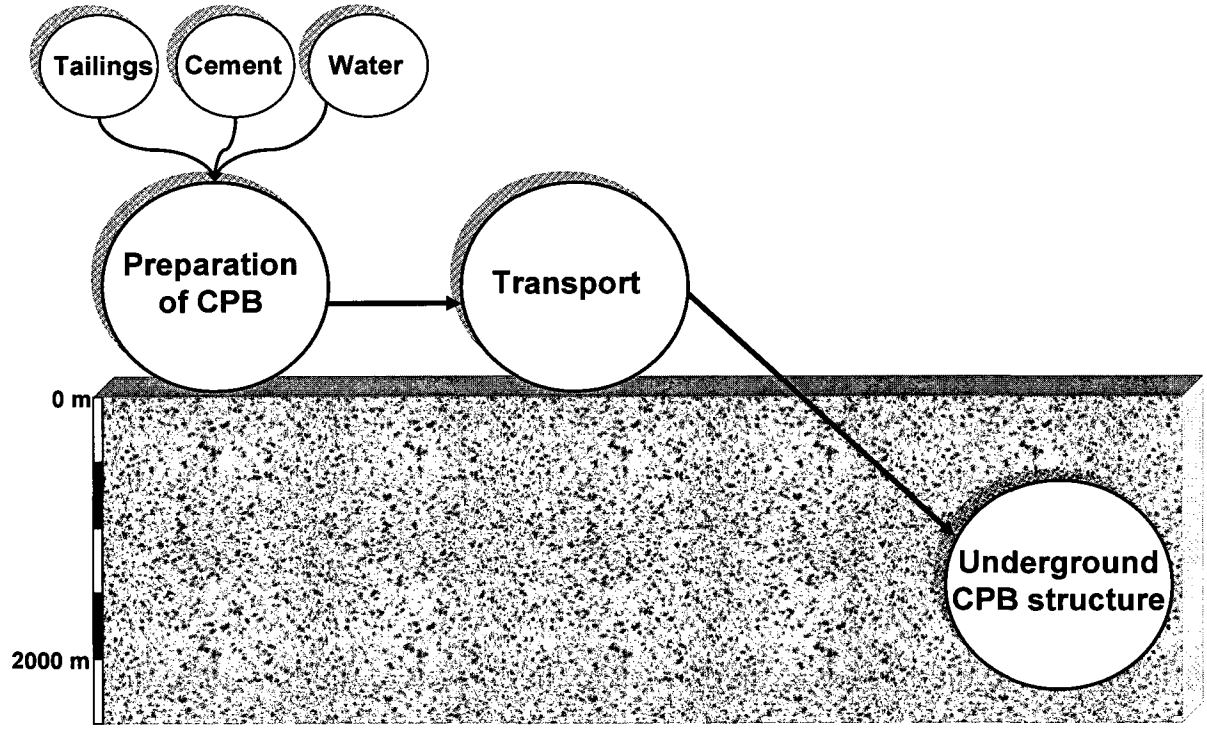

Figure 2.1 Schematic presentation of the different phases of CPB technology: preparation, transport and underground placing of the CPB, where it builds the CPB structure [7].

2.1.2 Advantages and disadvantages of the use of CPBs

As in every type of technology, the use of CPBs has its advantages and disadvantages, as described below.

2.1.2.1 Advantages of the use of CPBs

CPB technology has benefits for the stakeholders involved in mining operations from the following points of view:

- For the mining company, it allows an increase in the ratio of extraction since the stopes can be filled with the CPB and adjacent areas can be mined as well. This also improves the mine cycle and eventually, the company revenue [8].
- For mine workers, it contributes to the creation of a safer workplace since CPBs can be used as roof support and for the construction of barricades in underground mines [9].
- For communities, the underground disposal of tailings through CPBs reduces the footprint and total dimensions of surface tailings dams and therefore, there are fewer opportunities for catastrophic failures, such as those that occurred in Italy (Stava) [10] and Spain (Aznalcóllar) [11]. In addition, it can prevent undesirable conditions, such as acid mine drainage (AMD), since it reduces leachate generation in sulphidic tailings due to decreased permeability and better water retention in the paste [8,12,13].
- For other industries, it is an alternative method for underground disposal of byproducts, such as FA and slag.

Therefore, it can be said that the underground disposal of tailings has major environmental benefits [14].

2.1.2.2 Disadvantages of the use of CPBs

Among the disadvantages of using CPBs, Engels and Dixon [15] listed some of them, which are as follows:

- high cost due to the use of binders,

- increase in costs due to dewatering of tailings,
- lag times in extraction sequence to allow curing of the backfill,
- risk of liquefaction of the tailings if saturation is high and (seismic, blast) vibration is present,
- extra use of manpower and equipment, and
- ore dilution from poor quality fills.

Due to these disadvantages, it is recommended that a realistic assessment is performed on the long-term benefits to ensure that the CPB application can be sustained and also to secure financial resources. [16]

2.1.3 Process of production of CPBs

The production of CPBs is affected by the local conditions of the mine. The design of the whole process of production plays a primordial role because several factors must be controlled, such as [16]:

- rock mechanics requirements. A good understanding of rock mechanics is required in order to determine the stresses that will be transmitted to the adjacent rock mass. The allowable pressure in the rock has to be compared against the applied pressure by the CPB mass,

- environmental requirements and considerations. In this aspect, it is necessary to consider the bleed liquid, permeability of the CPB mass and that from the rock, and the chemical stability of the CPB,
- optimized paste system design. For this point, several actions might be taken as follows:
    - application of binder at the end of the pipeline,
    - balance between the workability of the mix and strength requirements,
    - pipeloop tests with different recipes, and
    - laboratory strength tests.

- considerations for the transportation of the CPB to the stope. For this aspect, several factors must be verified, such as:
    - the vertical and horizontal distances of the pipeline, which must be validated in order to ensure that there is no water hammer or unstable flow conditions. The use of pumps for surface transportation of the CPB might be required,
    - the usefulness of drilling boreholes directly into the stope that is going to be filled to determine if the rock is stable enough to allow the placement of the CPB without piping,
    - the CPB density, which must be optimal in order to guarantee a target value of strength and appropriate flow ability in the pipeline,

- the viscosity of the CPB, which should be monitored to obtain rheological data per batch. This can be achieved by using viscosity control loops which have been described by Hollinderbaumer and Mez [17] in Germany, and Wilkins et al. [18] in the UK , and
- the type of binder and the use of additives, which can also influence the transportability of the mix. In fact, some studies have proven that a reduction in the consumption of cement can be achieved by using mixtures of binders with FA, or other byproducts [19,20].

It is important to mention that one of the largest CPB operations in the world is carried out in the Kidd Creek Mine in Canada, at the Sudbury Basin. The plant for the production of CPBs allows the selection of multiple recipes according to the requirements of the mix and online monitoring of the paste underground distribution system [21]. Each CPB plant has its own customized process in accordance to local conditions. Some examples of CPB operations are listed below which show their capacity of production and references for further information in accordance to the compilation by Ilgner [16].

Table 2.1 Paste fill disposal systems (adapted from Ilgner 2002 in Paste and Thickened Tailings - A guide, Second Edition)

Mine/Location	Capacity	Reference
Mount Isa, Australia	308 m^3/h	Chen et al. [22]
Kidd Creek, Canada	400 tph	Lee and Pieterse [23]
Cabildo, Chile	104 tph	Martinson et al. [24]
Greens Creek, Alaska	84 tph	Lee and Wiedman [25]
Great River Energy's Coal Creek Station, USA	75 m^3/h	Jorgenson and Crooke [26]
Cannington, Australia	260 tph	Bloss and Revell [27]
Henty, Australia	30 tph	Henderson et al. [28]
Neves Corvo, Portugal	150 tph	Hepworth and Caupers [29]
Garpenberg, Sweden	120 m^3/h	Fredrikson et al. [30]
Boulby, UK	250 m^3/h	Wilkins et al. [31]

2.1.4 Strength requirements of CPBs

In order to guarantee an adequate stabilization of the stopes, the CPB structure must remain stable during the extraction of the adjacent stopes to avoid safety hazards and dilution of ore in the CPB mass [6]. The main parameter for the measurement of CPB stability is the UCS. UCS is simple to perform and easy to incorporate in the quality control activities of the mine [32]. For example, the stability of free standing CPB underground structures is usually evaluated by using Equation 1 developed by Mitchell [33]. Mitchell et al [34]. demonstrated that stability can be related to the UCS of the CPB through the conducting of centrifugal modeling tests The critical UCS ($UCS_{critical}$) is then given by:

$$UCS_{critical} = \frac{\gamma H}{1 + \frac{H}{L}}$$

Equation 1. Critical unconfined compressive strength of CPBs

where:

UCS = unconfined compressive strength (Pa)

H = height of fill exposure (m)

L = length of fill exposure or stope width (m)

γ = weight unit of fill (N/m^3)

The UCS value required for a given CPB structure basically depends on its function. In fact, when a CPB is used only for underground disposal or to fill voids during ore extraction, the target value ranges between 150 kPa and 300 kPa [35].

On the other hand, if the CPB structure is to be used for roof support, a UCS value of more than 4 MPa [36] can be required or even as much as 5 MPa [37]. However, some authors state that an appropriate UCS for a typical mine is between 0.7-2 MPa [38,39]. A liquefaction potential limit has been set at 100 kPa [40,41] and the UCS for free standing applications is commonly lower than 1 MPa [8,42]. A detailed formulation of the strength calculation in a given CPB structure has been provided by Belem and Benzaazoua [37].

2.1.5 Main factors that affect the strength of CPBs

During the past fifteen years, main research efforts have been mostly spent on understanding the factors that affect the strength of CPBs (e.g., [4], [8], [46], [4,43]). These studies have shown that aside from geomechanical factors, the CPB mix components and their characteristics (chemical, physical) and the curing temperatures have significant effects on the strength of CPBs. A brief explanation of how each factor affects the strength of the CPB is provided below.

2.1.5.1 Effects of tailings properties on the strength of CPBs

It has been noted that the physical properties of tailings (grain size and density) and chemical composition constitute important parameter in the development of the strength of the CPB mix [7].

With respect to the particle size distribution, the following findings have been noted [4,19,32]:

- Fine tailings grain size (20 μm particles > 60 wt.%) is not favourable for strength development. Medium (35 to 60 wt.% of 20 μm particles) and coarse (15 to 35 wt.% of 20 μm particles) tailings grain sizes are more favorable for CPB strength development (Figure 2.1). This can be mainly explained by, on the one hand, the decrease in the porosity of the matrix and thus, the refinement of the pores of the hardened cement matrix [4,32]. The decrease in porosity has been identified as beneficial for CPBs since it makes a more compact matrix. On the other hand, another cause of the increase of CPB strength with tailings coarseness is the influence of the tailings particle size on the specific surface of the tailings material as reported by Fall [32].

  It should be emphasized that an excessive proportion of fine tailings has a negative impact on the cost of the CPB due to higher binder consumption in order to achieve the same strength value. In addition, finer tailings means that more water is required to reach a desired consistency of the mix [4,19,32].

In relation to the density of the tailings, it has been found that for density values higher than 3.40 g/cm^3, the UCS increases (Figure 2.2). However, this increase is due to higher consumption of binder in volume and therefore, the cost of the CPB is also increased. Indeed, the study by Fall et al. [32] demonstrated that an almost

linear correlation exists between the tailings density and the binder consumption in terms of CPB cost.

On the other hand, the tailings chemistry is another factor that affects the strength of the CPB. The main aspect to consider is the percentage of sulphides. Thus, the amount of sulphides affects the density of the tailings and therefore, the binder consumption. In addition, higher sulphide content implies higher sulphate available in the mix as will be explained further in the current thesis.

It has been also demonstrated through oxygen consumption tests that sulphides have low reactivity within CPBs [44,45]. This can be explained by the high degree of saturation (usually very high) which inhibits the oxidation of the sulphide minerals and thus, restricts the production of sulphate ions within the CPB. This implies that sulphates which affect strength development are not produced within the CPB mass.

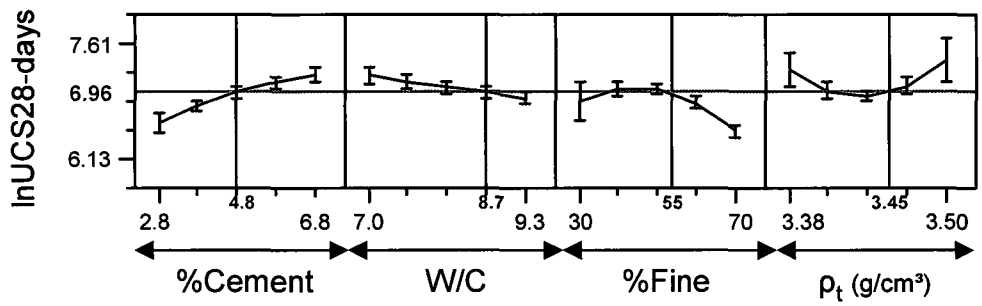

Figure 2.2 Effects of mix components of CPB on its UCS [7]

2.1.5.2 Effects of the binder on the strength of CPBs

In terms of the binder, the following aspects should be considered:

- type, and
- amount.

It has been found that depending on the type of binder, the strength development in the CPB can be different. For example, for binders made only of PC, the UCS value has been found to be less than those blended with ground blast furnace slag. This can be explained by the pozzolanic reaction induced by the slag and its filler effect that contributes to the obtaining of a higher strength in the long term [6]. However, it must be taken into consideration that studies have shown that FA does not confer good mechanical performances to the CPB [19]. In terms of the binder type, several studies have been conducted in order to explain the resistance of CPBs (durability) to chemical degradation (sulphate attack) which depends on the binder nature. In this regard, the study carried out by Kesimal et al. [46] is worth mentioning. In their study, it was found that CPB mixes made of binders with pozzolanic content (slag or FA) present a better resistance to sulphate than CPBs made only of PC. The study concluded that this greater stability in the UCS for the sulphated samples that use a pozzolanic binder can be attributed to the fact that the pozzolanic additives in the cement can increase the resistance of binders to sulphate attacks [46]. Therefore, it can be deduced that the type of binder strongly influences the UCS in conjunction with the chemistry of the tailings [2].

Aside from the binder type, the binder content also affects the UCS of a CPB (Figure 2.1). The UCS of a CPB increases as the binder content increases. This is illustrated by Figure 2.2 and also in a study conducted by Amaratunga and Yaschyshyn [38]. In this study, the binder used for the experiment is only PC. It was noticed that a variation of the percentage of binder from 3% to 7% of the mix

was accountable for almost twice the strength. This finding about the CPB agrees with most of the studies widely performed on concrete design mixes, where the cement consumption favors a higher strength and a more important implication is that the cost of the CPB is directly related to the binder consumption in the mix. The reason for this UCS increase is that higher cement content leads to the formation of more cement hydration products and thus to a higher strength of the cement matrix (Mehta, [47]).

2.1.5.3 Effects of the water/cement ratio (W/C) on the strength of CPBs

It is common knowledge that for cement based materials, the ratio between water and cement strongly influences the strength of the mix. The water cement ratio (W/C) ranges in CPBs are totally different, usually greater by far, than those used in structural concrete in order to obtain an appropriate workability of the mix that allows the transportation from the surface to its final disposal underground.

Generally, the W/C in CPBs is higher than 5 in comparison to W/C values around 0.4 for concrete [19]. However, some other studies consider values of W/C below 5, which ranges from 3.4 to 7.8, and in some cases, from 2.7 to 14.4 [38,46].

It has been demonstrated in the same studies that the strength of the CPB, as in concrete, is inversely related to the W/C ratio (Figure 2.2). These conclusions have been also corroborated in another study [4] in terms of the amount of water present in the mix. It is shown in this study that a higher amount of water means a lower

UCS of the sample. It is observed that a decrease in the UCS occurs due to an increase in the water proportion in the mix (Figure 2.2).

This behavior can be explained as follows: with a greater amount of water in the mix, the overall porosity increases once the hydration of the binder is achieved. Therefore, more water in the mix implies more voids once the cement is hydrated and as a result, there is more porosity in the matrix and a consequent low strength value [38].

2.1.5.4 Curing temperature of the CPB

The mechanisms of how the curing temperature affects strength development in cement based materials have been widely documented for concrete and mortars whereas the number of studies for CPBs is limited. Furthermore, the effects of curing temperature on the UCS of CPBs are not totally similar to that on concrete. However, it has been demonstrated through experiments that the curing temperature strongly influences the mechanical performance of CPBs [6]. In this aspect, the results show that the effects of curing temperature on the CPB strength depend on the type of binder. In summary, it has been found that low temperatures contribute to poor mechanical performance of the CPB as noted below.

In a study carried out by Fall and Samb [6], it was noted that for a curing temperature of 0°C, the value of the UCS is low in comparison to the same sample cured at higher temperatures (≥20°C). In general terms, it can be stated that higher curing temperatures (20°C, 35°C-50°C) accelerate the development of strength in

the CPB whereas the samples with a curing temperature of 0°C show a very low rate of strength gain which can be attributed to the development of ice lenses in the CPB matrix or inhibition of the cement hydration at low temperatures [6] (Figure 2.3). Higher strength is associated with higher temperature because a higher temperature accelerates binder hydration.

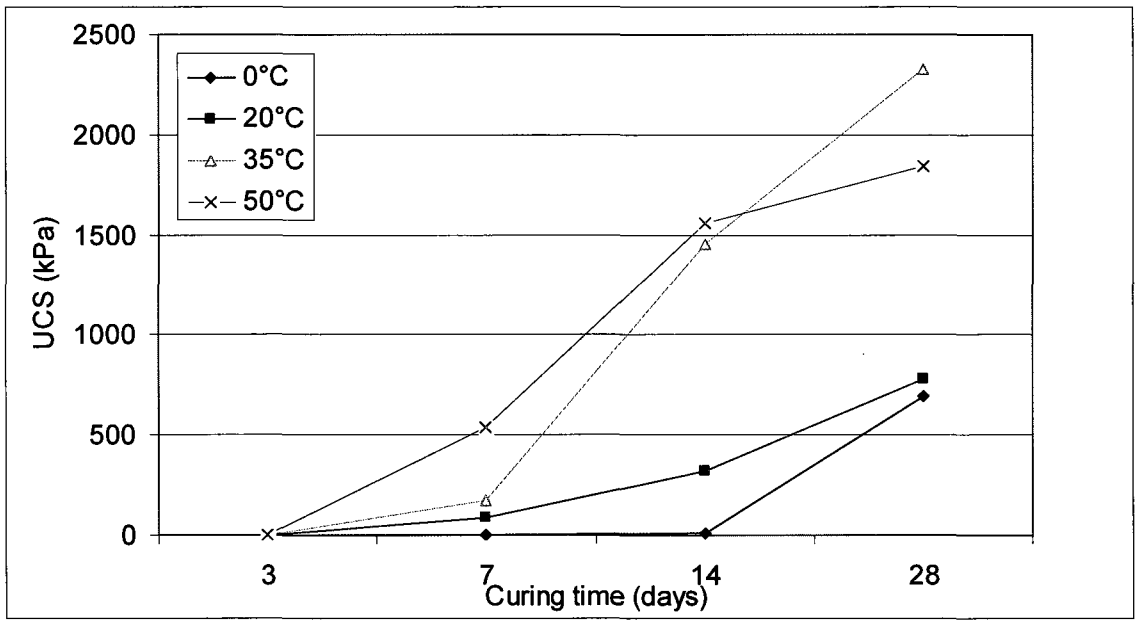

Figure 2.3 Effects of curing temperature on strength development of paste backfill cemented with PCI/Slag (20/80) [6]

2.1.5.5 Effects of sulphate on the strength of CPBs

Since CPBs are a cement based material, their long-term strength or durability can be affected by the same type of processes that affect regular concrete by the deterioration of their constituents. In fact, several studies have been carried out that evaluate the effects of sulphate on the strength development of CPBs ([48], [46]).

It is well known that in concrete, the presence of sulphate ions can deteriorate the cemented matrix of the concrete material, thereby leading to a drop in its strength. This is due to the precipitation of expansive minerals, such as gypsum ($CaSO_4.2H_2O$), ettringite ($[Ca_3Al(OH)_6{\cdot}12H_2O]2{\cdot}(SO_4)_3{\cdot}2H_2O$) or thaumasite ($Ca_3[Si(OH)_6{\cdot}12H_2O]{\cdot}(CO_3){\cdot}SO_4$) [49]. The term "sulphate attack" has been also defined as a synonym of the "deterioration of concrete"[50]. The occurrence of these precipitates in a hardened mass of concrete can lead to an increase in the initial solid volume by up to 2.8 times [51]. The same types of expansive minerals formed within the CPB are submitted to sulphate attacks. However, while the sulphate attacks on concrete and mortars are often external (external source of sulphate ions), the sulphate attacks on CPBs are essentially internal. A more detailed background on sulphate in CPBs is given in the first technical paper of this manuscript, which corresponds to the chapter where the ANN model is developed to predict the sulphate effects on CPBs.

2.1.5.6 Effects of extreme temperatures on the strength of the CPB

Sometimes, CPBs can be exposed to extreme (>100°C) temperatures. The main sources of high temperatures in underground mine operations are mine fires, and self-heating of the sulfidic rock masses adjacent to, or surrounding the CPB structures, due to the oxidation of sulphide minerals [52]. Additionally, an intensive cracking or collapse of CPB structures, which permits large amounts of air to access reactive moist paste, can lead to the self-heating of the CPB as observed in various Canadian underground mines [52]. In contrast to concrete, only few studies

[53,54,55] have dealt with the effects of extreme temperatures on the strength of CPBs. These studies have demonstrated that high temperatures have a great influence on the strength of CPBs as shown in Figure 2.4. First, an increase in the heating temperatures leads to an increase in the strength of CPBs mainly due to water that is driven out and additional binder hydration. However, at a certain level of temperature (>200°C), the coarsening of the pore structure of CPBs which results from the cracks and air voids that developed with increasing temperatures as well as the progressive decomposition of the hydrate phase, begin to negatively affect the final strength of the CPB [53]. However, it is found that the effects of extreme high temperatures on the strength of CPBs depend on the type of binder (Figure 2.5).

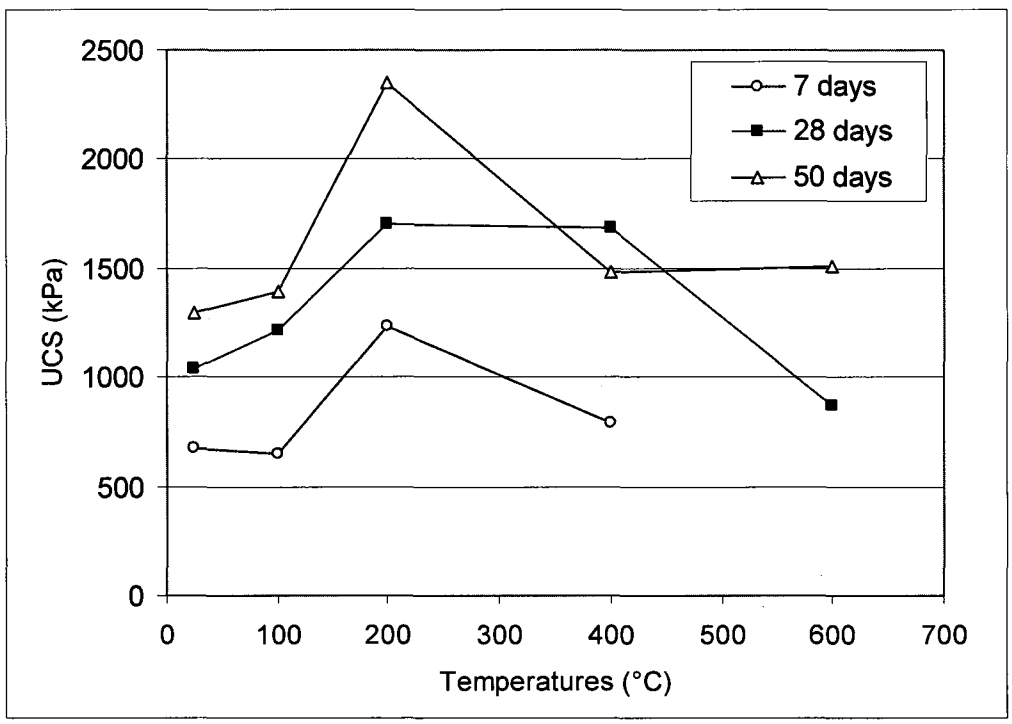

Figure 2.4 Effects of high temperatures on the strength of paste backfill cemented with PCI (4.5%; W/C=7) and cured at different times [55].

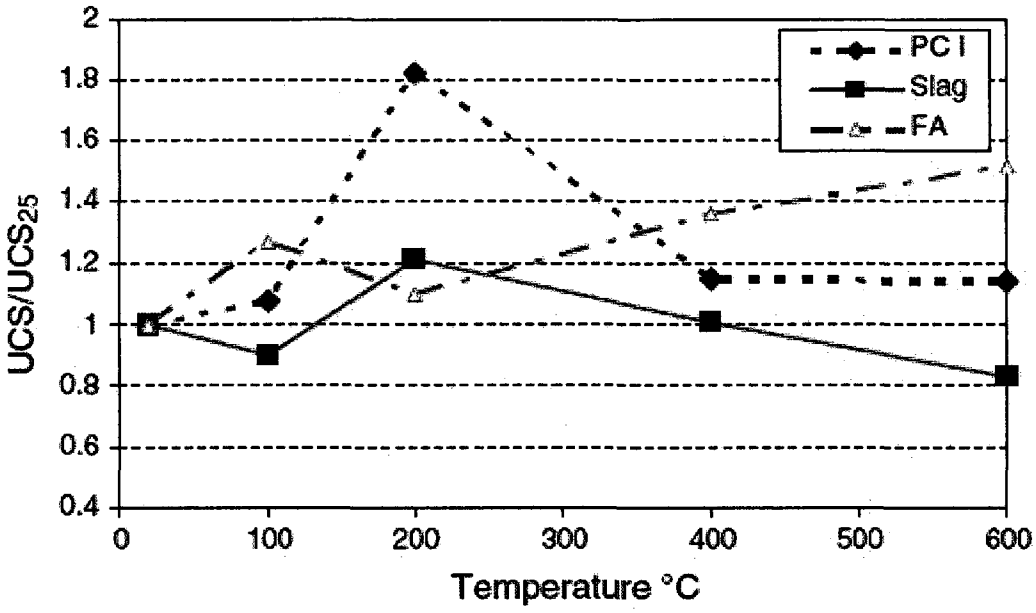

Figure 2.5 Relative UCS for CPBs with different binders [54].

2.1.6 Conclusions

An extensive literature review of the topic has been carried out and a detailed list of references is presented to facilitate further consultation. It is found that the underground disposal of CPBs has major environmental benefits and can also be seen as a mechanism to maximize safety and ore extraction in the mine. [8,9,12-14].The decision to establish a CPB operation in a mine should be the result of an integrated, regional resource and waste management strategy. [16]

The main factors that influence the strength of CPBs are as follows:

- W/C,
- binder type and amount,
- tailings fineness, density and chemistry,

- curing temperature of the CPB,
- mixing water chemistry (sulphate content), and
- extreme heating temperatures.

2.2 Background on ANN

2.2.1 Definition

In a general context, a neural network can be defined as "a machine that is designed to model the way in which the brain performs a particular task or function of interest" [56]. Certainly, the definition is very wide, but the analogy of how the process of knowledge and reactions to stimulus happen in the brain and in the artificial network itself, is most important.

The first studies on how the brain works can be attributed to Ramón y Cajál (1911) [57] who identified the neurons as the fundamental constituents of the brain. It is believed that there are 10 billion neurons and 60 trillion synapses or connections between them in the human cortex [58]. Thus, the brain can be an analogy to a highly complex, nonlinear and parallel computer [56]. The brain uses billions of neurons and neural networks to receive and process multiple stimuli that are simultaneously received from the environment and other parts of the body.
A typical configuration of a neuron can be seen in Figure 2.6.

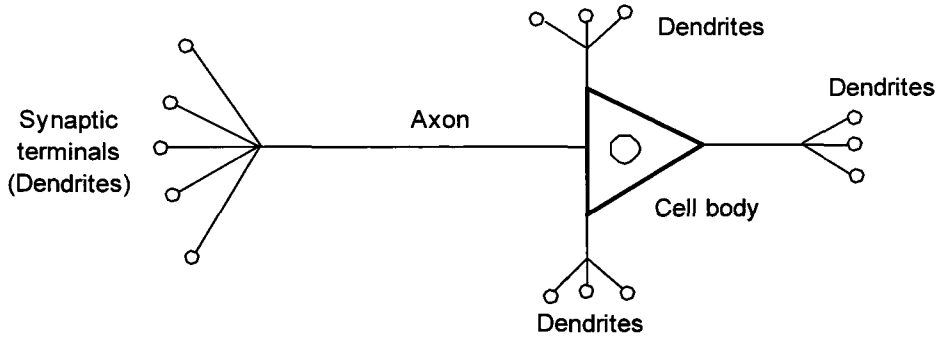

Figure 2.6 Schematic of a neuron

Accordingly, Aleksander and Morton [59] developed a more precise definition of an ANN, which was adapted by Haykin [56], as follows:

"A neural network is a massively parallel distributed processor that has a natural propensity for storing experiential knowledge and making it available for use. It resembles the brain in two respects:

1. *Knowledge is acquired by the network through a learning process.*
2. *Interneuron connection strengths known as synaptic weights are used to store the knowledge."*

From this definition, it can be noted that the network learns from "experience" in the same way that we do as individuals. Thus, vital elements in the network are the neurons connections or synapses. The signal from a neuron to another is transmitted by the cell body (axon) through the dendrites and synapses. Each synapse has a microscopical gap and a neurotransmitter to carry the signal from one cell to another. The intensity of the signal dictates the amount of neurotransmitter that is released and in the same way, the amount of signal that is

received and transmitted by the next neuron. Whether the neuron is assisted (excited), or inhibited by the incoming signals will depend on the amount of neurotransmitter that is released. This principle is the same as that used in the formulation of ANNs since their utilization in the early 1940s by McCulloh and Pitts [60].

In ANNs, each neuron constitutes a node or unit. The connection between nodes represents the axons and dendrites. The amount of neurotransmitter released in the synapses is the connection weight between the nodes, and the threshold (which dictates the ability to fire or inhibit the next node) corresponds to the activity in the soma of the cell. [61] A typical configuration of an ANN can be seen in Figure 2.7.

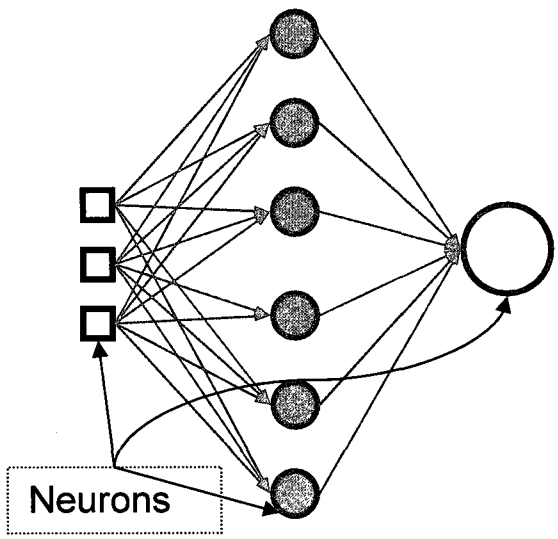

Figure 2.7 Typical ANN configuration

2.2.2 ANN history

A more detailed historical recount on neurocomputing can be found in the reference [62]; however, a brief description will be provided as follows.

The origins of neurocomputing can be traced back to 1890 with work on brain activity by William James [63]. However, it is believed that the actual start milestone is 1943 with a paper by McCulloh and Pitts on the ability of simple neural networks to compute arithmetic and logical functions [64]. The book "*The Organization of Behavior*" by Donald Hebb in 1949 explains the learning law for biological neurons which also contributes to the ulterior development of neurocomputing. Following the work of Hebb [65], advancement in computer simulation stimulated the development of neural networks. In this regard, the first neurocomputer, called the Snark, was built and tested at Princeton University in 1951 by Minsky. However, it was not until 1958 that the first successful neurocomputer, the Mark I Perceptron, was built at Cornell University by Frank Rosenblatt [64]. Mark I was designed to perform character recognition which is one of the multiple applications of neural networks. Nevertheless, Rosenblatt stated that the Perceptron only works for linear systems; therefore, the interest in ANN was redirected to other areas, mainly artificial intelligence, especially due to the discrediting work by other researchers such as Minsky and Pappert in their book "*Perceptrons*", which was published in 1969 [66].

The 70s was an era of low interest in neurocomputing due to the rise in interest on artificial Intelligence as a consequence of the Minsky and Pappert campaign. It was

only in 1986 that ANNs were brought to life by Rumelhart et al. with the rediscovery of the backpropagation (BP) algorithm which had been previously developed by Werbos in 1974 [67].

Since 1987, with the creation of the annual Institute of Electrical and Electronics Engineers (IEEE) International ANNs conference and the International Neural Network Society, research on ANNs have spread to many fields in science, both in theory and application [64].

2.2.3 Artificial neurons

In order to determine the way that a neural network can be used to predict physical processes, it is first required to understand how its fundamental units; the neurons, work. The following figure (Figure 2.8), can be used to identify its three basic elements as stated by Haykin [56].

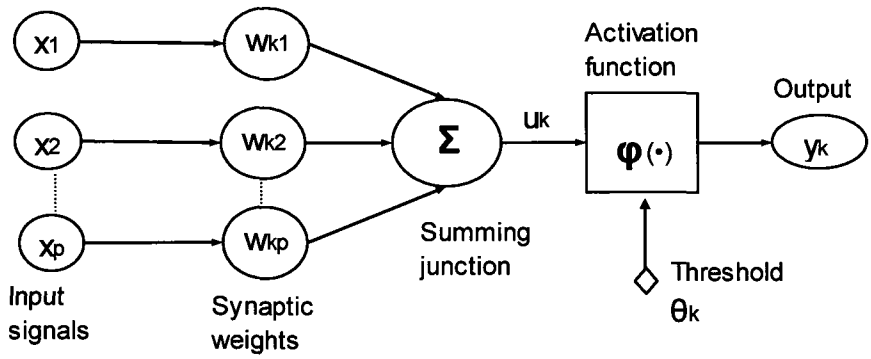

Figure 2.8 Model of a neuron per Haykin [56]

Haykin identified the three main components as follows [56]:

- "A set of synapses or connecting links. Each link has a weight or strength characteristic. The signal x_j, at the input of synapse j connected to neuron k is multiplied by the synaptic weight w_{kj}. The weight will be positive if it fires the neuron or negative if the response is inhibited."
- "An adder for summing the input signals, weighted by the respective synapses of the neuron."
- "An activation function for limiting the amplitude of the output of a neuron". This function it is also known as squashing function since it squashes (limits) the amplitude range of the output signal to some finite value [56].

There are several types of activation functions, which are depicted as $\varphi(\cdot)$ to follow the same notation as that used by Haykin in his textbook.

The first type of activation function is known as the "threshold function". The function is defined by Equation 2 and Figure 2.9.

$$\varphi(v) = \begin{cases} 1 \text{ if } v \geq 0 \\ 0 \text{ if } v < 0 \end{cases}$$ **Equation 2 Threshold function**

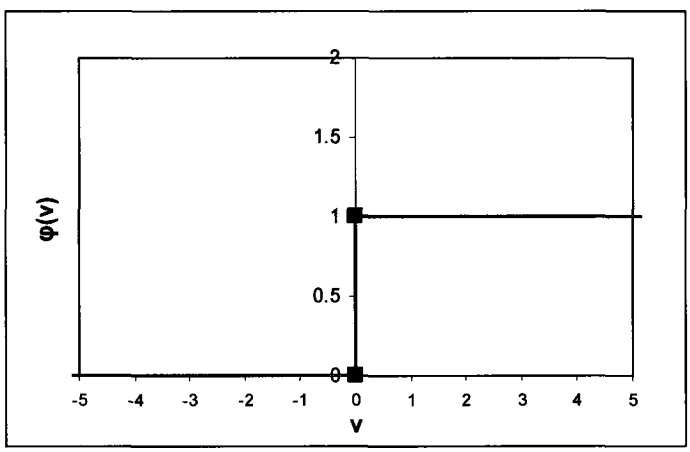

Figure 2.9 Threshold function plot according to McCulloh and Pitts model [60]

In the function, v_k is defined as the internal activity of the neuron according to the equation:

$$v_k = \sum_{j=1}^{p} w_{kj} x_j - \theta_k$$

where:

w_{kj} x_j = is the linear combiner output with w_{kj} as the weight of the synapse and x_j the input signal.

θ_k = is the threshold that is externally applied to the neuron. In this type of neuron, the output of the neuron is equal to 1 if the internal activity of the neuron is equal or greater than zero and the output will be zero if the internal activity is less than zero [56].

The second type of activation function is defined by Haykin as the 'piecewise-linear" function. In this type of function, the response of the neuron can take values between 0 and 1, which is not possible in the threshold function. An example of a "piecewise-linear" function can be seen in Figure 2.10.

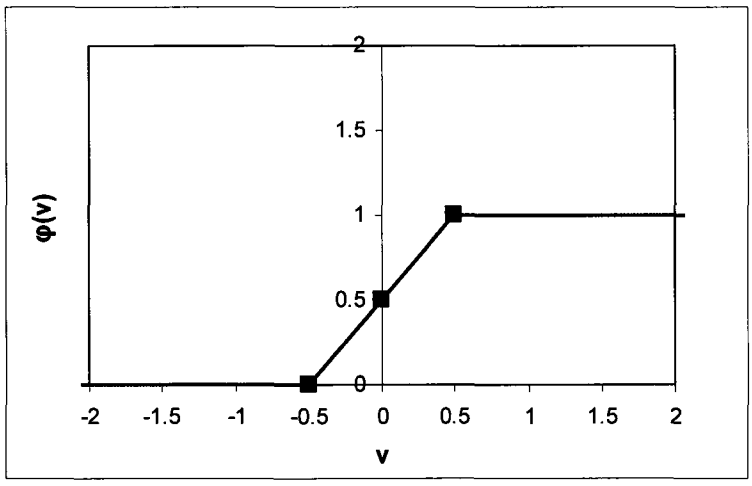

Figure 2.10 Piecewise function [56]

The third type of function and perhaps the most used in ANNs is the sigmoid function which is smoother than the two previous ones and has asymptotic properties. The "logistic function" is an example and defined by Equation 3.

$$\varphi(v) = \frac{1}{1+e^{-av}}$$ **Equation 3 Sigmoid function [56]**

where the term "a" is known as the slope parameter. A plot of the function with different slope values can be noted in Figure 2.11.

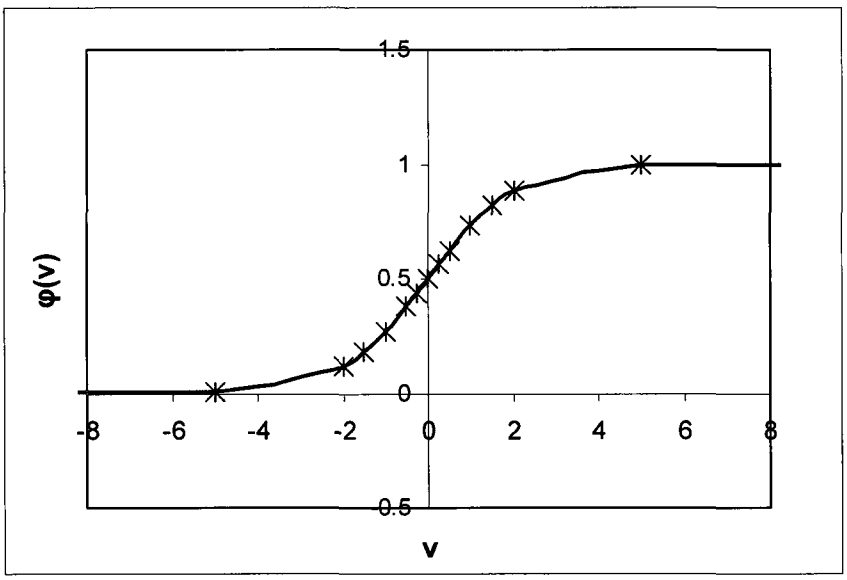

Figure 2.11 Sigmoid function plot (logistic) with "a" = 1

The sigmoid, threshold and "piecewise-linear" functions can only take values from 0 to 1. If the activation function is seen as the contribution of the particular neuron activity to an output variable, it can be said that this type of function only works for neurons that have a positive effect on the response. However, sometimes it is important to be able to model the negative effect of a certain input variable on the

output variable. In order to allow such a situation, a signum function can be used, as defined in Equation 3 or a special type of sigmoid, known as the hyperbolic tangent function, as defined by Equation 4 which was stated by Haykin [56] and shown in Figure 2.12.

$$\varphi(v) = \tanh\left(\frac{v}{2}\right) = \frac{1-e^{-v}}{1+e^{-v}}$$

Equation 4 Hyperbolic tangent function to simulate negative responses

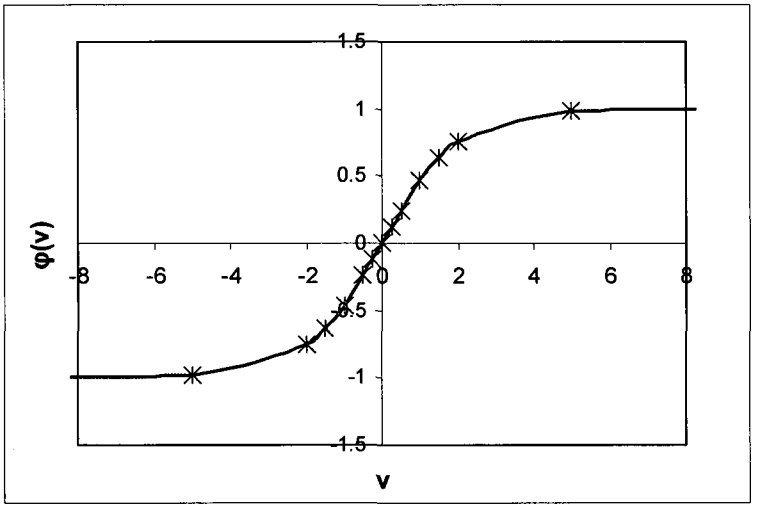

Figure 2.12 Hyperbolic tangent function plot

The piecewise function is also redefined to simulate such a situation by Equation 5 and shown in Figure 2.13.

$$\varphi(\mathrm{v}) = \begin{Bmatrix} 1\ if\ v > 0 \\ 0\ if\ v = 0 \\ -1\ if\ v < 0 \end{Bmatrix}$$

Equation 5 Piecewise function for negative value simulation

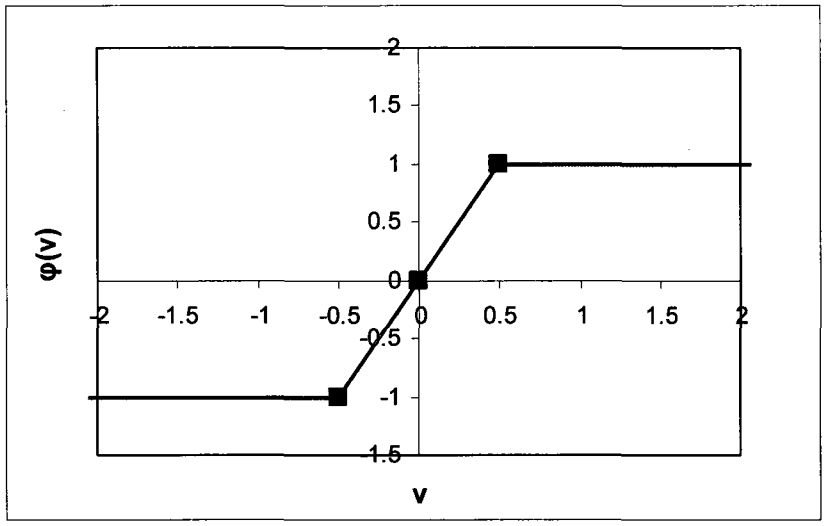

Figure 2.13 Piecewise function for negative and positive responses

2.2.4 Types of neural networks

The manner in which neurons are organized in the network will make a difference in the type of learning rules, also known as algorithms, which are used to train the network. In addition, the type of problem that needs to be solved will be the focus of the researcher in the decision of the type of network to use, since it has been noted that some networks perform better than others, depending on the application. The number of possible arrangements is abundant as some authors have found more than 50 different types [68]. Moreover, the available literature does not fully agree in the system of classification, where some use the learning rule to organize them, and others use the type of architecture as the organization criterion and some networks are identified by the name of the author that

developed them. In this regard, the classification of "popular ANNs" provided by Basheer [64], is worthy of mention.

In his work, Basheer [64] briefly described the following most commonly used ANNs as:

- Hopfield networks,
- adaptive resonance theory (ART) networks,
- Kohonen networks,
- BP networks,
- counter propagation networks,
- radial basis function (RBF) networks, and
- recurrent networks.

Among these types, the BP deserves special attention due to its flexibility and capacity to solve different types of problems as it is generally recognized in the ANN literature. Its concept and main characteristics will be further studied below.

2.2.5 Application of neural networks

According to Rumelhart et al. [69], the selection of a particular modeling technique to solve a given problem will depend on the availability of both the theory that explains the phenomenon and the data. In fact, according to Basheer et al. [64], ANNs are seen as "a perfect tool" for problems with plenty of data, but ambiguous theory; on the other hand, if good theory and data are available, a physical model (theoretical) may be developed. Finally, problems with poor data and theory

availability should follow the approach of the "expert systems" as stated by the aforementioned authors. Thus, the advantage of using ANNs is mostly seen in the following type of problems as listed by Basheer et al. [64]:

- pattern classification,
- clustering,
- function approximation (modeling),
- forecasting,
- optimization,
- association, and
- control.

In this regard, the function approximation characteristic is the most interesting one for the current type of research since our interest is to be able to model the strength of the CPB under certain conditions.

2.2.6 Backpropagation ANNs

BP ANNs are the most common type of neural networks. They are composed of multilayer perceptrons (MLP) that are trained by using the algorithm known as an error-backpropagation algorithm. [56] Its popularity may be due to its versatility in the type of problems that can be solved and the capability of MLPs to approximate any arbitrary function to any degree of accuracy as stated by Hecht-Nielsen [64,70]. A detailed formulation of such a statement is known as the universal

approximation theorem, stated by Cybenko in 1989 who said: "*a single hidden layer is sufficient for a multilayer perceptron to compute a uniform ε approximation to a given training set represented by the set of inputs* x_1, x_2,...., *xp and a desired (target) output* $f(x_1,x_2,.....x_p)$ [71 in 56].

As noted by Haykin [56], MLPs have three main characteristics:

- "The model of the neurons includes nonlinearity at the output and the nonlinearity is smooth." This is achieved by using transfer functions as the "logistic" type previously discussed in this chapter. This type of function is differentiable in its entire domain, which meets the smoothness requirement.
- "The network contains one or more layers of "hidden neurons" that are not part of the input or output of the network."
- "The network presents a high degree of connectivity."

The development of the BP algorithm for the training of MLPs is attributed to Werbos in 1974 [67]. However, it was not until 1986 with the publication of the book "Parallel Distributed Processing" by Rumelhart and McClelland that the algorithm was popularized [56].

The derivation of the algorithm was synthesized by Haykin [56] as follows:

- "A forward pass where the synaptic weights are unaltered in the network and the output is calculated according to the network configuration. For instance, the output signal of the neuron *j* is calculated as follows:

$$Y_j(n) = \varphi(v_j(n))$$

where $v_j(n)$ is the net internal activity of the neuron j, defined by:

$$v_j(n) = \sum_{i=0}^{p} W_{ji}(n) Y_i(n)$$

where p is the number of inputs applied to the neuron j, and $W_{ji}(n)$ is the synaptic weight connecting neuron i to neuron j, and $Y_i(n)$ is the input signal of neuron j (or the signal at the output of neuron i)." The calculation of the synaptic weights for the network is called an epoch.

- "A backward pass, that starts a the output layer by passing the error signals leftward through the network, layer by layer and computing the local gradient δ for each neuron".

The weight correction is defined by the delta rule:

$$\begin{pmatrix} Weight \\ correction \\ \Delta W_{ji}(n) \end{pmatrix} = \begin{pmatrix} Learning-rate \\ parameter \\ \eta \end{pmatrix} \bullet \begin{pmatrix} local \\ gradient \\ \delta_j(n) \end{pmatrix} \bullet \begin{pmatrix} input \\ signal \\ Y_i(n) \end{pmatrix}$$

Details on how to compute the weight correction in each layer can be found in the literature [56].

The application of the BP algorithm implies the following steps for any given data set:

- initialization. The network is initialized by assuming synaptic weights. The synaptic weights are usually assumed as small random numbers,
- presentation of the training samples, computation of forward and backward passes for the first data set,

- iteration. Computation of new forward and backward passes with the data available and the process is stopped until the average squared error is less than an acceptable level. The order of presentation of the training examples is ensured to be random from epoch to epoch.

In his book, Haykin [56] also gave interested readers some "hints" in order to improve the performance of the BP algorithm. These are:

- to use the hyperbolic tangent function as an activation function in the neurons;

$$\varphi(v) = a\tanh(bv) = \frac{2a}{1+e^{-bv}} - a$$
$$a = 1.716 \quad b = \frac{2}{3}$$

Equation 6 Hyperbolic tangent function suggested in reference [56]

- target values should be within the range of the sigmoidal activation function,
- to allow a random selection of the data sets during the training of the network,
- the order of how the training examples are presented to the network should be different from one epoch to the next,
- in order to have a valid generalization, the number of training samples N should be sufficient. The criterion used by Baum and Haussler [72] defined in the following equation could give an idea of the data set required:

$$N \geq \frac{32W}{\varepsilon}\ln\left(\frac{32M}{\varepsilon}\right)$$

Equation 7 Number of required samples per Baum and Haussler [72 in 56]

where:

N: number of data sets used in training the network,

W: number of synaptic weights in the network,

M: number of hidden neurons, and

ε: accuracy parameter, fraction of error permitted in testing the network.

Haykin deducted from Equation 7 that the number of data sets is directly proportional to the number of weights in the network and inversely proportional to the accuracy parameter ε and could be simplified as follows:

$$N \geq \frac{W}{\varepsilon},$$

Equation 8 Number of required samples per Haykin [56]

- the error on the training set is less than ε/2, and
- to use cross-validation to verify the generalization capabilities of the model. In this regard, the database should be partitioned into subsets as follows:
    - a training data set used for the estimation of the model,
    - a validation subset to evaluate the performance of the model, usually established as a 10% to 20% of the training set, and
    - a testing set that does not intervene in the model estimation and used to verify how accurate the model predicts the output variable. Although the size of the testing set is not defined by Haykin, some authors suggest 20% [64].

2.2.7 Other considerations in ANN modeling

Apart from cross-validation and database size mentioned in the previous section, there are some other recommendations that should be taken into account when modeling a problem with ANN. Most of these recommendations are found in the references and others are also the result of our own experience while building the models for the current research. The recommendations include the following:

- keep the input parameters in the same range of magnitude. A useful way is to use the data normalization of the input variables. Thus, saturation of the nodes is avoided and the larger numbers do not take priority over the small numbers [64]. In the literature, this issue is commonly referred as "scaling" [56]. The inconvenience of "scaling" can be avoided by using the standardization formula shown in Equation 9.

$$z = \left(\frac{x_i - \bar{x}}{\sigma_x} \right)$$

Equation 9 Standardization formula

where:

z= returns the standardized value of variable x_i.

x_i= value of the variable in vector X.

$\bar{x}$ = mean of the values of x in vector X.

σ_x = Standard deviation of the variable in vector X.

By using the normalizing formula, all values of the different inputs and outputs of the model will be converted into a small range in accordance to the dispersion of the data. The application of the formula can be done either on a conventional spreadsheet or by the command "zscore" if the model is developed in Matlab®,

- verify that the data set follows an approximated normal distribution of the output variable. Thus, a proper distribution of the input and output variables is guaranteed within the domain of study,
- verify that the input variables follow a close to uniform distribution inside the domain of study. This avoids bias of the output by over-represented classes [64],
- ensure that each sample in the data set is clearly identified and organized. This will allow an easy traceability of possible outliers within the database and within the outputs of the model, and
- start by doing simple simulations with the simplest architecture possible. Verify the degree of accuracy of the results and the time spent in obtaining the convergence of the network. Start to increase the number of hidden neurons in the model. It is noted that an initial number of hidden neurons should be twice the number of input variables in the first layer. The modification of the architecture (adding new hidden layers) is recommended by some authors; however, it has been found that an increase in the number of hidden cells in a single hidden layer of the problem would be almost equivalent to the creation of more layers in the model.

2.2.5 Engineering Applications

The possibilities of engineering applications of ANNs are as wide as the topic of neural networks itself. It is worth mentioning that most of the applications found in the literature are based on the BP algorithm, which is the same one used in the current research. It is also important to note that there are a great number of studies related to concrete strength research.

A quick view of the concrete strength problem shows that it perfectly fits the characteristics of a neural network study, such as:

- an important number of input variables (cement content, admixtures use, aggregate proportion, W/C, pozzolan content, etc.),
- an unknown interaction between the different input variables in order to produce a certain concrete strength,
- the fact that most of the existing models for concrete strength are the result of empiric formulations more than a precise theory, and finally,
- an important availability of data found in the literature and through specific research for each scenario. In this regard, the studies from Öztaş et al. [73], Sebastiá et al. [74], Lai and Serra [75], Cheng [76], and Kim et al. [77], among many others, are examples of successful applications of the neural network methodology in concrete strength research.

Other cases of utilization of neural networks in civil engineering can be found in geotechnical applications, such as the prediction of the settlement of shallow foundations by Shahin et al. [78], the prediction of slope stability by Lu and Rosenbaum [79], and ANNs applied to pile bearing capacity estimation by Abu Kiefa [80].

In terms of the application of ANNs to CPB, a paper by Rankine and Sivakugan [81] is perhaps the only reference available. However, the aforementioned study shows the great potential of ANNs in the mining industry due to a better design of the paste backfill by using ANN based models that can be translated into substantial savings for the operating companies. For that reason, it is believed that the present research will contribute to the range expansion of the applicability of ANN to CPB technology.

2.3 Background on cement and its hydration

Although concrete and CPBs exhibit different characteristics and applications, it has been demonstrated that CPBs show certain similarities with concrete in regards to strength development. This is mainly due to their common cement based nature. In order to better understand how the hydration of cement occurs, a brief background on the topic is provided to the reader in the following section.

2.3.1 Cement definition

In a general context, cement is a substance that is capable of making objects adhere to each other. However, from an engineering point of view, this general connotation is restricted only to calcareous cement and more specifically, to hydraulic cement, which has the property of setting and hardening under the presence of water due to a chemical reaction of its components [82]. For that reason, the common definition of cement is found in the dictionary as "*a powder of alumina, silica, lime, iron oxide, and magnesium oxide burned together in a kiln and finely pulverized and used as an ingredient of mortar and concrete*" [83].

2.3.2 Cement composition

In general, cement and specifically, PC as patented in 1824 by Joseph Aspdin in England, is a very complex material whose raw materials are mainly lime, silica, alumina and iron oxide which have been subjected to different processes of crushing, heating, cooling and grinding [82]. The composition of cement can not be expressed as a single formula and will differ from one cement plant to another as it depends on the process of fabrication and the minerals used in its manufacture. Thus, we may encounter as many different compositions as cement factories. However, it can be said that its composition is defined by four major compounds which are identified as "Bogue compounds" in honour of the work by R.H. Bogue and others on this topic. The compounds and notation, as it is known in cement chemistry, can be seen in Table 2.2 It is important to mention that each oxide is

identified by one letter, as follows: calcium oxide (CaO) = C; silicon dioxide (SiO_2) = S, aluminium oxide (Al_2O_3) = A, ferric oxide (Fe_2O_3) = F and hydrated cement, (H_2O) = H.

Table 2.2 Main compounds of Portland cement according to Bogue [84]

Name of compound	Oxide composition	Abbreviation
Tricalcium silicate	$3CaO{\bullet}SiO_2$	C_3S
Dicalcium silicate	$2CaO{\bullet}SiO_2$	C_2S
Tricalcium aluminate	$3CaO{\bullet}Al_2O_3$	C_3A
Tetracalcium aluminoferrite	$4CaO{\bullet}Al_2O_3{\bullet}Fe_2O_3$	C_4AF

There also exist 'minor compounds" as identified by Neville [82], which can be present in small fractions of the wt.% of cement. These minor compounds can be listed as magnesium oxide (MgO), titanium dioxide (TiO_2), manganese oxide (Mn_2O_3), potassium oxide (K_2O) and sodium oxide (Na_2O). From the list, special significance is usually given to K_2O and Na_2O, which are known as "alkalis", and can enter in reaction with certain types of siliceous aggregates which leads to concrete disintegration. Consequently, this has also been found to affect the rate of the strength gain of cement [85,86].

The strength of cement is mainly due to the presence of tricalcium silicate (C_3S) and dicalcium silicate (C_2S) which usually constitute about 75% of the cement weight [86]. C_3S is mainly responsible for the early strength of cement and produces a higher heat of hydration. On the other hand, C_2S is responsible for the

strength acquisition after 7 days. Tricalcium aluminate (C_3A) also contributes to the early strength and heat of hydration; however, it makes the cement vulnerable to sulphate and volume changes. Tetracalcium aluminoferrite (C_4AF) is formed due to the use of iron oxide in the kiln to lower the clinker temperature and as a catalyzer for the calcium silicate formation. The use of iron oxide will reduce the presence of C_3A; however, the C_4AF formed will act only as a filler with little contribution to the strength [86].

Most countries have their own standards for cement composition in an attempt to enhance or limit certain characteristics, such as high early strength, low heat of hydration, sulphate resistance, and so on [87]. Hence, according to Stegemann [87], a typical composition of unhydrated PC can be summarized as follows:

C_3S = 55%

C_2S = 20%

C_3A = 9%

C_4AF = 9%

Gypsum = 5% ($CaSO_4 \cdot 2H_2O$)

It is important to mention that the values previously given correspond to a typical "British" composition of cement provided by the aforementioned author. However, a typical compound composition supplied by Dobrowolski [86] is quite similar as noted below:

C_3S = 59.2%

C_2S = 15.5%

C_3A = 6.8%

C_4AF = 9.7%

2.3.3 Hydration of cement

In the presence of water, the compounds listed in the previous section in Table 2 react by forming products that in time will produce the hardened cement paste [82]. The hydration reaction is exothermic, i.e., heat is released during the reaction at an average of 120 cal/g. [86] Such a factor is favorable when the concrete is placed in cold weather and unfavorable when considerable quantities are poured into dams or massive foundations [86].

It can also be said that the main cementitious properties in PC come from the two calcium silicates; C_3S and C_2S, and hence, the physical properties of cement under hydration will correspond to those of the aforementioned silicates [81,88].

Since C_3S and C_2S are the major components of cement, the equations developed by Lea in 1971 show a good indication of how the hydration occurs [82,87] The equations are shown below, which follow the notation already used and use H for H_20:

For C_3S:

$$2C_3S + 6H \rightarrow C_3S_2H_3 + 3Ca(OH)_2$$

Equation 10 Hydration of C_3S

For C_2S:

$$2C_2S + 4H \rightarrow C_3S_2H_3 + Ca(OH)_2$$

Equation 11 Hydration of C_2S

$C_3S_2H_3$, which is commonly known as calcium silicate hydrate (CSH) in cement chemistry, and calcium hydroxide ($Ca(OH)_2$) which is denoted as CH (portlandite), are the main products of hydration of the two calcium silicates. The rate of hydration of C_3S and C_2S is completely different. According to the findings of Copeland and Brag [89] which are presented by Neville [82], after 10 days of hydration, C_3S reacts up to 50% meanwhile C_2S barely reaches 10%. Thus, it can be said that C_3S contributes more to the initial strength of the paste and C_2S to the long term strength. In fact, Neville stated that C_3S is responsible for most of the strength during the first four weeks and C_2S for the following four weeks [82,90]. Eventually, they will equally contribute to the final strength a year after commencement of hydration [91].

It must be said that the optimal solution to the hydration reactions presented in Equations 10 and 11 corresponds to the reaction of pure calcium silicates. In fact, it is likely that small impurities, as named by Neville [82], can be present in the C_3S and C_2S and therefore, have an effect on strength development.

As noted, the main two hydrates from C_3S and C_2S are CSH and CH. CSH is considered as the main component of the paste and CH as less stable since it can be attacked by magnesium and ammonium sulphates to produce gypsum and eventually, calcium sulphoaluminates that can have expansive effects in the hardened paste [92].

On the other hand, the presence of the other two compounds; C_3A and C_4AF, have less direct contribution to the strength [82]. It can be said that both of these compounds react in the first days of hydration, as noted by Copeland and Brag [89] who identified the fraction of C_3A and C_4AF that reacts the first day of hydration as 80% and 90%, respectively. In order to prevent the immediate reaction of C_3A with water and therefore, a "flash set", gypsum ($CaSO_4$•2H20) is usually added to the cement. Gypsum and C_3A react to form ettringite $C_6AS_3H_{32}$ (S=SO_3) and other calcium aluminate hydrates [82]. The formation of primary ettringite in the paste is favorable to the avoidance of a flash set; however, as noted later in the technical paper that involves sulphate attacks, the presence of "secondary" ettringite in the paste can lead to expansion and strength loss [50].The amount of C_3A and gypsum in the cement is usually limited by standards in order to avoid vulnerability of the hardened paste to sulphate attacks. Cements with low content of C_3A and C_3S are usually known as "low heat" types. Since these two compounds release the greatest amount of heat per gram of cement; 207 and 120 cal/g, respectively, [86] a reduction of their percentages produces a cement where under hydration, does not produce large amounts of heat, which is desirable when pouring massive concrete structures, such as dams or foundation mats.

In the case of C_4AF, its role in the strength development of cement paste is as "controversial" as the one of C_3A, as noted by Neville [82]. In fact, the aforementioned author stated that there is no "appreciable positive contribution" to

strength development by C_4AF. It is believed that C_4AF hydrates into the tricalcium aluminate hydrate and an amorphous phase as $CaO{\bullet}Fe_2O_3.nH_2O$ [82]. The work of Flint and Wells [88] established the possibility of a hydrated $CaO{\bullet}Fe_2O_3$ deposition on cement grains which acts as a retardant of hydration of other compounds. However, it should be noted that C_4AF presents a higher sulphate resistance than C_3A although the reasons are not clear [92]. The amount of C_3A in cement compositions can be reduced by increasing the amount of Fe_2O_3 in the initial dosage, and thus the alumina will turn into C_4AF which is the case in some European cements, known as "Ferrari-cements" [92].

To sum it up, it can be said that the hydration of C_3S and C_2S will positively contribute to the strength development of the paste, with the C_3S reaction as the most important for strength at the early age of hydration as noted before. On the other hand, the presence of C_3A and C_4AF in cement is justified by the manufacturing process where they act as a flux or catalyzer; the contribution of C_3A is mainly to the initial strength. However, its quantity is limited by standards and sudden hydration is decreased with the addition of gypsum to the clinker in the manufacturing process. Again, the amount of gypsum added is also controlled by specific ranges in the standards, which depend on the application of the cement.

2.3.4 References

1. Brackebusch, F., Shillabeer J., Use of paste for tailings disposal, in: Proceedings of the 6th International Symposium on Mining with Back-fill (Minefill 98) AusIMM, Publication no.1/98, 1998. p. 53-58

2. Benzaazoua, M., Belem, T., Bussiere, B., 2002. Chemical factors that influence on the performance of mine sulphidic paste backfill. Cement and Concrete Research 32 (7), 1133–1144.

3. Sofrá, F., Boger, D.V., Environmental rheology for waste minimisation in the minerals industry, Chemical Engineering Journal 86 (2002) p. 319–330.

4. Landriault D. Paste backfill mix design for Canadian underground Hard Rock Mining. 97th Annual General Meeting of CIM. Rock Mechanics and Strata Control Session. Halifax, Nova Scotia, 1995; 229-238.

5. Muldoon, Paul, CELA and Mark Winfield, CIELAP. Brief to the House of Commons Standing Committee on Natural Resources regarding Mining and the Environment. 1996. Included in report: "The Boreal Below". Mining Watch Canada. 2001

6. Fall, M., Samb, S.S., Influence of curing temperature on strength, deformation behavior and pore structure of cemented paste backfill at early ages. Construction and Building Materials (2006).

7. M. Fall a, M. Benzaazoua b, E.G. Saa, Mix proportioning of underground cemented tailings backfill, Tunnelling and Underground Space Technology 23 (2008) 80–90

8. Hassani, F., Archibald, J., 1998. Mine Backfill, CD-Rom, Canadian Institute of Mine, Metallurgy and Petroleum, Montreal, Que., 1998.

9. Fall, M., Geotechnical Hazards, Notes from lecture given by Dr. Fall to Graduate Students registered at the course Geotechnical Hazards. University of Ottawa, ON. Canada. 2007.

10. R.J. Chandler, G. Tosatti, The Stava tailings dams failure, Italy, July 1985, Proc. Inst. Civ. Eng. 113 (1995) 67–79.

11. Rico M., Benito G.Díez-Herrero A., Floods from tailings dam failures, Journal of Hazardous Materials 154 (2008) 79–87

12. Simms, P., Mine Waste Management, Notes from lecture given by Dr. Simms to Graduate Students registered at the course Mine Waste Management. Carleton University, Ottawa, ON. Canada. 2008

13. Yilmaz, E., Kesimal, A., Erçikdi, B., Evaluation of acid producing sulphidic mine tailings as a paste backfill.
Karadeniz Technical University, Department of Mining Engineering, 61080 Trabzon, Turkey. İstanbul Üniv. Müh. Fak. Yerbilimleri Dergisi, C. 17, S. 1, SS. 11-19, Y. 2004.
From the Website:
http://www.istanbul.edu.tr/eng/jeoloji/library/dergi/cilt_18_s_1/cilt17-s1-syf(11-20).pdf

14. Huynh, L. et al., Effect of polyphosphate and naphthalene sulfonate formaldehyde condensate on the rheological properties of dewatered tailings and cemented paste backfill. Minerals Engineering 19 (2006) 28–36

15. Engels, J., .Dixon-Hardy, D., An Expert Management System for Surface Tailings Storage, University of Leeds, 2006.
Website: http://www.tailings.info/index.htm

16. Ilgner, H. (2002) In Paste and Thickened Tailings – A guide. 2nd Edition. Australian Centre for Geomechanics, R.J. Jewell Ilgner and A.B. Fourie Editors., Natural Resources and the Environment Unit, South Africa.

17. Hollinderbaumer, E.W., Mez, W., Viscosity controlled production of high-concentration backfill pastes. Proceedings MINEFILL'98, 6th International Symposium on Mining with Backfill, Brisbane, Australia, 14-16 April, 1998, pp. 43-47.

18. Wilkins, M., Gilchrist, C., Fehrsen, M., Cooke, R., Boulby mine backfill system:design, commissioning and operation. Proceedings PASTE 2004, 7th International Seminar on Paste and Thickened Tailings, Cape Town, South Africa, March 2004.

19. Benzaazoua, M., Fall M., Belem, T., A contribution to understanding the hardening process of cemented pastefill, Minerals Engineering 17 (2004) 141–152

20. Nieminen, P., Seppamen, The use of blast furnace slag and other by-products as binding agets in consolidated backfilling at Outkumpu Oy's mine. In: Proceedings Int. Symp. on Mining with Backfill, Lulea, Sweden, June 1983, pp. 59-68.

21. Lee H.C., Pieterse E., Commissioning and operation experience with a 400 tph paste backfill system at Kidd Creek mine. Proceedings 8th International Seminar on Paste and Thickened Tailings, Paste 2005, Santiago, Chile, 20-22 April, 2005

22. Chen, J.J.Z., Potvin, Y. and Kuganathan, K., (1998). The investigation of high density and paste fills for the Enterprise Mine Expansion Project at Mount Isa. Proceedings MINEFILL'98, 6th International Symposium on Mining with Backfill, Brisbane, Australia, pp.29-33

23. Lee, C., and Pieterse, E.,(2005) Commissioning and operation experience with a 400 tph paste backfill system at Kidd Creek mine. Proceedings 8th International Seminar on Paste and Thickened Tailings, Paste 2005, Santiago, Chile, 20-22 April, 2005.

24. Martinson, R., Cooke, R. and Stipo, N., (2005), Cabildo mine backfill system. roceedings 8th International Seminar on Paste and Thickened Tailings, Paste 2005, Santiago, Chile, 20-22 April, 2005, pp.317-327.

25. Lee, C. and Wiedman, P., (2002) Undeground paste plant at Green Creek mine, International Seminar on Paste and Thickened Tailings.

26. Jorgenson, R.R. and Crooke, D.R. (2001) Fly ash paste utilization for placement as mine and landfill backfill at Great River Energy's Coal Creek Station. Proceedings 7th International Symposium on Mining with Backfill (cancelled), Society of Mining Engineers, Seattle, USA, September 2001, pp.187-194.

27. Bloss, M. and Revel, M., (2000) Cannington paste fill system – achieving demand capacity. Proceedings MassMin 2000, Brisbane, Australia, 29 October – 2 November, 2000

28. Henderson A., Jardine G. and Woodall C., The implementation of paste fill at the Henty Gold Mine, Sixth Sym. Min. Backfill, 1998, 299.

29. Hepworth N. and Caupers, D.J.D. (1998) Geotechnical aspects of paste fill introduction at Neves Corvo mine. Proceedings 7th International Symposium on Mining with Backfill (cancelled), Society of Mining Engineers, Seattle, USA, September 2001, pp. 223-236.

30. Fredrikson, A., Krauland, N., Still, H. and Stromberg, S. (1993) Improved undercut-and-fill mining at the Garpenberg Mine, Proceedings MINEFILL'93, South African Institute of Mining and Metallyurgy (SAIMM), Johannesburg, South Africa, pp.17-23

31. Wilkins, M., Gilchrist, C., Fehrsen, M. and Cooke, R. (2004) Boulby mine backfill system:design, commissioning and operation. Proceedings PASTE 2004, 7th International Seminar on Paste and Thickened Tailings, Cape Town, South Africa, 31 March- 2 April, 2004

32. Fall M., Benzaazoua, M., Ouellet, S., Experimental Characterization of the effect of tailings fineness and density on the quality of cemented paste backfill. J. Miner Eng. 2005; 18 (1)

33. Mitchell RJ (1983) Earth structures engineering, Chapter 6. Allen & Unwin, London.

34. Mitchell RJ, Olsen RS, Smith JD (1982) Model studies on cemented tailings used in mine backfill. Canadian Geotechnical Journal 19(1):14–28

35. Bloss, M., Below ground disposal (mine backfill) In: Paste and Thickened tailings: A guide. Jewell, Fourie Lord Editors. University of Western Australia, 2002. p. 103-126

36. Belem, T., Fall, M., Aubertin, M., Li, L., Développement d'une méthode intégrée d'analyse de stabilité des chantiers miniers remblayés Preliminary Report., IRSST project 2005, 28 p.

37. Belem, T., Benzaazoua, M., Design and Application of Underground Mine Paste Backfill Technology, Geotech. Geol Eng (2008) 26:147–174, Published online: 13 October 2007. Springer Science&Business Media B.V. 2007

38. Amaratunga, L.M., Yaschyshyn, D.N., Development of a high modulus paste fill using fine gold mill tailings.
Geotechnical and Geological Engineering Volume: 15, Issue: 3, 1997, pp. 205-219

39. Brackebusch, F.W. Basics of paste backfill systems, Mining Engineering (1994) No. 46, 1175–8

40. Grice AG (1998) Underground mining with backfill, The 2nd Annual Summit—Mine Tailings Disposal Systems, 24–25 November 1998, Brisbane, Australia, 14 pp

41. Le Roux KA, Bawden WF, Grabinsky MWF (2002) Assessing the interaction between hydration rate and fill rate for a cemented paste backfill. In: Proceedings of the 55th Canadian geotechnical and 3rd joint IAH-CNC groundwater specialty conferences. Niagara Falls, Ontario, 20–23 October, pp 427–432

42. Stone DMR (1993) The optimization of mix designs for cemented rockfill. In: Proceedings of fifth international symposium on mining with backfill, MINEFILL'93, Johannesbourg, SAIMM, pp 249–253

43. Fall, M., Belem, T., Benzaazoua, M., (2005). Tensile and compressive properties of underground paste backfill. 58th Canadian Geotechnical Conference; and 6th Joint IAH-CNC and CGS Groundwater Speciality Conferences 18-21 September 2005 in Saskatchewan, Canada, 8p.

44. Elberling, B., Nicholson, R.V., Reardon, E.J., Tibble, P., Evaluation of sulphide oxidation rates: laboratory study comparing oxygen fluxes and rates of oxidation product release. Canadian Geotechnical Journal 31 (1994), 375-383

45. Benzaazoua, M., Belem, T., Ouellet, S., Fall, M., 2003. Utilisation du remblai en pâte comme support de terrain, Partie II: comportement à court, à moyen et à long termes. In: Symp. int. Après-mines, GISOS, Gisos ed., Nancy, France, 5–7 Fèvrier.

46. Kesimal, A. et al., Effect of properties of tailings and binder on the short-and long-term strength and stability of cemented paste backfill. Materials Letters 59 (2005) p. 3703 – 3709.

47. Mehta, P.K., 1986. Concrete: Structure, Properties, and Materials. Prentice-Hall, Inc., Englewood Cliffs, NJ.

48. Fall, M., Benzaazoua, M., Modeling the effect of sulphate on strength development of paste backfill and binder mixture optimization, Cement and Concrete Research 35 (2005) p. 301–314

49. Glasser, F.P., Marchand, J., Samson, E., Durability of concrete — Degradation phenomena involving detrimental chemical reactions, Cement and Concrete Research 38 (2008) p. 226–246.

50. Collepardi, M., A state-of-the-art review on delayed ettringite attack on concrete, Cement & Concrete Composites 25 (2003) p. 401–407

51. Sezer, A. et al, Image analysis of sulfate attack on hardened cement paste, Materials and Design 29 (2008) 224–231

52. Bernier, L.R., High Temperature Oxidation (Heating) of Sulfidic Paste Backfill: A Mineralogical and Chemical Perspective. Proceedings from the 2003 Mining & the Environment Conference, Sudbury. Canada. http://www.ott.wrcc.osmre.gov/library/proceed/sudbury2003/sudbury03/prof11.html

53. Fall, M., Samb, S.S., Pore structure of cemented tailings materials under natural or accidental thermal loads, Materials Characterization (2007), MTL-06252; No of Pages 10.

54. Orejarena, L., Fall, M., Mechanical response of composite mine tailings materials to extreme heat loads, Directed Study, University of Ottawa, Faculty of Engineering, 2007.

55. Fall M., Samb S.S., Effect of high temperature on strength and microstructural properties of cemented paste backfill Fire Safety Journal 44 (2009) 642–651

56. Haykin S., Neural Networks – A Comprehensive Foundation, Macmillan College Publishing Company Inc., 1994, p.8, 138.

57. Ramón y Cajál S., 1911. Histologie du système nerveux de l'homme et des vertébrés., Paris :Maloine ; Edition Française Revue : Tome I, 19952 ; Tome II, 1955 ; Madrid: Consejo Superior de Investigaciones Científicas.

58. Shepherd G.M., Koch C., "Introduction to synaptic circuits" In The Synaptic Organization of the Brain, g.M. Shepherd Ed., pp.3-31, 1990, New York, Oxford University Press.

59. Aleksander I., and Morton H., 1990, An Introduction to Neural Computing. London: Chapman & Hall

60. McCulloh, W.S., Pitts, W., 1943. A logical calculus of the ideas immanent in nervous activity, Bulletin of Mathematical Biophysics 5, 115-133.

61. Jain A.K., Mao J., Mohiuddin K.M., Artificial neural networks: a tutorial. Comput. IEEE, 1996, March, 31-44

62. Anderson J.A., Rosenfeld E., Neurocomputing: Foundations of Research, MIT Press, Cambridge, MA., 1988

63. Nelson M., Illingworth W.T., A practical guide to neural nets. Addison-Wesley, MA, 1990.

64. Basheer I.A., Hajmeer M., Artificial neural networks: fundamentals, computing, design, and application, Journal of Microbiological Methods 43 (2000) 3–31 from Hecht-Nielsen R., Neurocomputing, 1990. Addison-Wesley, MA.

65. Hebb D.O., The organization of behavior, Wiley, New York, 1949

66. Minsky, M., Pappert, S., Perceptrons, 19696, MIT Press, Cambridge, MA.

67. Werbos, P.J., 1974, Beyond regression: new tools for prediction and analysis in the behavioral sciences, PhD Thesis, Harvard University.

68. Pham D.T., Neural networks in Engineering. In: Rzevski, G. et al. (Eds.), Applications of Artificial Intelligence in Engineering IX, AIENG/94, Proceedings of the 9th International Conference. Computational Mechanics Publications, Southampton, pp. 3-36

69. Rumelhart D.E., Durbin R., Golden R., Chauvin Y., Backpropagation: the basic theory. In: Rumlehart D.E., Yves C. (Eds), Backpropagation: Thoery, Architecture and Applications. Lawrence Erlbaum, NJ, 1995, pp. 1-34

70. Hecht-Nielsen R., 1990, Neurocomputing. Addison-Wesley, MA.

71. Cybenko, G., Approximation by superpositions of a sigmoidal function, Mathematics of Control, Signals and Systems, 303-314.

72. Baum, E.B., Haussler D., 1989, What size net gives valid generalization?, Neural Computation 1, 151-160

73. Öztaş et al., Predicting the compressive strength and slump of high strength concrete using neural network, Construction and Building Materials 20 (2006) 769-775

74. Sebastiá M., Fernández I., Irabien A., Neural Network prediction of unconfined compressive strength of coal fly ash – cement mixtures, Cement and Concrete Research 33 (2003) 1137-1146

75. Lai S., Serra M., Concrete strength prediction by means of neural network, Construction and Building Materials Vol. 11, No.2, pp 93-98, 1997.

76. I-Cheng Yeh, Analysis of strength of concrete using design of experiments and Neural Networks, Journal of Materials in Civil Engineering, July-August 2006, pp. 597-604

77. Kim J., Kim D.K., Feng M.Q., Yazdani F., Application of neural network for estimation of concrete strength, Journal of Materials in Civil Engineering, May-June 2004, pp. 257-264.

78. Shahin M.A., Jaksa M.B., Maier H.R., Predicting the settlement of shallow foundations on cohesionless soils using back-propagation neural networks, University of Adelaide, Research report No. R 167, February 2000.

79. Lu P., Rosenbaum M.S., Artificial Neural Networks and Grey Systems for the prediction of slope stability, Natural Hazards (30) 383-398, 2003.

80. Abu Kiefa M.A., General Regression Neural Networks for Driven Piles in Cohesionless Soils, Journal of Geotechnical and Geoenvironmental Engineering, Volume 124, Issue 12, pp. 1177-1185 (December 1998).

81. Rankine R.M., Sivakugan N., Prediction of Paste Backfill performance using artificial neural networks, James Cook University, Townsville, QLD, Australia, document available on the web at http://www.jcu.edu.au/eps/idc/groups/public/documents/journal_article/jcuprd_049651.pdf

82. Neville A.M., Properties of Concrete, Pitman Publishing limited, 2nd edition, 1973

83. Merriam-Webster dictionary on line from: http://www.merriam-webster.com/dictionary/cement

84. Bogue R.H., Chemistry of Portland Cement, New York, Reinhold, 1955

85. Neville A.M., Role of cement in creep of mortar, Journal ACI 55, pp.963-984, March 1959.

86. Dobrowolski J.A., Concrete Construction Handbook, Mc Graw Hill, Fourth Edition, 1998, p.1.13-1.18

87. Stegemann J.A., Neural Network analysis of the effects of contaminants on properties of cement pastes, Imperial College of Science, Technology and Medicine, London, England, PhD Thesis, 2001, pp.30-31

88. Flint E.P., Wells L.S., Study of the system CaO-SiO2-H2O at 30°C and the reaction of water on the anhydrous calcium silicates, J.Res. Nat. Bur. Stand., No. 687, pp.751-783, 1934.

89. Copeland L.E., Bragg R.H., Determination of Ca(OH)2 in hardened pastes with the X-ray spectrometer, Porltand Cement Association Rep., Chicago, 14th May 1953.

90. Woods H., Starke H.R., Steinour H.H., Effect of cement composition on mortar strength, Engr. News Rec., 109, No.15, pp.435-437, New York, 1932

91. Davis R.E., Carlson R.W., Troxell G.E., Kelly J.W., Cement investigations of the Hoover Dam, J. Amer. Concrete Institute, 29, pp.413-431, 1933

92. Czernin, W., Cement Chemistry and Physics for Civil Engineers, Chemical Publishing Co., Ireland, 1962, p.91

Chapter 3 – Technical paper I:

The Use of Artificial Neural Networks to Predict the Effect of Sulphate Attack on the Strength of Cemented Paste Backfill

ABSTRACT

The growing use of cemented paste backfill (CPB) as a ground support method in mining and also as an environmentally friendly alternative for mine waste disposal demands a better understanding of the different processes that affect its strength. Due to its nature as cement based material, CPB is prone to the progressive loss of strength originated by sulphate attacks under certain conditions. The purpose of this study is to develop a model based on artificial neural networks (ANN) to analyze the impact of such a phenomenon on the unconfined compressive strength (UCS) of the CPB. A general background about sulphate attacks in CPB is provided in the first part of the study as well as the different parameters used for the model development. The model is carried out using the Neural Network Toolbox from MATLAB™ software. The input data used for the model is obtained from UCS tests performed in previous studies on CPB. The results obtained through the model are validated against the actual tests. They suggest that ANN is an effective tool for predicting the effects of sulphate on the strength of CPB. It is demonstrated through the model that sulphate attacks decrease the UCS of the

CPB mix. As part of the study, some conclusions are presented by the authors for avoiding the harmful effect of sulphate attacks in the mix.

3.1. INTRODUCTION

The use of cemented paste backfill (CPB) technology in mining operations is considered beneficial from both economical and environmental points of view and is currently used in Canada and several other countries (Brackebusch and Shillabeer 1998; Yilmaz et al. 2004, Fall, Benzaazoua and Ouellet, 2005, Orejarena and Fall 2008). Used as support for the overlying ground, CPB can contribute to substantially reducing the amount of tailings for disposal on the surface and thus reducing the environmental impact of mining operations (Sofrá and Boger 2002). In addition, the use of CPB allows the mine operator to obtain a greater recovery of ores and therefore, a better profitability from the mine (Nasir and Fall, 2009).

CPB can be defined as an engineered mixture of wet fine process tailings (75%-85% solids by weight), a hydraulic binder (3-7% by total dry paste weight) and mixing water (Kesimal et al. 2005).

Consequently, the mechanical properties of CPB are strongly marked by the nature of the tailings as demonstrated in several studies (e.g. Fall, Benzaazoua and Ouellet, Kesimal 2005). Usually the binder is Portland cement which is frequently mixed with blast furnace slag, which confers to the mix, a better compressive strength and reduces the binder use (Kesimal 2005). However, a

specific strength value needs to be complemented with an adequate durability of the material in order to meet the structural requirements for ground support, new pillar configuration, ore recovery maximization and to guarantee a safe operation of the mine.

One of the factors for consideration in the design of a CPB structure is the presence of sulfides in the tailings, since under certain conditions, they can cause a process known as acid mine drainage (AMD) or acid rock drainage (ARD) (Fall, Benzaazoua and Ouellet 2004). Although the oxidation of the tailings has a low probability of occurrence in CPB due to its high degree of saturation (Benzaazoua, Fall and Belem 2004, Fall and Benzaazoua 2005), such a process can occur before the tailings are mixed with the binder and therefore, a considerable quantity of sulphate ions might be trapped in the CPB matrix. This may cause a progressive loss of strength of the material due to the decomposition of its constituent phases, a phenomenon that summarizes the sulphate attack process and has been documented in some other studies (e.g., Bernier, Li and Moerman 1999, Sofrá and Boger 2002, Fall and Benzaazoua 2005).

In concrete, the sulphate attack is due to external sources of sulphate ions, whereas in CPB, the sulphate attack is mainly due to internal sources or their constituents (Fall and Benzaazoua 2005). Explaining sulphate attacks in concrete is still a subject of study and there are several lines of thinking that seem to explain the different mechanisms that trigger such phenomena in concrete (Collepardi

2003). On the other hand, due to the increasing use of CPB in the mining industry, the importance of understanding the behavior of CPB structures under sulphate attacks is almost mandatory to ensure an appropriate stability of the stopes during the extraction of the minerals for a safe and cost effective operation (Fall and Benzaazoua 2005). However, the rationale of the strength development in CPB is complex and only a few studies have been carried out with respect to this specific topic (e.g. Bernier, Li and Moerman 1999, Fall and Benzaazoua 2005, Fall, Benzaazoua and Sae 2008). These studies are mostly experimental.

The objective of this work is to develop a model based on artificial neural networks (ANN) that can predict the impact of a sulphate attack on CPB. To the best knowledge of the author, there is no ANN based tool that reproduces the effect of a sulphate attack on CPB. In order to attain this objective, this study is organized as follows:

- A general background of the sulphate attack phenomena in cementitious materials will be presented to the reader.
- A general background on ANN methodology will be outlined.
- A description of the different parameters used in the design of the model to predict the effect of a sulphate attack on the uniaxial compressive strength (UCS) of the CPB will be provided.
- An outline of the different considerations taken in the model development concerning the ANN architecture will be presented.

- A summary of the results obtained by means of the developed model and a comparison against available data will be included.
- Finally, some conclusions of the study and the model will be provided to the reader.

3.2. BACKGROUND

3.2.1 Background on sulphate attack

Since CPB is a cement based material, its long-term strength or durability can be affected by the same type of processes that affect regular concrete by the deterioration of its constituents. In fact, only a few studies have been carried out that evaluate the effect of sulphate on the strength development in CPB (e.g. Kesimal et al. 2005; Benzaazoua, Fall and Belem 2004; Fall and Benzaazoua 2005). The occurrence of a sulphate attack in cementitious material is generally described as a chemical decomposition process (Czernin 1962) or "deterioration of concrete" (Collepardi 2003). The loss of adhesion and strength in the cemented material has been noted in previous studies as the main consequence of a sulphate attack (Metha 1995, Fall and Benzaazoua 2005).

In cement-based materials, the reaction between sulphate ions with ionic species of the pore solution can lead to the precipitation of minerals, such as gypsum ($CaSO_4.2H_2O$), ettringite ($[Ca_3Al(OH)_6{\cdot}12H_2O]_2{\cdot}(SO_4)_3{\cdot}2H_2O$) or thaumasite ($Ca_3[Si(OH)_6{\cdot}12H_2O]{\cdot}(CO_3){\cdot}SO_4$) (Glasser, Marchand and Samson 2008). Due to

the precipitation of these minerals, the structure of the hardened paste can be deteriorated by the excess of stress within the material, producing expansion, loss of strength, spalling and degradation (Glasser, Marchand and Samson 2008). The type of degradation depends on the type of sulphate attack occurring in the material. In this regard, a classic sulphate attack involves ettringite and/or gypsum formation and a physical sulphate attack is related to the crystallization of sulphate-rich salts (Brown 2002, Neville 2004). Thus, the hydrated phases of the cement, including calcium aluminate hydrate and calcium hydroxide, react with the sulphate ions to generate the aforementioned precipitates which can lead to an increase in the initial solid volume up to 2.8 times (Sezer 2008). The stresses generated by the expansion can produce cracking and loss of cohesion between its components which eventually lead to loss of strength and severe degradation (Glasser, Marchand and Samson 2008; Sezer 2008). However, there is still controversy on whether gypsum formation generates expansion since its softening effect, mass and strength loss are more acceptable (Mather 1997; Cohen 1991; Bing and Cohen 2000). However, it is also accepted that gypsum is formed initially and eventually, expansive calcium sulphoaluminates, which have been identified as responsible for the final damage to the concrete (Czernin 1962).

In order for a sulphate attack to occur, several conditions have to be met. As stated by Collepardi (2003), sulphate attacks in concrete have more chances to occur if the following conditions are present concurrently:

- Environmental sulphate (from water or soil) penetrating the existing concrete structures,

- Permeable concrete, and
- Moist environment which facilitates the diffusion of SO_4 through the aqueous phase of capillary pores.

It is noted that in most cases, a sulphate attack in concrete is produced by external sources, for example, groundwater in certain type of clays (Neville 1977). In this regard, it has been noted that certain regions of South Australia, the Canadian Prairies, California and England are prevalent in sulphate-rich soils (Neville 2004).

It is also important to mention that not all ettringite is harmful for concrete. Indeed, primary ettringite occurs homogeneously and when concrete is still in a plastic stage. The formation of this ettringite is attributed to ground gypsum which reacts with calcium aluminates of the Portland clinker phase to produce set regulation or sulphate-based expansive agents in shrinkage compensating concretes (Collepardi 2003). This ettringite formation happens in the first hours or days of the concrete pouring. Therefore, the formation of secondary ettringite or delayed ettringite, as referred by Collepardi (2003), is the process that deteriorates the concrete.

The processes of a sulphate attack on CPB have several resemblances. However, in CPB, the sulphate ions are usually present in its components and therefore, the process succumbs as a result of internal sources (Fall and Benzaazoua 2005).

There are four main internal sources of sulphate in the CPB system (tailings, water and binder). First of all, we mentioned that CPB is formed in great percentage by fine tailings (Kesimal 2005). Depending on the type of mineral extraction, it is common to find pyrite (FeS_2) as an important constituent of these tailings. In fact, several studies denote up to 60% of pyrite in the tailings (Kesimal et al. 2005) and concentrations of the ion SO_4 of up to 24,000 ppm.

It is also known that the oxidation of pyrite produces acidity and releases metals from the sulphides (Moreno and Neretnieks 2006). This oxidation has been defined as a complex biogeochemical process (Nordstrom 1982) that involves hydration, oxidation and hydrolysis and can be summarized in the following reaction proposed by Stumm and Morgan in 1981:

$$FeS_2 + 3.75O_2 + 3.5H_2O \rightarrow Fe(OH)_3 + 2H_2SO_4$$

Equation (1)

Equation 1 basically summarizes the process known as ARD which leads to a dramatic increase in the acidity of the ground water and the release of sulphate ions as noted in the following equations (Moses et al. 1987):

$$FeS_2 + \frac{7}{2}O_2 + H_2O \rightarrow Fe^{2+} + 2SO_4^{2-} + 2H^+$$

$$FeS_2 + 14Fe^{3+} + 8H_2O \rightarrow 15Fe^{2+} + 2SO_4^{2-} + 16H^+$$

Equations (2) and (3)

Thus, the availability of sulphate in the paste can be due to the presence of pre-oxidized tailings. However, once the tailings are mixed with the binder, it is considered that tailings oxidation is negligible due to the high degree of saturation of CPB which impedes the oxygen diffusion through the paste. Therefore, the sulphate attack will be caused mainly by the process water ions (Fall and Benzaazoua 2005).

Another source of sulphates in CPB, apart from sulfur rich tailings, is the process of sulfur dioxide/air used for destruction of cyanides in gold mining. In this process, SO_2 is used to oxidize the cyanide to the less toxic cyanate OCN^- according to the following reaction (Akcil 2003):

$$SO_2 + O_2 + H_2O + CN^- \xrightarrow{Cu^{2+}\ catalyst} OCN^- + SO_4^{2-} + 2H^+$$

Equation (4)

Thus, this process can also contribute to the presence of sulphates in the CPB if the slurry is used for underground disposal and the mine processing water is used in the CPB mix (Fall and Benzaazoua 2005).

Sulphates can also enter into the CPB mass depending on the type of cement used for the mix. It is known that often gypsum ($CaSO_4.2H_2O$) or anhydrite ($CaSO_4$) is added in the clinker to control the setting of the cement and therefore, small amounts of sulphate are introduced into the mix (Fall and Benzaazoua 2005).

Finally, the water added to the mix for obtaining appropriate workability for underground disposal may contain free sulphate ions either from pre-oxidized tailings or the sulphur dioxided/air process described above.

3.2.2 Background on artificial neural networks

Ramón and Cajál (1911) contributed to the understanding of how the human brain works by introducing neurons as the constituents of the brain (Haykin 1994). However, the history of ANN actually started in the 1940s with the publication of a paper by McCulloh and Pitts (1943). A comprehensive narrative can be found by Basheer and Hajmeer (2000) for the reader who is interested in details about ANN development. Nonetheless, it must be mentioned that the use of the neural network methodology increased dramatically after the Hecht-Nielsen theorem (Hecht-Nielsen 1989) stated that any vector function y=f(x) may be calculated using a suitable neural network.

ANN is identified as a regression tool that exhibits an exceptional performance especially when used for pattern recognition and function estimation (Ji and Lin 2006). In fact, some authors refer to ANN as a generalization of classic regression

or "super regression" (Wythoff 1993), or more recently, as a form of nonlinear statistical regression (Rumelhart et al. 1995).

The basic principle of every ANN is to imitate the behavior of biological learning and the decision-making process through mathematical and computational processes (Kim et al. 2004). The increasing importance of ANN tools in function approximation is their ability to generalize complex processes that can not be easily formulated through available theory or simple regression. Consequently, a model developed using ANN methodology can capture the complex interactions among the input/output variables without any prior knowledge about the nature of such interactions (Ji and Lin 2006).

It has been noted that the backpropagation networks (BP) are the most widely used (Basheer and Hajmeer 2000) among the wide spectra of ANNs, and its application in engineering has been proven in several studies, especially in regards to concrete strength prediction (Lai and Serra 1997; Kim et al. 2004; Öztaş 2005; Ji and Lin 2006;). A BP can simply be described as a multilayer perceptron consisting of two exterior layers as follows: an input layer with units or nodes (artificial neurons or cells) representing the variables of the problem, and an output layer that corresponds to the variables that are modeled (dependent variables). In the middle of these two main layers, one or more layers of artificial neurons called hidden layers can be found. A schematic of a BP is presented in Figure 3.1.

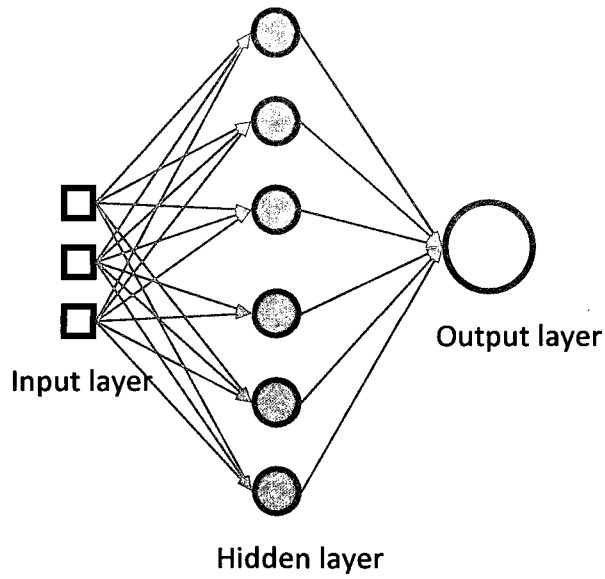

Figure 3.1 Schematic of a Backpropagation Neural Network

For approximation problems, it has been stated that one hidden layer is enough to model continuous functions (Basheer 2000).

Since a neural network can be seen as a machine that is designed to model the way in which the brain performs a task or function, it exhibits two main characteristics that resembles the brain (Haykin 1994):

- Knowledge is acquired by ANN through a learning process.
- Interneuron connection strengths (synaptic weights) are used to store the knowledge.

The learning process is performed in the BP through a technique known as error-correction learning, in which the error that is found when comparing the output with the actual result is distributed backwards to the neurons in the middle and input

layers in order to adjust the synaptic weights. Once the weights have been adjusted, the network sends a signal forward to produce a second output. This result is once again compared against the actual value (obtained from empirical data) and the cycle is repeated until an appropriate convergence or error is achieved in the result.

It is worth mentioning that in order to develop a model using ANN methodology, there are three main processes that must be completed prior to implementing the model for forecasting the dependent variable. These main processes are known as training, testing and validation (Basheer and Hajmeer 2000).

Once the architecture of the network has been chosen, the different weights between the units (artificial neurons) need to be calibrated. This is achieved by using the BP technique as described above, through a series of data. This process is known as training (learning) of the network. During this stage, it is recommended that the data are selected uniformly in order to cover the whole range of experiments where the network is being developed (Kim et al. 2004). The training is regularly interrupted to test the accuracy of the network in the prediction of the modeled variable. This is accomplished, by means of data sets that are not included in those used in training and whose results for the modeled variable are known. Thus, the ability of the network for generalization is tested, which is called the testing phase. It has to be mentioned that the operator must pay attention to the variation in the error during the training and testing sets. It is important to identify that after consecutive iterations during the training phase, the error should decrease and in the same way for the testing sets. The operator could continue

training the network indefinitely. However, once the testing error starts to increase (or the training error is very similar to the testing error), the training should be stopped in order to avoid overtraining, which implies that even if the training error is minimum, the network loses its capacity to generalize data and can be used only as a look-up table (Basheer and Hajmeer 2000; Wythoff 1993). It is expected that when the testing and training errors are reasonably close together, the network is prone to generalize (Sebastiá et al. 2003).

The validation process is carried out with a different data set that is not used in the learning (training and testing) phases after selecting the best network to determine its accuracy and before implementing the model by the final user (Basheer and Hajmeer 2000). However, it is important to note that most authors and also the software used in the development of the model identify the testing as data that is "not seen" by the network during the learning and validation as part of the learning process. This topic will be considered further in the section on partitioning.

3.3 DEVELOPMENT OF THE ANN

3.3.1 Parameters considered in the design of the model

The first step in the development of a model based on the ANN methodology is to clearly identify the input variables of the problem for generalization. In order to identify the possible variables that can affect the output of the problem, some previous studies are used as the starting point for the model development. In such

regards, references, such as Benzaazoua, Fall and Belem (2004), Fall and Benzaazoua (2005), Fall, Benzaazoua and Saa (2008), are selected as those with the ability to better explain the possible input variables that affect the UCS of CPB.

Based on the aforementioned studies, the main input variables or parameters can be stated as follows:

- water/cement ratio,
- amount and type of binder used for the CPB,
- type of tailings; fineness, density and chemical composition,
- curing temperature of the CPB,
- curing time, and
- Sulphate amount.

A brief description of how each parameter is defined is presented as follows.

3.3.1.1 Water/Cement Ratio (W/C)

It is common knowledge that for cement-based materials, the ratio between water and cement strongly influences the strength of the mix. The range of water cement ratio (W/C) in CPB is entirely different, usually by far larger than those used in structural concrete in order to achieve an appropriate workability of the mix that allows its transportation from the surface to its final underground disposal.

Generally, the W/C in CPB is higher than 5 in comparison to W/C values around 0.4 for concrete. However, some other studies will consider values of W/C below 5, ranging from 3.4 to 7.8, and in some cases, from 2.7 to 14.4 (Grice 1998, Kesimal et al. 2005).

It has been demonstrated in the same studies that the strength of the backfill, as in concrete, is inversely related to the W/C. These conclusions have been also corroborated in the references (Benzaazoua, Fall and Belem 2004) in terms of the amount of water present in the mix. It was shown in that study that a higher amount of water means a lower UCS of the sample. Hence, it can be said that for lower values of W/C, a high UCS should be obtained in the CPB. This behavior can be explained since with a greater amount of water in the mix, the overall porosity increases once the hydration of the binder is achieved (Amaratunga and Yaschyshyn 1997).

Based on the previous studies, the interval assumed in this study for the W/C parameter is between 4.4 and 10.8.

3.3.1.2 Amount and type of binder

Several studies (e.g. Fall, Benzaazoua and Saa 2008, Amaratunga and Yaschyshyn 1997) have demonstrated that the amount of binder in the CPB mix is directly proportional to the expected strength of the material as it is in concrete.

According to the studies here, a cited variation from 3% to 6% of binder can account for almost twice the final strength of the CPB. The importance of determining a proper amount of binder relies on the cost of the mix, since the binder is the most costly material as it does not come from the mine operation. In fact, it has been found that binders can account up to for the 75% of the cost of the backfill (Grice 1998).

In the selection of the binder for the CPB, usually furnace blast slag (slag) or fly ash are combined with Portland cement type I (PCI) due to their cementing properties and to take advantage of their pozzolanic characteristics that allow a greater hydration of the cement and formation of C-S-H with its subsequent increase on strength. The use of slag and fly ash is popular in the concrete industry because of their beneficial effects on the cement microstructure and durability (Frías and Rodríguez 2007). In addition, since they are by-products, the cost of the binder decreases. Therefore, this mix of binders is seen in mining operations nowadays (Benzaazoua, Fall and Belem 2004). Moreover, it has been already suggested in the early 90s that the use of pozzolans might be the only option for producing a cost-effective CPB (Lamos 1993).

In their study, Fall, Benzaazoua and Saa (2008) found that the optimum amount of binder in the mix is around 4.8% (Fall, Benzaazoua and Saa 2008) for binders with 20% PCI and 80% slag. On the other hand, the use of fly ash has shown contradictory results since some studies obtained low values of UCS (Benzaazoua, Fall and Belem 2004) and others actually recommend its use in order to obtain a higher UCS in the long term (Amaratunga and Yaschyshyn 1997).

The range of binder amount currently used in the industry varies from 3% to 7% (Amaratunga and Yaschyshyn 1997).

Since the best results of UCS have been obtained using slag in conjunction with PCI, this combination is hence used in the present study. A replacement of 0% up to 80% of cement by slag (blast furnace slag) is considered in the database used for the model development. The range of binder as a percentage of the total weight

of the mix used in the present study is 3% to 7.5% which covers the range used in the mining industry (Benzaazoua, Fall and Belem 2004).

3.3.1.3 Type of tailings

It has been noted that the physical properties of tailings (grain size and density) and chemical composition constitute an important parameter in the development of the strength of the CPB mix (Amaratunga and Yaschyshyn 1997, Fall et al. 2005, Kesimal et al. 2005, Fall, Benzaazoua and Saa 2008).

In order to avoid any chemical interactions between the tailings and cement which may bring about significant uncertainties in the outcome of the study, and since tailings oxidation inside the CPB mass is almost negligible (Fall and Benzaazoua 2005), the chemical composition of the tailings is taken as constant in this stage of the study. Hence, the model assumes that no oxidation of tailings will be present in the CPB matrix. The manner in which the sulphate parameter is introduced in the model will be discussed later in Section 3.1.6. On the other hand, in order to ensure that the chemical composition of the tailings is constant, the present research uses ground silica tailings since this material will not produce any reactions with the binder that can affect the results. The selection of these constant values has been based on the results of recent studies and aims to obtain the best results of UCS in the model (Fall, Benzaazoua and Saa 2008).

In regards to the physical properties, the density and fineness of the tailings (proportion of fine tailings <20 μm) are narrowed to 2.7 g/cm^3 for the former and 45% for the latter. In this way, the study seeks to reduce possible noise in the

results of the model. Assuming a fineness of 45% is intended to obtain the best results of UCS according to the conclusions of the study performed by Fall, Benzaazoua and Saa (2008).

The grain size distribution of the tailings used in the study is shown in Figure 3.2 and is very close to the average of 9 Canadian mine tailings as referred in a previous study (Orejarena and Fall 2008), and also used in the study by Benzaazoua, Fall and Belem (2004).

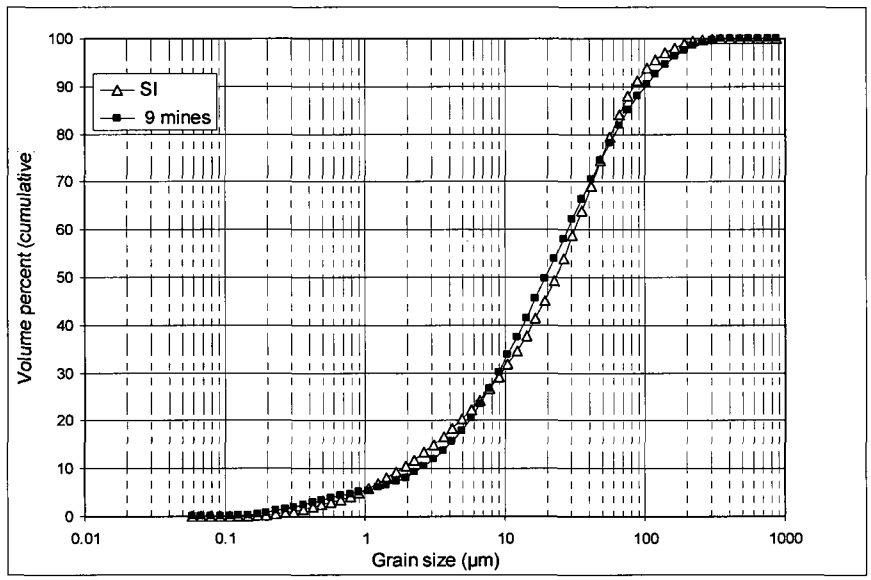

Figure 3.2 Grain size distribution curves of the tailings used (Orejarena and Fall 2008).

3.3.1.4 Curing temperature of the CPB

It has been demonstrated by previous studies that the curing temperature strongly influences the mechanical performance of CPB (Fall and Samb 2006). In the present study, this parameter is considered constant to centre the results of the model in the sulphate attack phenomena. The curing temperature of the data set used for the ANN model is room temperature (~20°C).

3.3.1.5 Curing time

It is normally understood that the strength development of a cemented material is a function of its curing time. Similar to concrete design, early and advanced strength is important for consideration during the design of a CPB. The early age strength is important since it triggers the ability of early exploitation of adjacent stopes and the stability of underground barricades usually built to facilitate the mining process (Fall 2007).

On the other hand, long term strength in CPB is important for reducing the occurrence of ground subsidence in mining operations, to guarantee the operability of secondary stopes in the mine and the long term stability of the backfilled stopes. It has been observed that sulphate attack reactions can last several months or even years after they have started (Glasser, Marchand and Samson 2008; Fall 2007). Indeed, it has been demonstrated that the long term UCS value decreases when it is assumed that sulphate attack reactions take place (Kesimal et al. 2005). Thus, the UCS values obtained through the model will be evaluated at 150 days in order to simulate the effect of a sulphate attack on the strength of mature CPB.

3.3.1.6 Sulphate amount

It is established in other studies (e.g. Ouellet and Servant 2000; Fall and Benzaazoua 2005) that CPB has a low permeability and remains saturated or highly saturated in the field. Therefore, the oxidation of the sulphides present in the

CPB is almost negligible. This is because oxygen cannot diffuse easily in the matrix of the CPB. Therefore, the sulphide reactivity of the tailings is very limited in CPB (Fall et al. 2004).

In order to simulate this effect and since the tailings chemistry in this study is considered constant by using ground silica (no presence of sulphides in the tailings minerals), the sulphate attack will be modeled providing a sulphate concentration from 0 ppm up to 35,000 ppm in the mixing water.

This range is selected in consideration of normal values in the industry and previous studies (Benzaazoua, Fall and Belem 2004, Fall et al. 2004).

The parameters mentioned above can be summarized in Figure 3.3 as follows:

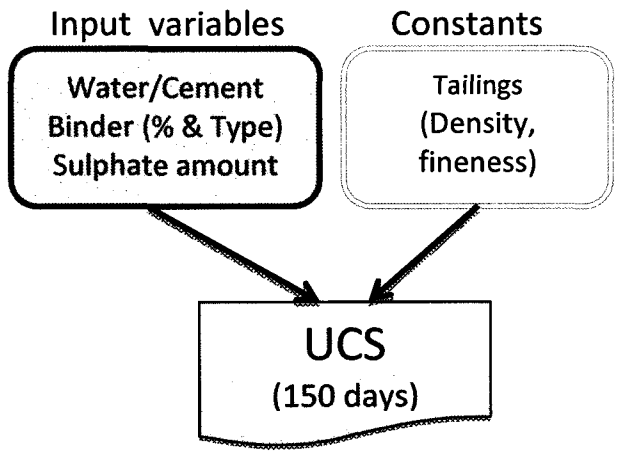

Figure 3.3 Summary of parameters used to develop the ANN model.

3.3.2 Database used in the model development

3.3.2.1 Preprocessing

Before building the model in Matlab™, the database was selected from data available from previous experimental studies on CPB (e.g. Fall and Samb 2006, 2008, Fall et al. 2008, Celestin 2008, Muskesh 2008) taking into account a uniform distribution of the output variable along the domain of study. A consolidated data set of 150 experiments was used to build the model. All samples were cured at room temperature for the present model.

The ranges for the input variables and the output (UCS) in the database are shown in Table 3.1. As it can be inferred from the output range, the model should be able to predict the UCS value of a CPB mix up to 3 MPa. It must be taken into account that ANNs are used as interpolators. Therefore, for greater values of UCS, a different model should be considered (Basheer and Hajmeer 2000).

Table 3.1 Ranges of variables in database used for the model

Input variables	**Minimum**	**Maximum**
Portland Cement Content (PCI %)	20	100
Slag Content (%)	0	80
Binder (%)	3.0	7.5
Water / Cement ratio (W/C)	4.4	10.8
Sulphate content (ppm)	0	35,000
Output variable	**Minimum**	**Maximum**
Unconfined compression strength at 150 days (UCS 150d - Kpa)	43	3,400

In order to guarantee an appropriate fitting of the model in the domain of study, a normal distribution shape of the output variable in the database is recommended. The database used in the model development exhibits a close behaviour to a normal distribution as evident in Figure 3.4.

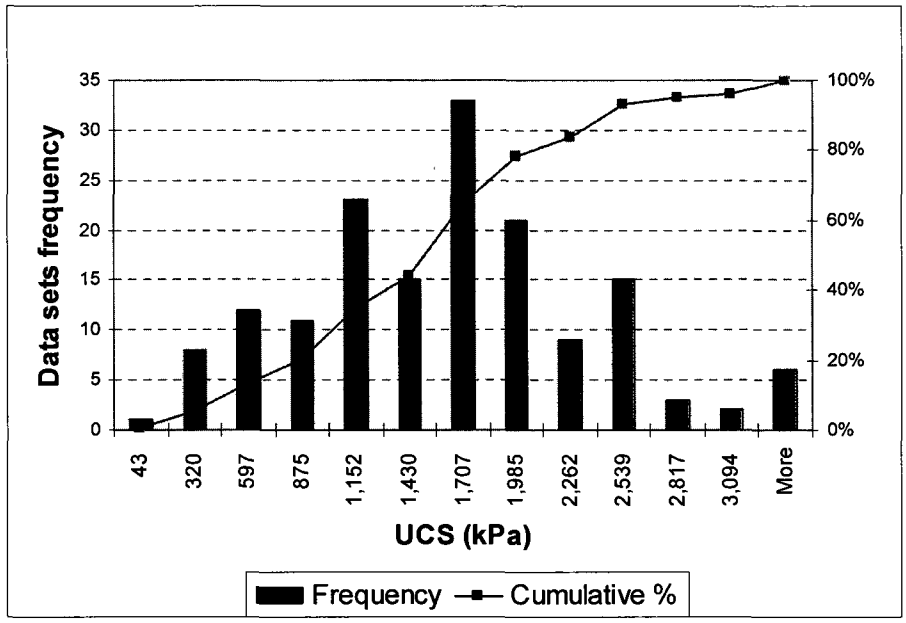

Figure 3.4 Distribution of the output variable in the domain of study.

The database was sorted from the lowest to highest value of UCS. The complete set of data can be found in Orejarena (2009). Since the input variables have a different scale or numerical range, a typical standardization was used in order to avoid the saturation of the model towards the variables with bigger numerical values. The standardization of a variable in a vector is obtained through the application of Equation 5.

$$z_i = \frac{(x_i - mean(X))}{stdev(X)} \qquad \text{Equation (5)}$$

z_i: Standardized value ("zscore" function in Matlab ®)

X= Vector or variable analyzed.

Mean, stdev: Mean and standard deviation as known in statistics analysis.

3.3.2.2 Database size and partitioning

Before proceeding with the model development, some key parameters were estimated based on similar studies and the literature available (Haykin 1994; Basheer and Hajmeer 2000). The first considered parameter is the database size and its partition between training, testing and validation subsets. In a study by Sebastiá et al. (2003), the data set was divided into 80% for training, 10% for testing (also called verification) and 10% for validation. The total database size in the study was 712 cases, considering between 5 and 20 input variables. Some of the different approaches recommended for estimating the size of the training subset are described in Table 3.2.

Table 3.2 Approaches to estimating the training subset size

Author	Parameter
Baum and Haussler (1989)	Minimum size to be equal to the number of weights in the network times the inverse of the minimum target error.
Dowla and Rogers (1995) and Haykin (1994)	Example to weight ratio (EWR) > 10
Masters (1994)	EWR > 4

In order to estimate the database size for the sulphate attack ANN model, the preliminary architecture of the neural network is conceived as follows:

- Type of neural network: Multilayer perceptron is trained through the error back-propagation algorithm (this is the most used type of ANN and its application to function approximation has already been proven in several studies) (Basheer and Hajmeer 2000; Rumelhart et al. 1995).

- Neurons in the first layer: 5 (from the parameters mentioned above in Section 3.1 and Table 1).
- Hidden layers: 1. It has been found that a single hidden layer presents satisfactory results for many problems (Ji and Lin 2006).
- Neurons in hidden layer: 10. Generally, it is assumed as twice the number of neurons in the first layer and taken from empirical criteria (Lai and Serra 1997).
- Number of outputs: 1 (UCS at 150 days).

As a result of such a configuration, the ANN preliminary architecture is shown in Figure 3.5. The number of weights that need to be adjusted during the training process is therefore 60. It is worth mentioning that it is considered a neural network that is fully connected for the estimation of the data base size.

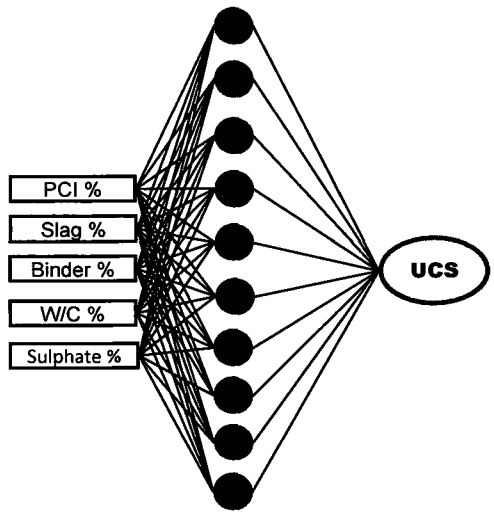

Figure 3.5 ANN initial configuration

Thus, the training set size is estimated following the recommendations that are described in Table 2. Based on the approach proposed by Masters (1994), it would have been necessary to have 240 data sets for developing the network for the proposed architecture. However, the values presented here should be taken only as a reference. On the other hand, the first two neurons (PCI and slag) can be considered dependent between themselves since the content of Portland cement plus the content of slag in the binder mix will always be equal to 100%. In this case, the number of fully independent neurons can be read as 4 and therefore, the number of weights and required data sets would drop to 40 and 160 respectively. In addition, in several studies (e.g. Kim et al. 2004; Lai and Serra 1997; Öztaş 2005), reliable ANN models with a high degree of accuracy were developed, where the number of data used for the model development is lower than those recommended by the authors mentioned in Table 2. Based on the aforementioned facts and taking into consideration that the database available for the present study comes from UCS tests performed under well-controlled conditions and on CPB samples whose composition is well-known (i.e. reliable source of data), 150 data sets are used for developing the ANN model. The database is divided as follows:

- Training: 80%
- Validation: 10%
- Testing: 10%

It is worth mentioning that the testing subset corresponds to data sets not used in the model development and therefore, the error obtained in the modeled results of

the testing vector is an indication of the ability of the ANN model to generalize. The denomination of the testing vector as data "not seen" by the ANN was made to avoid confusion when entering the data into the software used for the model development.

3.3.3 Artificial neural network parameters

The commercial software MATLAB® was used for the development of the model. A script was developed and adjusted several times until the error criteria were met in the modeling of the results. It was found that by increasing the number of hidden neurons to 12 instead of 10, the convergence of the model improves drastically and the accuracy of the results increases in the same way.

In order to avoid overtraining of the network as described in the literature (Basheer and Hajmeer 2000), the training was stopped when the testing error increased. This feature is automatically set up in the software. The training of the network was stopped when the MSE in each vector (training, validation and testing) was equal or less than 5%. MSE is the average squared difference between outputs and targets. Lower values are better, and zero MSE means that there is no error. Regression R values measure the correlation between outputs and targets an R value of 1, which means a close relationship (Demuth, Beale and Hagan 2008).

$$MSE = \frac{\left(\sum_j \left[t_j - o_j\right]^2\right)}{n}$$ Equation (6)

$$R = \sqrt{1 - \frac{\left(\sum_j [t_j - o_j]^2\right)}{\sum_j (o_j)^2}}$$ Equation (7)

where "t" is the target value, "o" is the output value obtained through modeling and "j" indicates the number of the sample in the data set (Öztaş 2005).

The training method used in the model development was the Levenberg-Marquardt algorithm which exhibits the fastest convergence in problems of function approximation with only a few hundred weights (Demuth, Beale and Hagan 2008), which is the case of the selected architecture.

The transfer function between the neurons is defined by Equation 8, known as tangent sigmoid, which is differentiable in its entire domain and has been proven to have a good performance in ANN models because it leads to a faster convergence (Vogl et al. 1988).

$$a(n) = \frac{2}{1 + e^{-2n}} - 1 \approx \tanh n$$ Equation (8)

Gradient descent with momentum weight and bias learning function was used during the training of the neural network. The values of the backpropagation learning rate and momentum constant were 0.01 and 0.9 respectively. The use of a momentum term when updating the weights helps to prevent the network falling

into local minima and improves stability of the results (Haykin 1994; Basheer and Hajmeer 2000).

3.4 Model results and discussion

The results of the model once the training was performed can be seen in the following figures (Figures 3.6 to 3.8). It must be said that training an ANN model is not a single step process. Thus, several adjustments during the process of modeling were necessary. The comprehensive results of the development of the neural network are shown in Figures 3.6 to 3.8. The results demonstrate that the proposed ANN models are suitable and predict very closely, the UCS values to experimental values as discussed below.

Figure 3.6 shows how the predicted results from ANN differ from the actual outputs. The dots that are closer to the continuous line in Figure 3.6 indicate the accuracy of the prediction.

The MSE value obtained through MATLAB® for each vector is shown as follows:

- Training Vector MSE: 0.039074
- Validation Vector MSE: 0.007426
- Testing Vector MSE: 0.030850

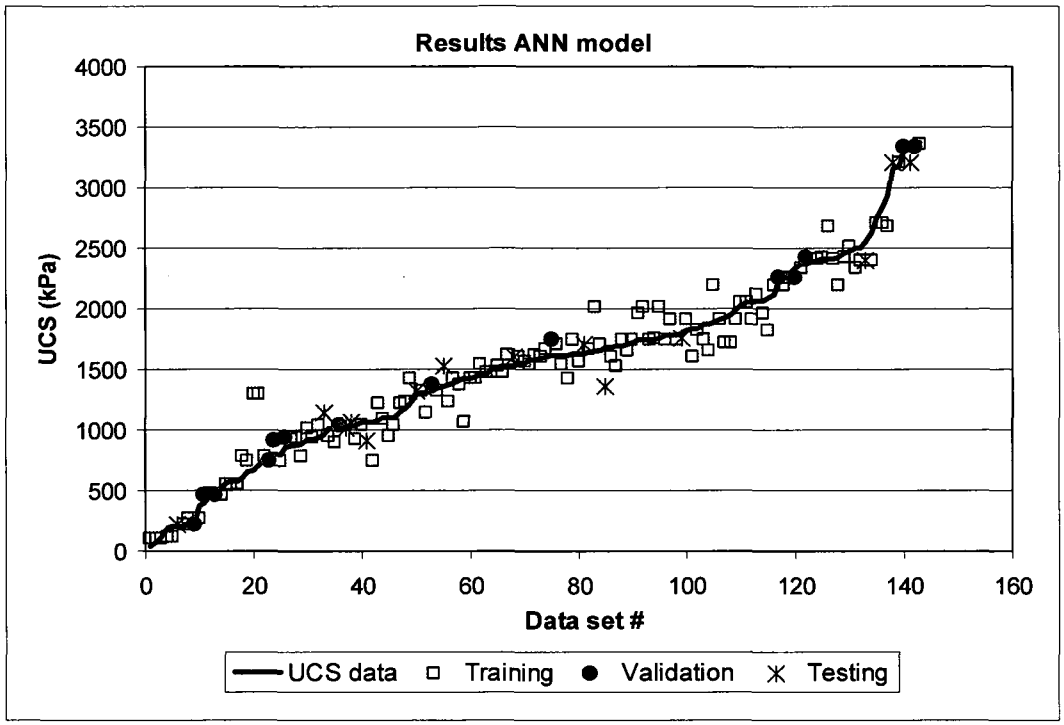

Figure 3.6 Data sets vs. output results for the ANN model

In Figure 3.7, the results obtained through ANN are compared against the measured values of UCS. Figure 3.7 shows R^2 of 0.9646 or a regression value R of approximately 0.982, which is acceptable for the model purposes on the basis that a value of 1 would imply perfect correlation. Furthermore, the accuracy of the results of the model is easily corroborated by Figure 3.8 which shows how the error is distributed in a histogram of frequency. It can be noted that most of the error (approximately 70%) occurs in a range between 57 and 114 kPa. This is because a 50 kN computer controlled compression machine was used to perform UCS tests on the CPB samples. The accuracy of the testing machine is reduced when the UCS value is lower than 80 kPa.

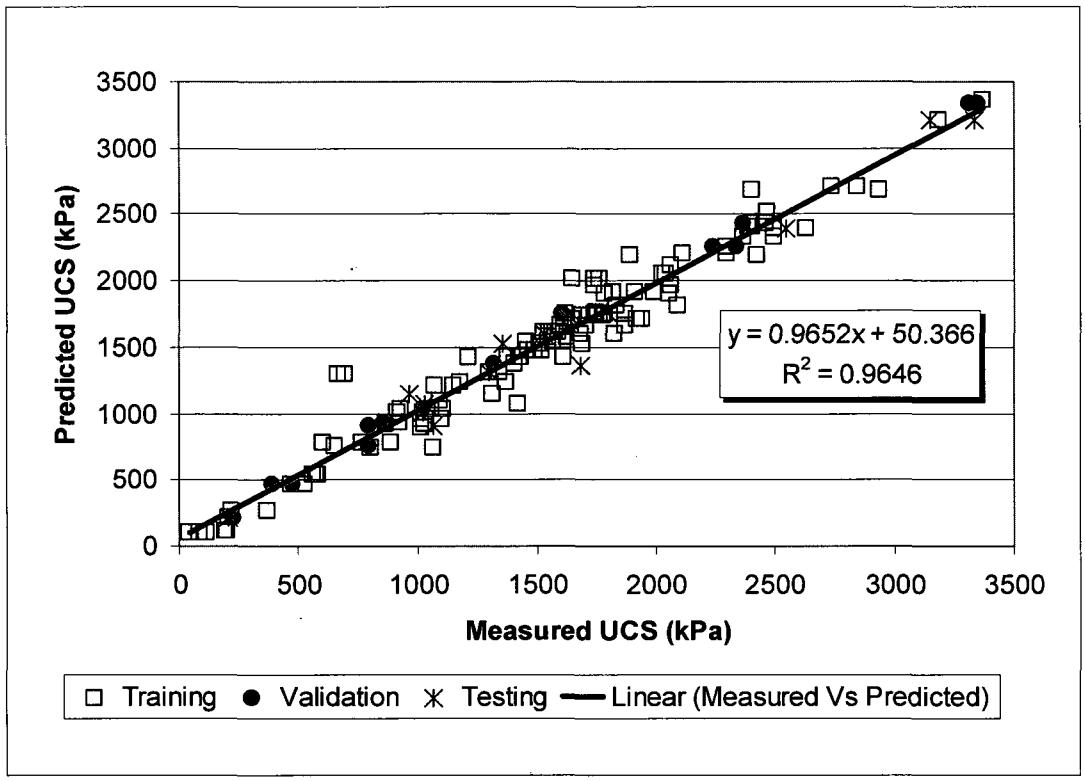

Figure 3.7 Parity plot for UCS prediction

It is worth mentioning that such results were achieved after initializing the neural network 77 times in order to obtain an MSE less than 5% in each vector and the final weights of the network were obtained in the 6th epoch or simulation.

Once the model was refined and an appropriate accuracy in the estimation of the UCS values was achieved, the next step of the study was to use the model to simulate the behavior of CPB samples under a sulphate attack, which will be explained in the following section.

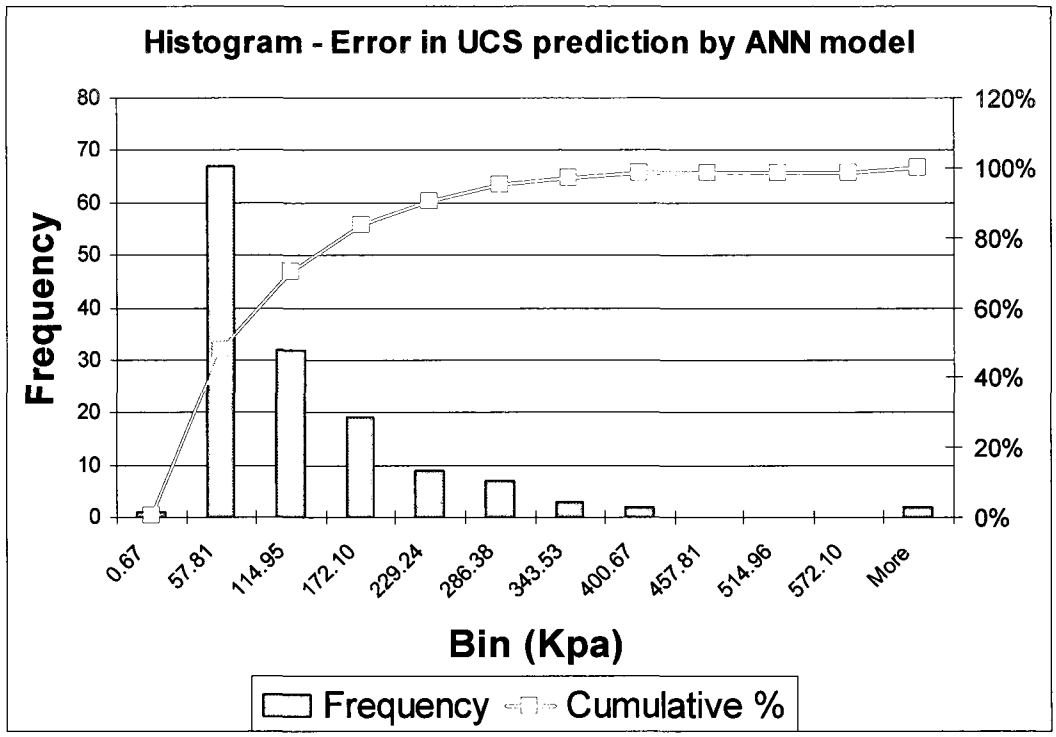

Figure 3.8 Frequency histogram of the error in UCS prediction

3.5 Effect of ANN model parameters on its response

Following the development and validation of the ANN model as described above, the next step of the study was to use the model to simulate the effect of the input parameters on its response (predicted UCS). This allows us to study the impact of CPB mix components on its resistance to a sulphate attack. In this scenario, the main variables studied are the binder content, binder composition (PCI/slag ratio), W/C and the amount of sulphate in the mix as noted in Table 1. The different scenarios used to simulate the behavior of the UCS under sulphate attack in MATLAB can be seen in Table 3.3.

Table 3.3 Different scenarios simulated through ANN

1- Binder percentage (%)				
PCI	Slag	% binder	w/c	Sul (ppm)
50	50	3	11.09	variable
50	50	4.5	7.6	variable
50	50	6	5.69	variable
2- Binder composition (PCI/slag)				
PCI	Slag	% binder	w/c	Sul (ppm)
25	75	4.5	7.6	variable
50	50	4.5	7.6	variable
75	25	4.5	5.69	variable
3- Water Cement Ratio (W/C)				
PCI	Slag	% binder	w/c	Sul (ppm)
50	50	4.5	6	variable
50	50	4.5	7.6	variable
50	50	4.5	9.2	variable
50	50	4.5	10	variable
Sulphate amount: 5,000 - 25,000 ppm at intervals of 5,000 ppm				

3.5.1. Effect of binder content on sulphate attack resistance of CPB

For the first scenario (% binder, Table 3), the goal was to obtain the behavior of the output variable (UCS) by changing the sulphate content and binder proportion in the mix. It should be noted that the W/C used in each data set corresponds to those that would produce the same consistency in the mix (slump of 18 cm). Once the vectors for the first scenario were organized, the values were normalized using Equation 5 and then the software was used to simulate the responses to the new set of input variables. The results obtained through such a procedure can be noted in Figure 3.9.

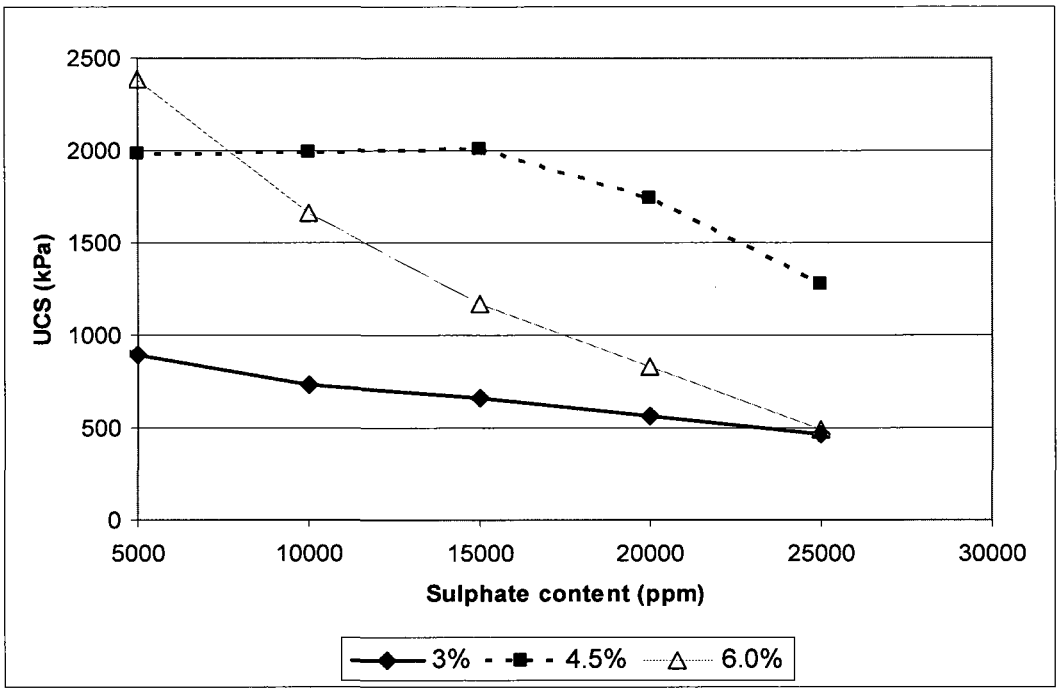

Figure 3.9 Effect of binder content on the response of CPB to sulphate attack

Some interesting features in the behavior of the UCS can be seen in Figure 3.9 as follows:

- Mixes with low to medium binder content exhibit a better resistance to sulphate attack since the drop in their UCS value is not as high as the drop for a mix with the highest binder content. It is remarkable to notice that for the mix with 4.5% of binder in weight, even for a high value of sulphate (15,000 ppm), the UCS value is practically the same as for 5,000 ppm. Similar observations were made in experimental studies conducted on CPBs by Muskesh (2008).
- The mix with the highest content of binder (6.0%) shows the steepest decrease in the UCS value under a sulphate attack. However, it also shows the highest value of UCS for low sulphate concentration.

Figure 3.9 confirms the general behavior of a cementitious material under a sulphate attack which is summarized as a drop in the UCS value depending on the quantity of sulphate ions that are present in the material. From Figure 9, it can also be noted that with more availability of binder, the loss of strength is greater. This can be attributed to the fact that there is a greater formation of expansive phases in the material (ettringite, gypsum) due to a major availability of C_3A and CH (Fall and Benzaazoua 2005).

3.5.2 Effect of binder composition on sulphate attack resistance of CPB

In the second scenario (binder composition, Table 3.3), the purpose is to analyze the UCS value by varying the sulphate content and content of PCI and slag in the binder composition. The binder content was kept constant at 4.5 wt.%. The reason for selecting this percentage is its common use in the actual industry and the relatively good performance of mixes with this binder content as noted before. Again, it should be noted that the W/C used in each data set corresponds to those that would produce the same consistency in the mix (slump of 18 cm). The results of the simulation were plotted and they can be seen in Figure 3.10.

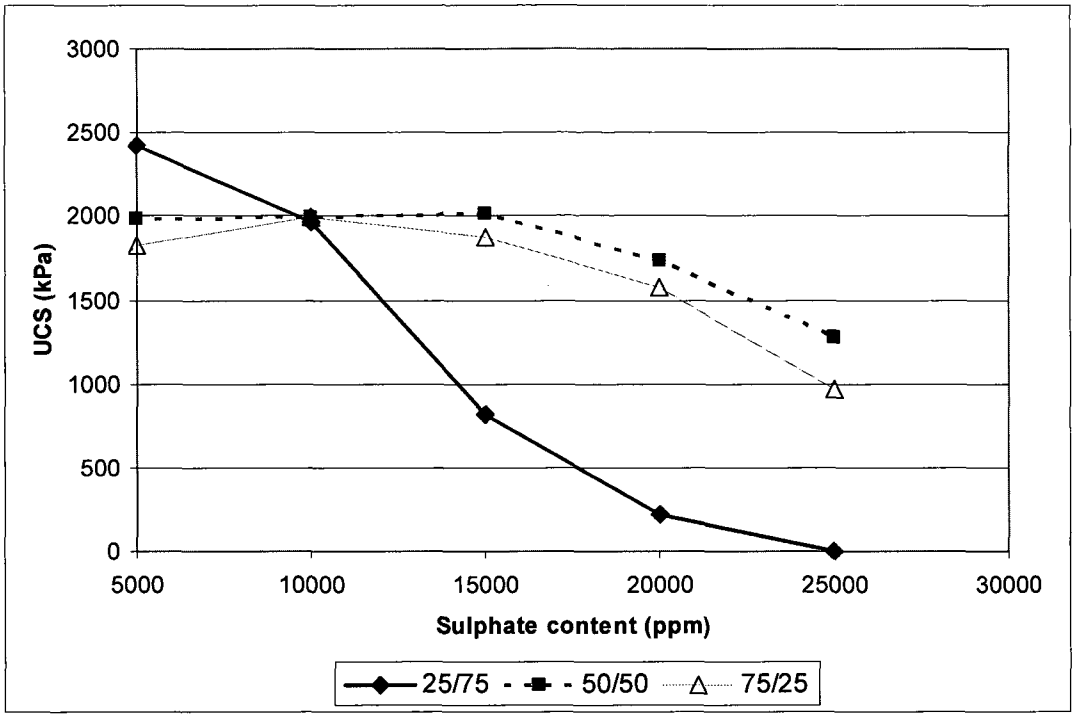

Figure 3.10 Effect of binder type on the resistance of CPB to sulphate attack

From Figure 3.10 the following findings can be noted:

- The binder composition with the best performance under a sulphate attack is 50% PCIt and 50% slag (PCI/Slag: 50/50). This dosage seems to have a good effect on the UCS since the paste is rich enough in the hydrated products of the cement and benefits the pozzolanic reaction of the slag. The formation of gypsum and ettringite due to the presence of the sulphate ions apparently do not significantly affect the strength value for low to medium sulphate concentrations (less than 15,000 ppm). However, after this value, the expansion created by gypsum and ettringite as a subproduct of the sulphate reaction is detrimental for the UCS value. This behavior is consistent with the results obtained by previous experimental studies (e.g. Fall and Benzaazoua 2005, Muskesh 2008).

- Mixes with a high Portland cement content (PCI/slag ratio of 75/25) behave in a similar pattern than the mix with 50/50 proportion. However, the value of UCS is always smaller than the 50/50 proportion. This can be attributed to the formation of a higher amount of gypsum and ettringite that affect the hardened paste to a larger extent than the 50/50 mix.

- The worst performance is obtained by the mix with a low content of PCI (25%) in relation to the slag (75%), which shows the most unstable conditions under a sulphate attack and a total loss of strength at a sulphate concentration of 25,000 ppm. This type of behavior justifies that using this proportion of slag content should be discouraged if the CPB is subjected to sulphate attacks during its service life span. A possible explanation for this type of response could be due to a lack of adequate clinker portions for the strength in CPB with a high slag proportion (PCI/Slag: 25/75). Indeed, the partial (75%) replacement of PCI with slag provides this blended cement with only 25% of C_2S and C_3S in comparison to PCI. These proportions are not high enough to produce enough C-S-H in CPBs made of the blended cement (PCI/slag: 25/75). It is well known that C-S-H is mainly responsible for the strength of cementitious materials (Mehta 1986; Fall and Benzaazoua 2005). Thus, CPBs with lower amounts of C-S-H will offer less resistance to the expansive pressure developed by ettringite and gypsum (i.e. to sulphate attack) than those with a higher amount of C-S-H. In addition, it has been demonstrated by experimental studies that slag based binders exhibit a poor performance in terms of UCS in the presence

of sulphate ions due to the inhibition of the hydration reaction (Sofrá and Boger 2002).

3.5.3 Effect of W/C on sulphate attack resistance of CPB

In the last scenario (W/C, Table 3.3), the purpose is to analyze the UCS value by varying the sulphate content and W/C in the mix. The binder content was maintained constant at 4.5 wt.% and the same was for the binder composition (50/50 – PCI/slag). The results of the simulation were plotted and they are shown in Figure 3.11.

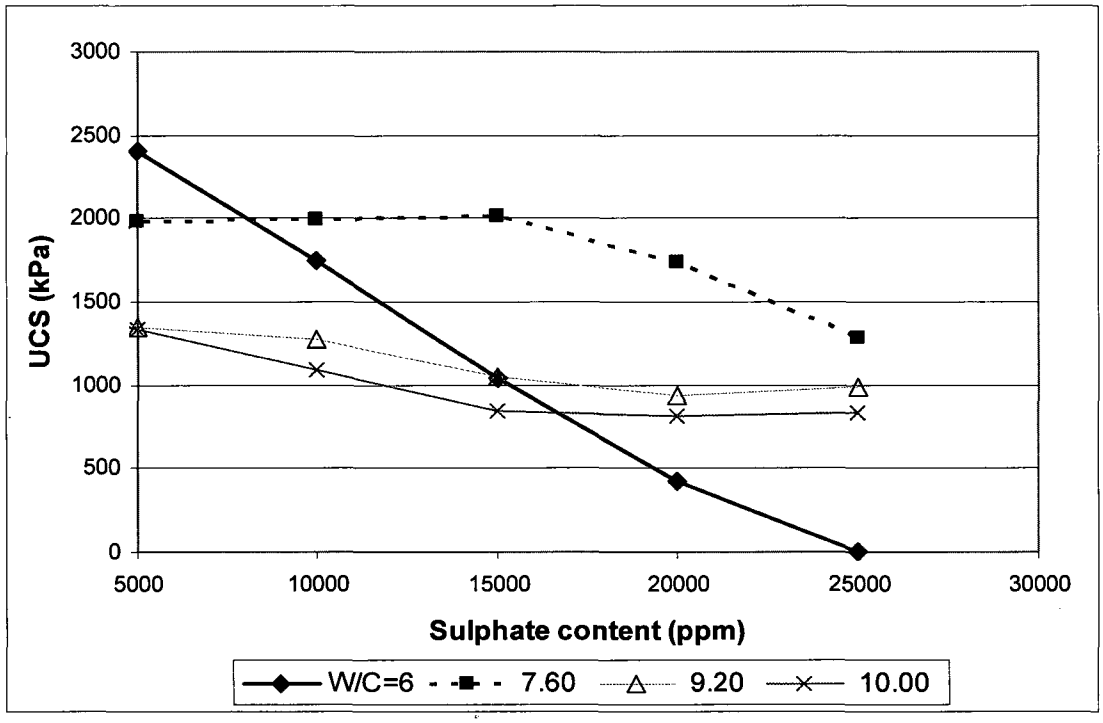

Figure 3.11 Effect of W/C on the resistance of CPB to sulphate attack

From Figure 3.11, some obvious features deserve to be mentioned:

- Mixes with a W/C equal to 7.6 show the best performance under a sulphate attack. Their UCS value is consistently higher for medium to high concentrations of sulphate ion (10,000 to 25,000 ppm).
- Although the loss of strength is considerable for a W/C of 9.2, the value of UCS for high sulphate contents is very close to 1,000 kPa which is a common value in the design of CPB structures for free-standing applications. It is also remarkable that all mixes modeled with a W/C between 7.6 and 10 shows a UCS higher than 700 kPa which is another common target value of UCS found in the literature (Brackebusch 1994; Amaratunga and Yaschyshyn 1997).
- In general, for W/C from 7.6 to 10, Figure 3.11 shows a diminution of the strength with an increase in the W/C. This decrease is greater with the presence of higher concentrations of sulphate. This behavior is consistent with the findings in several studies (Amaratunga and Yaschyshyn 1997; Benzzazoua, Fall and Belem 2004; Fall, Benzaazoua and Saa 2008). However, the strength losses due to a sulphate attack combined with increases in the W/C are not as critical as the ones shown with binder variations (Figures 3.9 and 3.10). This can be explained by the fact that with a higher content of water, the porosity of the material increases and therefore, the UCS value decreases. Nevertheless, a greater presence of voids in the cement matrix can help in accommodating a higher amount of expansive minerals under the sulphate attack reactions.
- The behavior obtained for the lowest W/C shows a high instability of the UCS value under different sulphate concentrations. Although the strength value is

the highest at low sulphate concentrations (≤5000 ppm), the UCS drops sharply as the sulphate concentration increases and becomes smaller than the other mixes after 20,000 ppm. It can be said from observing Figure 3.11 that for low sulphate concentrations, a low W/C guarantees low porosity in the cement matrix and therefore, a higher value of UCS (Amaratunga and Yaschyshyn 1997). However, once the sulphate concentration exceeds a certain limit value (in this case, 10,000 ppm) the formation of expansive phases leads to strength loss. Since the porosity of the material is low, the expansive minerals (gypsum and ettringite) deteriorate the structure of the material and therefore, its strength (Fall, Benzaazoua and Saa 2008).

3.6. SUMMARY AND CONCLUSIONS

In this study, a general background on sulphate attacks and ANNs was provided in order to understand both the implications of such phenomena in CPB structures and the details of the model development. An ANN model is developed to predict the impact of sulphate on the strength of CPB. It has been demonstrated that ANN represents a reliable technique for modeling the effect of sulphate on the strength of CPB. It is also proven that ANN forms a good basis for understanding and predicting the effect of CPB's mix components on its resistance to a sulphate attack. The validation tests that are completed show good agreement between the experimental and modeling results.

Finally, some important facts are determined once the model is used to simulate different mixes by changing the input variables. This is probably the most

interesting feature of the ANN methodology; the ability to simulate and explain complex processes once an appropriate model is developed. Thus, some of the most important findings are listed as follows:

- From the different binder dosages introduced in the model, a binder content of 4.5% shows the best performance under a sulphate attack. A high content of cement does not guarantee the best performance under a sulphate attack as noted in Section 3.4.
- A proportion of 50% PCI and 50% slag is believed to provide the best results under a sulphate attack. Mixes made from binders with a low proportion of cement against slag should be evaluated carefully under a sulphate attack since the response of the model shows a steep loss of strength after 10,000 ppm.
- The response of the model for a low W/C (W/C = 6) shows the highest strength value for low sulphate concentrations. However, the strength is dramatically reduced for higher concentrations of sulphate.

3.7. ACKNOWLEDGMENTS

The writers would like to acknowledge the National Sciences and Engineering Research Council of Canada (NSERC), University of Ottawa and Cement Lafarge Inc.

3.8. REFERENCES

Akcil, A., Destruction of cyanide in gold mill effluents: biological versus chemical treatments, Biotechnology Advances 21 (2003) p. 501– 511

Amaratunga, L.M., Yaschyshyn, D.N. , Development of a high modulus paste fill using fine gold mill tailings, Geotechnical and Geological Engineering, 1997, 15 p. 205–219

Basheer, I., Selection of Methodology for modeling hysteresis behavior of soils using neural networks. J. Comput.-aided Civil Infrastruct., Kansas State University, 2000., 435 pp.

Basheer, I.A., Hajmeer, M., Artificial neural networks: fundamentals, computing, design, and application, Journal of Microbiological Methods 43 (2000) p. 3–31

Benzaazoua, M., Fall, M., Belem, T. A contribution to understanding the hardening process of cemented paste fill. Minerals Engineering 17 (2004) p. 141–152

Bernier L.R, M.G. Li, A. Moerman, Effects of tailings and geochemistry on the physical strength of paste backfill, Proceedings of Sudbury '99, Mining and the Environment II, in: D. Goldsack, Belzile, P. Yearwood, G. Hall (Eds.), Laurentian University, Sudbury, Canada, 1999, pp. 1113–1122.

Bing, B., Cohen, M.D., Does gypsum formation during sulphate attack on concrete lead to expansion, Cem. Concr. Res. 30 (1) (2000) 117– 123.

Brackebusch, F., Shillabeer J., Use of paste for tailings disposal, in: Proceedings of the 6th International Symposium on Mining with Back-fill (Minefill 98) AusIMM, Publication no.1/98, 1998. Pp. 53-58

Brackebusch, F.W. (1994) Basics of paste backfill systems, Mining Engineering, 46, 1175–8.

Brown, P.W., Thaumasite formation and other forms of sulfate attack, guest editorial, Cem. Concr. Compos. 24 (3– 4) (2002) 301– 303.

Celestin, J.C. Geotechnical properties of cemented paste backfill and tailings liners: effect of mix components and temperature. M.A.Sc. thesis, University of Ottawa, 2008, 221p.

Cohen, M.D., Mather, B., Sulfate attack on concrete-Research needs, ACI Mater J 88 (1991) 62–69.

Collepardi, M., A state-of-the-art review on delayed ettringite attack on concrete, Cement & Concrete Composites 25 (2003) p. 401–407

Czernin, W., Cement Chemistry and Physics for Civil Engineers, Chemical Publishing Co., Ireland, 1962, p.91

Demuth, H., Beale, M., Hagan, M., Artificial Neural Network Toolbox™ 6, User's Guide, MATLAB, p 1-18, 2008.

Fall, M., Benzaazoua, M., Saa, E.G., Mix proportioning of underground cemented tailings backfill, Tunnelling and Underground Space Technology 23 (2008) p. 80–90

Fall, M. et al., Civil Engineering Department, University of Ottawa, Studies on CPB properties, 2008.

Fall, M., Benzaazoua, M., Modeling the effect of sulphate on strength development of paste backfill and binder mixture optimization, Cement and Concrete Research 35 (2005) p. 301–314

Fall, M., Geotechnical Hazards, Notes from lecture given by Dr. Fall to Graduate Students registered at the course Geotechnical Hazards. University of Ottawa, ON. Canada. 2007.

Fall, M., Samb, S.S., Influence of curing temperature on strength, deformation behaviour and pore structure of cemented paste backfill at early ages, Construction and Building Materials (2006).

Fall M., Benzaazoua M., Ouellet S. Experimental characterization of the effect of tailings fineness and density on the quality of cemented paste backfill. Journal Minerals Engineering 2005; 18: 41-44.

Fall M., Benzaazoua M., Ouellet S. Effect of tailings properties on paste backfill performance. Proceedings of 8th International Symposia on Mining with Backfill. In Beijing, China 2004;193-202.

Frias, M., Rodriguez, C., Effect of the incorporating the ferroalloys industry wastes as complementary cementing materials in the properties of blended cement matrixes, Cement & Concrete Composites(2007)

Glasser, F.P., Marchand, J., Samson, E., Durability of concrete — Degradation phenomena involving detrimental chemical reactions, Cement and Concrete Research 38 (2008) p. 226–246.

H.F.W. Taylor, Cement Chemistry, 3rd edR, Academic Press Publisher, New York, 1990, 475 pp.

Haykin, S., Neural Networks A Comprehensive Foundation, MacMillan College Publishing Company Inc, 1994, 696 pp. ISBN 0-02-352761-7.

Hecht-Nielsen, R., Theory of back propagation neural networks, In: International Joint Conference on Neural Networks, 1989.

Ji, Tao, Lin, Tingwei, Lin, Xujian, A concrete mix proportion design algorithm based on artificial neural networks, Cement and Concrete Research 36 (2006), Elsevier, p. 1399-1408.

Kesimal, A., Yilmaz E, Ercikdi B., Alp I, Deveci H., Effect of properties of tailings and binder on the short-and long-term strength and stability of cemented paste backfill. Materials Letters 59 (2005) p. 3703 – 3709.

Kim, J-I et al., Application of Neural Networks for Estimation of Concrete Strength, Journal of Materials in Civil Engineering, ASCE, May/June 2004, pp. 257-264

Lai, S., Serra, M., Concrete strength prediction by means of neural network, Construction and Building Materials, Vol11, No.2, pp. 93-98, 1997.

Lamos, A.W., An assessment of the effects of ultrafine aggregate components on the properties of mine backfills (1993), in Minefill 93, South Africa Institute of Mining and Metallurgy, Johannesburg, pp. 173–9.

Mather, B. Discussion of The process of sulfate attack on cement mortars by Shen Yang, Xu Zhongzi, and Tang Mingshu, Adv. Cem. Based Mater., (1997) 109-111.

McCulloh, W.S., Pitts, W., A logical calculus of the ideas immanent in nervous activity. Bull. Math. Biophys. 5, 1943, pp.115-133.

Mehta, P.K., 1986. Concrete: Structure, Properties, and Materials. Prentice-Hall, Inc., Englewood Cliffs, NJ.

Metha, P.K. , Sulphate attack on concrete—a critical review, in: J.Skalny (Ed.), Materials Science of Concrete III, American Ceramic Society, Ohio, USA, 1995, pp. 105– 130.

Moreno, L., Neretnieks, I., Long-term environmental impact of tailings deposits, Hydrometallurgy 83 (2006) p. 176–183

Moses, C., Nordstrom, D.K., Herman, J.S., Mills, A.L., Aqueous pyrite oxidation by dissolved oxygen and by ferric iron, Geochimica et Cosmochimica Acta Vol 51, pp. 1561-1571, Pergamon Journals Ltd., 1987.

Nasir, O., Fall, M, (2008). Modeling the heat development in hydrating CPB structures. Journal of Computer and Geotechnics (submitted).

Neville, A., Properties of concrete, Pitman Publishing, 1977, p. 392., ISBN 0 273 36150 3.

Neville, A., The confused world of sulfate attack on concrete, Cement and Concrete Research 34 (2004) 1275–1296.

Nordstrom, D.K. 1982. Aqueous pyrite oxidation and the consequent formation of secondary iron minerals. In: Acid Sulfate Weathering (eds J.A. Kittrick, D.S. Fanning & L.R. Hossner), pp. 37-56. Soil Science Society of America, Madison, WI

Orejarena, L., Fall, M., Mechanical response of a mine composite material to extreme heat, Bulletin of Engineering Geology and the Environment, Springer, 21.05.2008, vol. 67, no. 3, pp. 387-396

Orejarena, L., Prediction of Unconfined Compressive Strength of Cemented Paste Backfill using Artificial Neural Networks. University of Ottawa, Department of Civil Engineering, 2009, Masters Thesis in development.

Ouellet S., Bussiere B., Mbonimpa M., Benzaazoua M., Aubertin M., Reactivity and mineralogical evolution of an underground mine sulphidic cemented paste backfill, Minerals Engineering 19 (2006) 407–419

Ouellet, J., Servant, S., 2000. In-situ mechanical characterization of a paste backfill with a self-boring pressuremeter. CIM Bulletin 93 (1042), 110–115.

Ouellet, S., Bussiere, B., Mbonimpa, M., Benzaazoua, M., Aubertin, M., Reactivity and mineralogical evolution of an underground mine sulphidic cemented paste backfill, Minerals Engineering 19 (2006) 407–419

Öztaş, A. et al., Predicting the compressive strength and slump of high strength concrete using neural network, Construction and Building Materials, 2005, Elsevier.

Pokharel, M.Geotechnical en environmental responses of paste tailings systems to coupled thermo-chemical loadings. M.A.Sc. thesis, University of Ottawa, 2008, 248 p.

Ramón y Cajál, 1911, Histologie du système nerveux de l'homme et des vertébrés. Paris, Maloine ; Edition Française Revue : Tome I, 1952 ; Tome II, 1955 ; Madrid : Consejo Superior de Investigaciones Científicas.

Rumelhart, D.E., Durbin, R., Golden, R., Chauvin, Y., Backpropagation: the basic theory. 1995. In: Rumelhart, D.E., Yves C. (Eds.), Backpropagation:Theory, Architecture and Applications. Lawrence Erlbaim, NJ, pp. 1-34

Sebastiá, M. et al., Neural Network prediction of unconfined compressive strength of coal fly ash-cement mixtures, Cement and Concrete Research 33 (2003), pp.1137-1146.

4. Chapter 4 - Technical paper II:

Artificial Neural Network Based Modeling of the Coupled Effect of Sulphate and Temperature on the Strength on Cemented Paste Backfill

Abstract

Among the different options for mine waste management, CPBs have become important in mining operations around the world due to their environmental and economic benefits. The key design parameter of a CPB structure is its mechanical stability, which is commonly evaluated by the UCS of the CPB material. Experimental studies have shown that the sulphate present within the CPB and the curing temperatures can significantly affect the strength of CPBs. The increasing use of CPBs in underground mine operations as well as the subjection of CPBs to a large variability of thermal (curing temperature) and chemical (sulphate content) loads, make it necessary to model and quantify the coupled effect of sulphate and curing temperature on the strength of CPBs. Therefore, the main objective of this study is to develop a methodological approach and a mathematical model based on an ANN to analyze and predict the strength of mature CPBs which contain different amounts of sulphate and cured at various temperatures. Based on the experimental results of UCS tests from previous studies on CPBs from several Canadian mines, the author has developed an ANN model by using an ANN methodology implemented through MATLAB™. The developed model is validated

with experimental data that is not used for the model development. The validation shows good agreement between the predicted and experimental data. The results from the ANN model of this study show that the coupled effect of curing temperature and sulphate significantly affects the strength of CPBs. This effect can be positive (strength increase) or negative (strength decrease) depending on the initial amount of sulphate content, the curing temperature and type of binder. Furthermore, this study demonstrates that ANN can be used as a valuable tool to evaluate the coupled influence of sulphate and temperature on the strength of CPBs, i.e., it is a suitable tool for the optimization of a CPB mixture.

4.1. Introduction

The Canadian mining industry generates an average of 650 million tons of waste per year and over 95% of all solid waste generated in Canada annually [1]. Since the Bad Grund Mine in Germany first used CPBs in the late 1970s, it has been noted as an alternative method for the reduction in the disposal of waste on the surface by returning up to 60% of the extracted material underground [2,3]. In fact, it has been suggested that the application of this technology to mines should be supported by government incentives to guarantee the maximization of the extraction of ore, proper reclamation of mined areas, better waste management and control of groundwater [4].

CPB technology is beneficial for stakeholders involved in mining operations from the following points of view:

- For the mining company, it allows an increase in the ratio of extraction since the stopes can be filled with the CPB and adjacent areas can be mined as well. This also improves the mine cycle and eventually, the company revenue [8].
- For mine workers, it contributes to the creation of a safer workplace since CPBs can be used as roof support and for the construction of barricades in underground mines [9].

- For communities, the underground disposal of tailings through CPBs reduces the footprint and total dimensions of surface tailings dams and therefore, there are fewer opportunities for catastrophic failures, such as those that occurred in Italy (Stava) [10] and Spain (Aznalcóllar) [11]. In addition, it can prevent undesirable conditions, such as AMD, since it reduces leachate generation in sulphidic tailings due to decreased permeability and better water retention in the paste [8,12,13].
- For other industries, it is an alternative method for underground disposal of byproducts, such as FA and slag.

Therefore, it can be said that the underground disposal of tailings has major environmental benefits [9].

CPB is basically made of dewatered tailings combined with a hydraulic binder. The binder is usually PC. However, PC can be blended with FA or Slag to mainly reduce the binder cost [3]. The concentration of binder and tailings in the mix is usually between 3% to 7%, and 70% to 85% by weight, respectively [2].

One of the most important performance properties of CPBs includes mechanical stability. It is commonly evaluated by using the UCS [3,5]. Several studies [e.g., 5,6,10,11] have demonstrated that the initial sulphate content of a CPB can significantly decrease its long-term UCS. This means that one of the major durability concerns in the design of CPBs or factors that cause the deterioration of CPB structures is internal sulphate attacks. Furthermore, recent studies [e.g.,12,13] have demonstrated that the effect of sulphate on the strength of CPBs

is strongly dependent on the curing temperature. In other words, the coupled effects of sulphate and temperature can significantly affect the strength of CPBs. Despite the significant contribution of the aforementioned studies to the understanding of the coupled effects of sulphate and temperature on the strength of CPBs, our understanding is still limited. Additionally, the mathematical approach for related analysis and modeling has not been considered until now, nor has the prediction of CPB mechanical strength been subjected to coupled chemical (sulphate) and thermal (temperature) loads.

Considering the problems mentioned above and the fact that several underground CPB structures in Canada and worldwide are subjected to various chemical and thermal loads during their lifetime, the goal of the research is to develop an efficient approach and mathematical prediction model based on ANNs, which will allow us to do the following:

– find the relationship between the quantity of sulphate, curing temperature and strength of mature CPB, i.e., to better understand the coupled effect of sulphate and temperature on the long-term strength of cemented backfill; and

– quantitatively evaluate and predict the coupled effect of sulphate and temperature on the mechanical strength of mature CPBs.

In order to achieve this goal, the research is outlined as follows:

- a general background on temperature and sulphate sources and their coupled effect on CPBs will be first presented,
- the development of a modeling approach and an ANN model will be then provided,

- the main results of the modeling and verification of the ANN model will be presented and discussed, and
- the main conclusions of the study will be outlined.

4.2. Background on temperature and sulphate sources and their effects on CPBs.

4.2.1 Source of temperature and sulphate in CPB operations

- **Sources of temperature**

Nowadays, mining operations often require an ability to carry out extraction of ore from greater depths than those in the past. Stopes that are located deeper means that the CPB will be exposed to higher temperatures due to geothermal gradient which has been identified as one the sources of underground heat and can account for up to 15°C/km to 40°C/km [14]. From reference [15], it was found that in a South African mine, the current depth of extraction is 3,500 m and the temperature can reach 54°C; similarly in reference [16], the author estimated a temperature of 46°C at 3,000 m in the Sudbury Basin in Canada. It is also known that with greater mine depths, the auto-compression of the surface air that has been introduced in the mine for ventilation also contributes to the increase of the mine temperature by up to 10°C per kilometer of vertical depth; especially in warm climates. [14]

In addition to the factors mentioned above, the hydration of cement is a process that contributes to the increase in temperature in CPB structures and mine

environment. The heat produced by cement hydration is one the most important sources of heat in CPB technology. Field [50] and a number of other studies [e.g., 17,18] have demonstrated that after only a few days (~ 4 days) of curing, the backfill temperatures increase up to approximately 50°C. However, the amount of the increase depends on several factors, such as the binder content, filling rate, shape of the stope, initial CPB temperature and CPB specific heat [18].

Another factor that can come into play is the probability of self-heating of sulfidic rocks that are adjacent to stopes. The occurrence of this event not only has a strong effect on the strength of the CPB, but also in the safe operation of the mine and the impacts on the environment as found in reference [19]. Furthermore, it must be said that this type of heat requires specific conditions to occur and is not within the scope of the current work. For more information on the extreme heat effect on CPBs, the reader is encouraged to review reference [20].

Temperature variations in an underground mining operation can also come from other various sources, such as mine machinery, blasting operations, lighting, ventilation, fires, etc. However, the size of the CPB structures is often too large to be significantly affected by these heat sources [21]. Furthermore, moderate heat can also be added to the CPB to increase its early strength in order to speed up the mine cycle [22].

- **Source of sulphates in CPB technology**

On the other hand, the availability of sulphate in the CPB mix can be due to the presence of pre-oxidized tailings, free sulphate ions in the process water, use of sulfur dioxide/air process in gold mining, gypsum ($CaSO_4.2H_20$) or anhydrite ($CaSO_4$) added in the binder. The presence of sulphate ions in the CPB can lead to the strength loss of the CPB structure as noted in previous experimental studies [3,23,24,25]. A more detailed background on sulphate and its effect on CPB strength can be found in those references and also in [26].

4.2.2 Coupled effect of sulphate and temperature on cementitious materials

The discussion and development of models with respect to the effects of curing temperature on cement hydration has been the subject of extensive research over time. A common finding in these studies is the increase in temperature during the curing time which accelerates the early hydration of the cement constituents and therefore, favors early strength development as mentioned in references [27,28]. Similarly, research in concrete has demonstrated that high curing temperatures (40°C) will improve high early strength although in the long-term, the strength can be lower than those of samples cured at lower temperatures [28,29], mainly due to the formation of hydrates of poorer physical structure with greater porosity in detriment of the strength [30]. On the other hand, low curing temperatures can lead to a strength decrease up to 30% for ordinary concrete which is cured at 10°C. The results are more critical if the temperature is 0°C with a 62% decrease of the strength ratio according to the results from reference [31].

Notwithstanding the profuse research on curing temperature and sulphate in concrete, the same cannot be said in terms of their coupled effect in concrete and this sort of research is even scarcer for CPB applications. In this regard, it is worthwhile to mention the study in reference [32], where it was found that sulphate concentrations up to 15,000 ppm and curing temperatures up to 35°C have a positive effect on the long term UCS of a CPB mixture.

On the other hand, when the mine is located in a permafrost region, temperatures below zero in some areas of the mine can be expected. The presence of low curing temperatures on CPBs has a deleterious effect since the inclusion of ice lenses in the matrix of the paste leads to lower values of strength due to more porosity in the paste and inhibition of the hydration of cement [2,33].

4.3. Development of the ANN model

4.3.1 Parameters considered in the model

The first step in the application of modeling with the use of neural networks is to have an appropriate definition and formulation of the problem [34]. Thus, the parameters considered in the design of the model to simulate the coupled effect of curing temperature and sulphate on CPB strength are listed below and a schematic is provided in Figure 4.1.

- W/C

- Amount and type of binder used for the CPB (%)
- Sulphate content (parts per million (ppm))
- Curing temperature
- Curing time
- Type of tailings: fineness, density and chemical composition. They are considered as a constant in this study because the sulphate and temperature exclusively affects the hydraulic binders and cement matrix

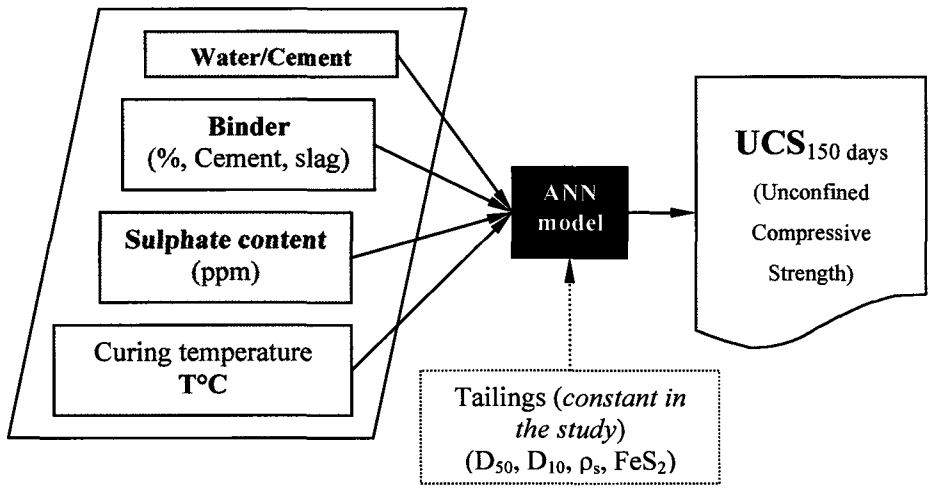

Figure 4.1 Parameters considered in the ANN model development

4.3.1.1 Water/cement ratio

CPB mixtures require a W/C ratio greater than in concrete to be able to transport the mix to its underground location. Thus, values for W/C higher than 5 are common in CPB mixes in comparison to 0.5 or less in concrete. However, despite the difference in range, the strength of CPB follows an inversely proportional relationship with the W/C ratio as it does in concrete mixes. The aforementioned fact has been confirmed by several experimental studies (e.g., [10,11,35]). Based

on these previous studies, the range of values of W/C used in the study of the development of the ANN model is between 4.4 and 10.8 as shown in Table 4.3.

3.1.2 Amount and type of binder (%)

By means of experimental studies such as those in references [10,11,35], it has been found that the amount and type of binder has a direct effect on the UCS value of the CPB mix. The relevance of this parameter resides not only in its influence on the strength, but also in the final cost of the mixture, since it is in most of the cases the only component of the CPB that is not produced in the mine and therefore, the most costly. The binder can represent up to 75% of the costs [35]. The effect of the binder on the strength depends on the amount added to the mix. It was found that a variation in the binder dosage from 3% to 6% can affect the UCS up to twice the initial value [35]. The most common binder used in the preparation of CPB is Portland cement type I (PCI). However, due to the relatively high costs of PC, other by-products commonly designated as mineral admixtures (e.g. Slag, FA) are sometimes substituted for PC in various amounts to produce blends of lower costs [36]. Nevertheless, while the use of Slag results in higher strength of a mature CPB, the use of FA leads to lower strength [10,11]. For the aforementioned reason, PCI and Slag are used as the binders. PCI was used alone or blended with Slag in various weight proportions (0/100, 25/75, 50/50, 75/25 and 100/0).

These binders are often used for CPB mixtures in mines located in eastern Canada.

4.3.1.3 Sulphate content (ppm)

High sulphate concentrations; sometimes more than 25 000 ppm, can be present in fresh CPBs, particularly when mine processing water is used to prepare the CPB and/or the pore water of the filtered tailings is rich in sulphate.

In order to simulate the effect of sulphate on the CPB strength, an initial sulphate concentration that varies from 0 ppm to 35,000 ppm will be considered. This range has been chosen by taking into account the available data and considering a typical range found in the industry according to previous studies [25,37].

4.3.1.4 Curing temperature of the CPB

According to the study from reference [2] the curing temperature of CPBs has a strong effect on the UCS value, especially at early ages of the material. In the study, it was found that for curing times up to 28 days, an increase in curing temperature increases the strength of the CPB. However, low curing temperatures (0, 2°C) mainly show the lowest strength and lowest strength rate development [2]. The inhibition of cement hydration at low temperatures can be the explanation for low UCS values according to reference [33]. On the other hand, the hydration of the binder may be accelerated at high curing temperatures and therefore, a greater UCS value is obtained in the first days after the CPB is poured as corroborated by the results of differential thermal analyses performed on samples in the study by reference [2]. For the present study, the range of curing temperatures will vary

from 2°C to 50°C. This temperature range covers the most common thermal loading conditions of CPBs [14,18,20].

4.3.1.5 Curing time

It is well known that the strength development of a cementitious material is dependent on the curing time mainly due to the time-dependent evolution of the cement hydration process. Furthermore, It has been observed that sulphate attack reactions can last several months or even years after they have started [25,38]. Indeed, it has been demonstrated that the long term UCS value of CPBs can decrease when it is subjected to sulphate attacks [39]. This decrease is commonly due to the formation of excessive amounts of expansive minerals (ettringite, gypsum) which results from the reaction between the sulphate ions and C_3A of the cement (formation of ettringite) as well as between the sulphate ions and cement hydration product; CH (formation of gypsum). These expansive minerals can exert excessive pressure on the pore structure of the CPB and damage its cemented matrix. Thus, the UCS values obtained through the model will be evaluated at 150 days in order to simulate the effect of a sulphate attack on the strength of a mature CPB, or in other words, on its durability.

4.3.1.6 Type of tailings

Since sulphate and temperature exclusively affect the hydration of hydraulic binders, the chemical and physical characteristics of the tailings are kept constant in this study. This is achieved by using tailings (SI) exclusively made of quartz as

tailings materials. This maintains the level of uncertainty at a minimum level when studying the coupled effect of sulphate and temperature on the strength of CPBs. Indeed, while the quartz does not react with the cement, some natural tailings may contain various (uncontrollable) minerals (e.g., sulphide minerals) and chemical elements that can react with the cement and thus, influence the outcome of the study. Figure 4.2 shows a grain size distribution of the tailings used, which is close to the average of 9 Canadian mine tailings. Table 4.1 gives the main physical and chemical characteristics of the tailings used. It can be observed that SI, with about 41-45 wt.% fine particles (<20 μm), can be classified as medium tailings (Figure 4.2).

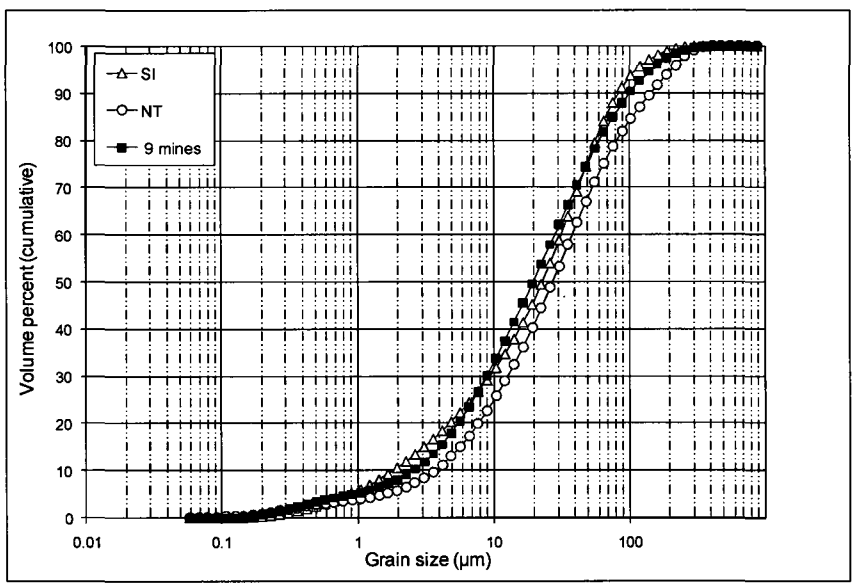

Figure 4.2 Grain size distribution of the tailings (SI, NT) used and the average grain size distribution of tailings from 9 Canadian mines. (SI: Silica Tailings, NT: Natural tailings)

Table 4.1 Physical properties of the tailings used

Element	G_s	D_{10}	D_{30}	D_{50}	D_{60}	C_u	C_c
unit	-	μm	μm	μm	μm	-	-
SI	2.7	1.9	9.0	22.5	31.5	16.6	1.3

Table 4.2 Main chemical elements in the tailings used

Element	Al	Ca	Si	Fe	Na	Pb	S	K
unit	wt %	wt %	wt %	wt %	wt %	wt %	wt %	wt %
SI	0.1	<0.01	99.8	<0.01	<0.01	0.0	0.0	0.0

4.3.2 Database

Once all the different parameters that can potentially affect the output variable, which is UCS in this case, have been properly identified, the next step is the proper selection of the database that will be used to construct the model. Thus, UCS results from various previous studies [18,22,26,32] are used. The UCS tests were carried out on CPB samples (5 cm in diameter and 10 cm in height) by using a computer-controlled mechanical press which follows the standard ASTM C39. The details on specimen preparation and the experimental procedures are given in the aforementioned references. A total of approximately 300 data sets were taken initially as the main database to develop the model.

4.3.3 Pre-processing

In order to prevent saturation of the results by variables of greater numerical values, the different data sets were standardized before the training of the ANN. The standardization of a variable is made by the application of the following equation:

$$z_i = \frac{\left(x_i - mean(X)\right)}{stdev(X)}$$

Equation 12 – Variable standardization

z_i: Standardized value ("zscore" function in Matlab ®)

X= Vector or variable analyzed

Mean, stdev: Mean and standard deviation as known in statistics analysis.

A first trial with the entire database was carried out in order to verify if some degree of correlation could be obtained. At this stage of the development, the correlation value is less than 0.9, but high enough to continue with the process. Thus, some of the data sets were left apart in order to obtain a close to normal distribution of the UCS values. In addition, this stage is also necessary since from a previous study (150 data sets), the temperature was kept constant at 20°C and therefore, the data was reorganized to give approximately the same number of data sets to each temperature (from 2°C to 50°C). Eventually, the best results in the model were obtained by using a database size of 165 samples and a distribution of the UCS values as shown in Figure 4.3. Special attention was given to the outliers during the training of the ANN since every time the neural network was trained; the UCS predicted values were compared against the expected values obtained through the experiments. Depending on the different variables involved in each one of the data sets, they were even maintained or set aside for the subsequent training iteration. In this regard, the ANN process can be tedious since it requires the appropriate expertise to determine how the database is organized and how the variables are expected to interact between themselves during the training.

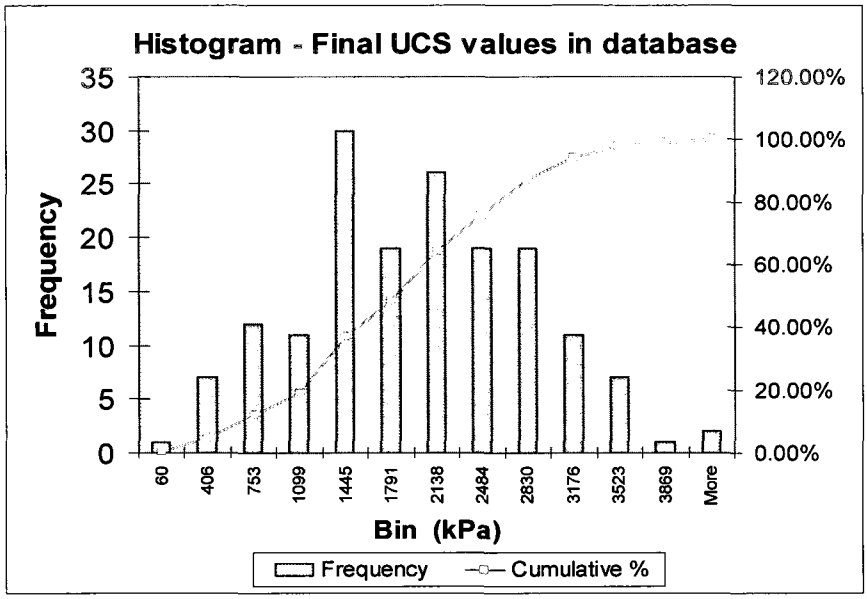

Figure 4.3 Distribution of the output variable in the domain of study

From an analysis of Figure 4.3, as expected, the model predicts the UCS of the CPB within a range of 0 to 4,000 kPa. In this regard, it is worthwhile to mention that ANNs should be used as interpolators [34]. Therefore, for UCS values greater than those shown here, the ANN must be trained with a different database.

The final ranges for the input variables (curing temperature, sulphate content, binder content and composition, and W/C) and the output variable (UCS at 150 days of curing time) are presented in Table 4.3.

Table 4.3 Range of variables in the final database

Input variables	Minimum	Maximum
Portland Cement Content (PCI %)	20	100
Slag Content (%)	0	80
Binder (%)	3.0	7.5
Water / Cement ratio (W/C)	4.4	10.8
Sulphate content (ppm)	0	35,000
Curing temperature (°C)	2	50
Output variable	**Minimum**	**Maximum**
Unconfined compression strength at 150 days (UCS 150d - Kpa)	60	4,215

4.3.4 ANN architecture

In ANNs, the type of network and architecture will vary in accordance to the type of problem that needs to be solved. In most cases, a BP neural network has been found adequate for this type of function approximation problem. Whereas an ANN that works for CPBs is very scarce, the spectrum in concrete applications is very wide as it can be verified through references, such as the following [40, 41, 42]. In addition, for a detailed description of the type of networks and the different training algorithms, references [34,43] may suffice for the avid reader.

In the present study, the type of network and architecture used is a BP neural network with a single hidden layer, as mentioned above. Attempts to use multiple hidden layers did not return the best accuracy on the predictions and therefore, those models were discarded.

The number of neurons used in the hidden layer was 18. This optimal number was obtained through numerous trials. Thus, the key parameters that define the final architecture of the ANN model for the present study can be summarized as follows:

- type of ANN: multilayer BP network,
- number of input neurons: 6 (PC content, slag content, binder content, W/C, curing temperature and sulphate content),
- number of neurons in hidden layer: 18,
- number of outputs: 1 (UCS at 150 days), and
- number of data sets: 165.

A simplified schematic of the architecture is shown in Figure 4.4 as follows.

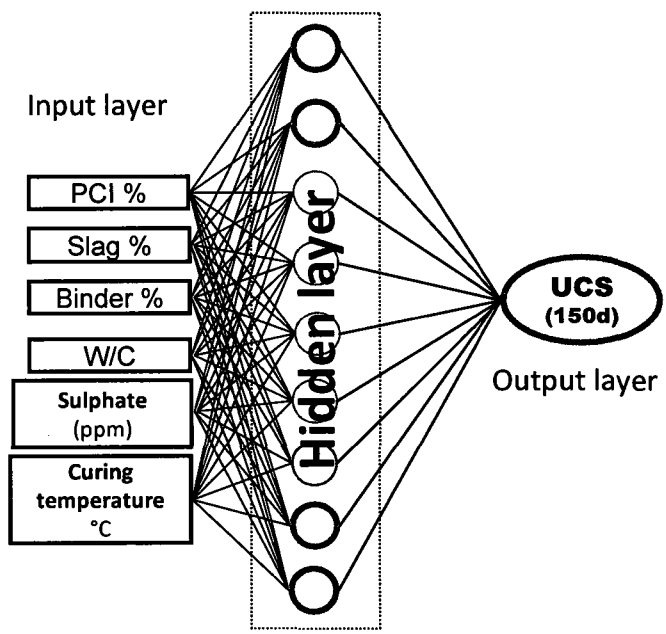

Figure 4.4 Schematic of the ANN architecture

4.3.5 Training

The commercial software MATLAB® was used to train the network by using a BP algorithm. The final partition of the database consists the following:

- training vector: 80%,
- validation vector: 10%, and
- testing vector: 10%.

The partitioning demonstrated proper results in a previous study by the author [26] and again, in this case, proved to generate the best results. It was noted that increasing the training vector as much as possible facilitates the convergence of the model. However, it must be taken into account that a significant number of validation and testing data sets are required in order to ensure that the model will have adequate generalization capabilities.

A script in MATLAB® was developed to achieve the intended precision in the model. In this regard, the mean square error (MSE) and the regression (R) coefficient concepts come into play. The MSE can be defined as the average squared difference between the outputs and targets as shown in Equation 2 as follows.

$$MSE = \frac{\left(\sum_j [t_j - o_j]^2\right)}{n}$$

Equation 13 Mean square error

where "t" is the target value, "o" is the output value obtained through modeling and "j" indicates the number of samples in the data set.

The R coefficient value measures the correlation between the outputs and targets; an R value of 1 means a close relationship. The corresponding formula is given in Equation 3 [44].

$$R = \sqrt{1 - \frac{\left(\sum_j \left[t_j - o_j\right]^2\right)}{\sum_j \left(o_j\right)^2}}$$

Equation 14 Regression coefficient

Generally, the training is stopped when the testing error increases. In this regard, it is worthwhile to mention that the testing vectors are data sets that are not used during the training (data not seen by the model) and therefore, indicates how accurate the model is in the prediction of the outputs with new data.

The basic criteria established was to obtain a total MSE that is less than 0.20 (through training, validation and testing) and an MSE for the training vector less than 0.1. The convergence was achieved after several hundreds of iterations.

Another important parameter for the ANN model is the type of transfer function used between the neurons. In this case, the tangent sigmoid function is used between the input neurons and hidden layer. Such a function can be approximated through Equation 4. For the transfer of the response between the hidden and

output layers, a linear function was used. The advantage of using these two functions is that the tangent sigmoid is continuous between -∞/+∞ and sets up certain limits for the response (due to its asymptotic behavior). The linear function is useful for the output layer since it transmits the response which comes from the previous layer. The use of the tangent sigmoid in ANN problems has been recommended since it leads to a faster convergence of the model [45].

$$a(n) = \frac{2}{1+e^{-2n}} - 1 \approx \tanh n$$

Equation 15 Tangent sigmoid

4.3.5 Data enrichment

The development of the model for the coupled effect of sulphate and curing temperature by using neural networks is more challenging than the model of sulphate attack on CPBs previously developed by the author in reference [26]. This can be explained in terms of the complexity of the interactions between the different factors that affect the strength of the CPB. In order to obtain the expected accuracy in the model, it is necessary to enhance the database of experiments with additional data from the results of the experimental study in reference [32]. Approximately 20 datasets out of 165 in the final database were obtained through direct interpolation between two immediate UCS experimental values from the aforementioned study. The data sets obtained by this mean are properly identified in Appendix No.2 where the total data base is presented.

4.4. Model results

Satisfactory results for the model were achieved after training the neural network by using the BP algorithm. Several iterations were carried out in order to obtain the appropriate level of accuracy. The results can be analyzed through the figures shown further below.

The MSE value obtained for each vector is shown as follows:

- training vector MSE: 0.086211,
- validation vector MSE: 0.050427, and
- test vector MSE: 0.023158.

Figure 4.5 gives an illustration of how close the outputs generated by the model are to the continuous line (experimental values), which can be better appreciated in Figure 4.6 through a parity plot.

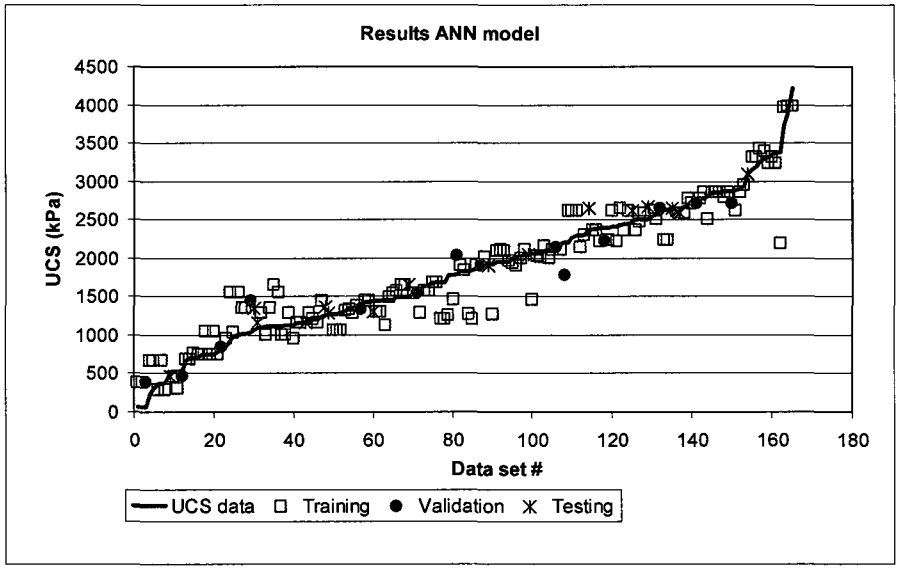

Figure 4.5 Data sets vs. output results for the ANN model

In Figure 4.6, a perfect correlation between the measured and predicted UCS values are depicted by a y=x line (R^2=1). In this regard, it can be noted that the training and testing vectors are very close to the ideal situation. The validation trend line is not shown for clarity purposes.

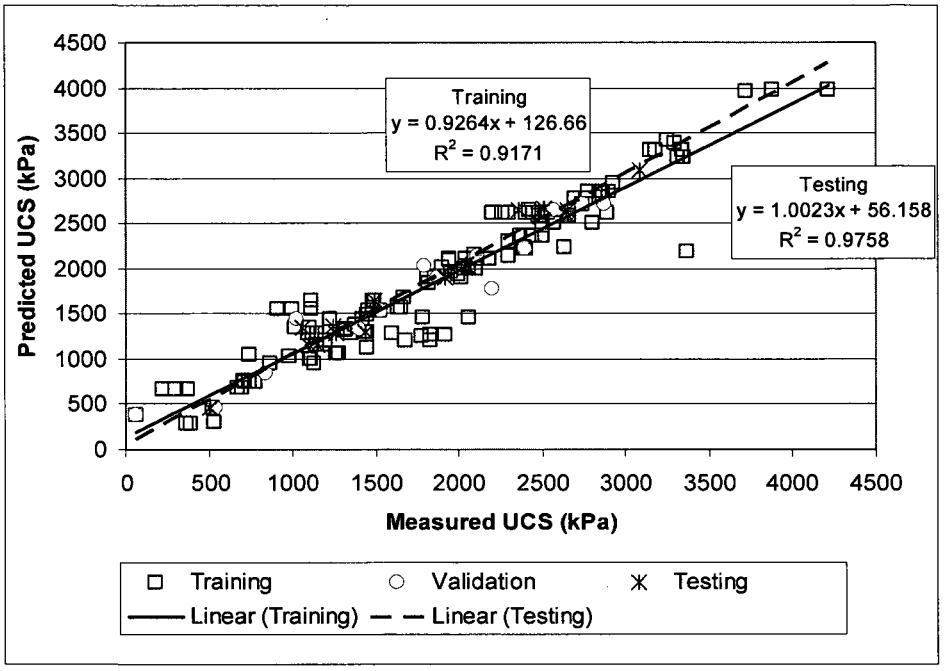

Figure 4.6 Parity plot for UCS predicted by the ANN model

A similar representation is illustrated in Figure 4.7 where the total database is shown and also the obtained correlation and the ideal y=x situation. Figure 4.6 shows that R^2=0.92 or an R value of 0.96, which is acceptable for modeling purposes since a value of R=1 would imply perfect correlation.

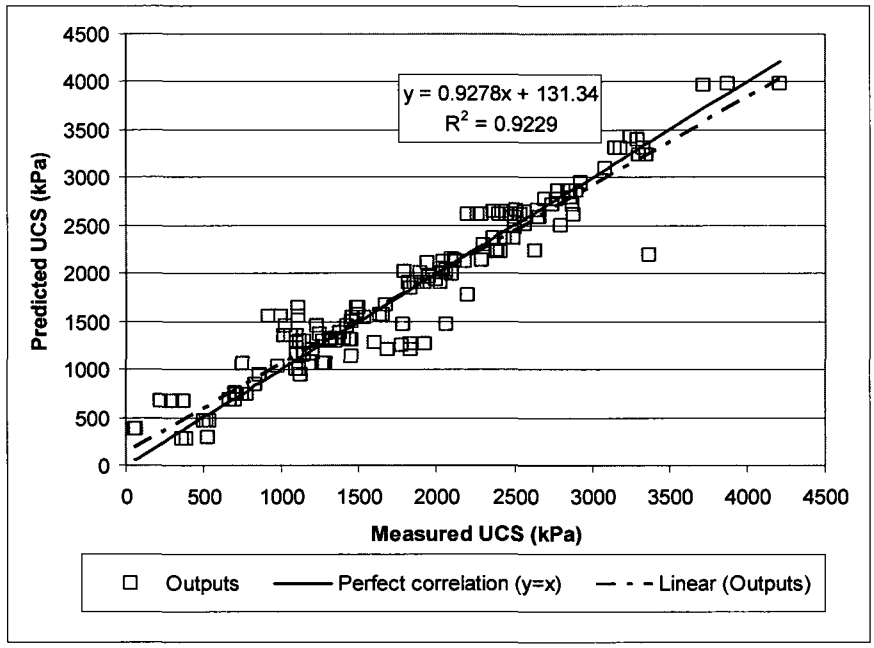

Figure 4.7 Parity plot for the total database

Another interesting plot is the one shown in Figure 4.8, which shows the magnitude of errors in the UCS prediction. From Figure 4.8, it is noted that approximately 70% of the absolute error in the UCS predicted is less than 200 kPa.

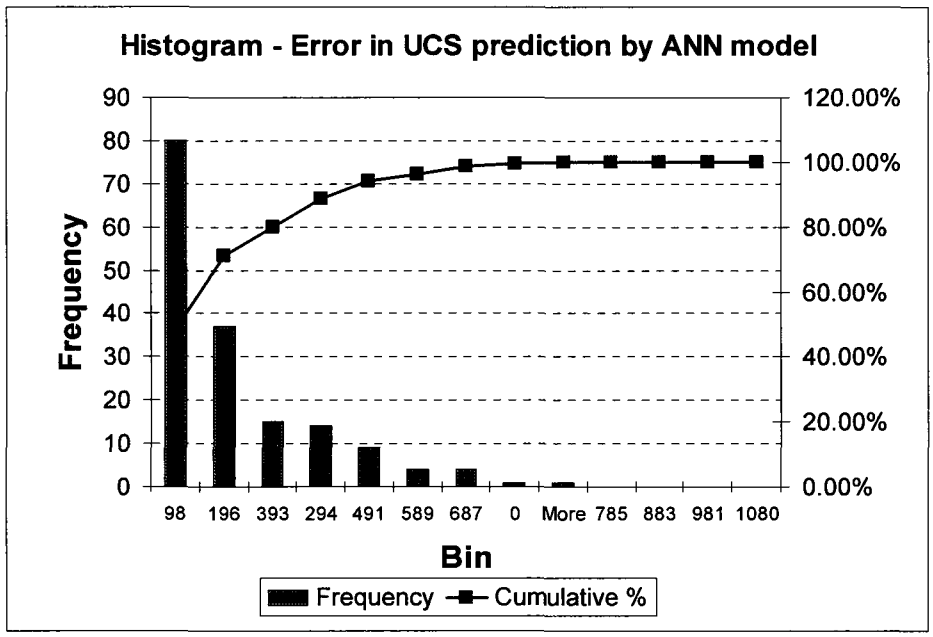

Figure 4.8 Frequency histogram of the error in UCS prediction

Based on the results shown above, it can be concluded that the ANN model is comfortably accurate enough to simulate the coupled effect of sulphate and curing temperature on CPB strength.

4.5. Simulation of the coupled effect of curing temperature and sulphate on the UCS of CPBs

Once the model was refined until the level of accuracy in the prediction of the UCS was adequate, the next step of the study was to simulate the coupled effect of sulphate and curing temperature on the UCS of a mature CPB. In order to do so and also as a cross-check against the experimental study in reference [32], an ANN model is used to predict the UCS for the following scenarios (Table 4.4):

Table 4.4 CPB mixes used for UCS simulation on ANN

PCI	Slag	Binder %	W/C	Sulphate (ppm)	T °C
50	50	4.5	7.6	Variable 0-25,000	Variable 2 -50°C
100	0	4.5	7.6	Variable 0-25,000	Variable 2 -50°C

The results of the simulation of these two basic scenarios are shown in Figures 4.9 and 4.10. Figures 4.9 and 4.10 show the simulation results of the coupled effects of sulphate and curing temperature on the strength of CPBs; one in which the binder is made of a mix of PCI and Slag with a weight proportion of 50/50, and

another with only PCI. The binder content considered is 4.5%. The experimental results obtained by [32] are also presented in Figures 4.9 and 4.10 for comparison purposes. From these figures, it can be noted that the predicted UCS (solid lines) follows approximately the same behavior as the one obtained through the experiments (dotted lines) except for 50°C at 25,000 ppm of sulphate content where the experiments show a decrease in the UCS and the model predicts a slight increase with respect to the UCS at 35°C. This behavior can be explained by the fact that limited data is available for CPBs with 25,000 ppm and cured at 50°C. An enrichment of the data sets at this curing temperature and initial sulphate content will result in a better fit between the experimental and modeling results for the aforementioned point. However, it is worthwhile to mention that ANN models capture the general trend of the data and not only the results of particular data sets.

From Figures 4.9 and 4.10, it can be noticed that the UCS of Slag-CPBs and PCI-CPBs at an advanced age is significantly dependent on the coupled effects of the initial sulphate content and curing temperature. As the curing temperature increases, the UCS of sulphate-free and sulphated Slag-CPBs increases. The mechanisms responsible for this UCS increase are experimentally demonstrated by [46,47,48]: (i) more binder hydration products (e.g., CSH, CH) will be formed with higher temperatures due to the acceleration of the clinker phases and slag pozzolanic reactions (for Slag-CPB only); and (ii) higher curing temperatures are associated with refinement of the pore structure of the CPBs due to the increased binder hydration products formed.

From Figures 4.9 and 4.10, it can be also observed that regardless of the curing temperature, the UCS of the sulphated CPBs with sulphate content ≤15,000 ppm is higher than that of sulphate-free CPBs. This results from the refinement of the pore structure of the CPBs through the precipitation of expansive minerals that are not excessive in the empty pores (e.g., [25,27,28,46]). However, it can be noted that once the sulphate amount is greater than 15,000 ppm, the UCS drops. Figures 4.9 and 4.10 show that for most of the temperature range (20°C to 50°C) the UCS values are lower for 25,000 ppm samples than those at 15,000 ppm sulphate concentration. This lower strength is attributed to the combined effect of two mechanisms: (i) creation of internal stress in the CPB matrix as a result of the formation of excessive amounts of expansive minerals during the sulphate reactions. This would physically damage the cemented matrix and thus, increase the porosity of the CPB. Therefore, a strength drop occurs [10,25,27,28,46]; and (ii)

the inhibition of the cement hydration by high sulphate content (25,000 ppm) (e.g., 25,46). Indeed, it is well known that a high sulphate content inhibits cement hydration (especially C_3A) [25,49].

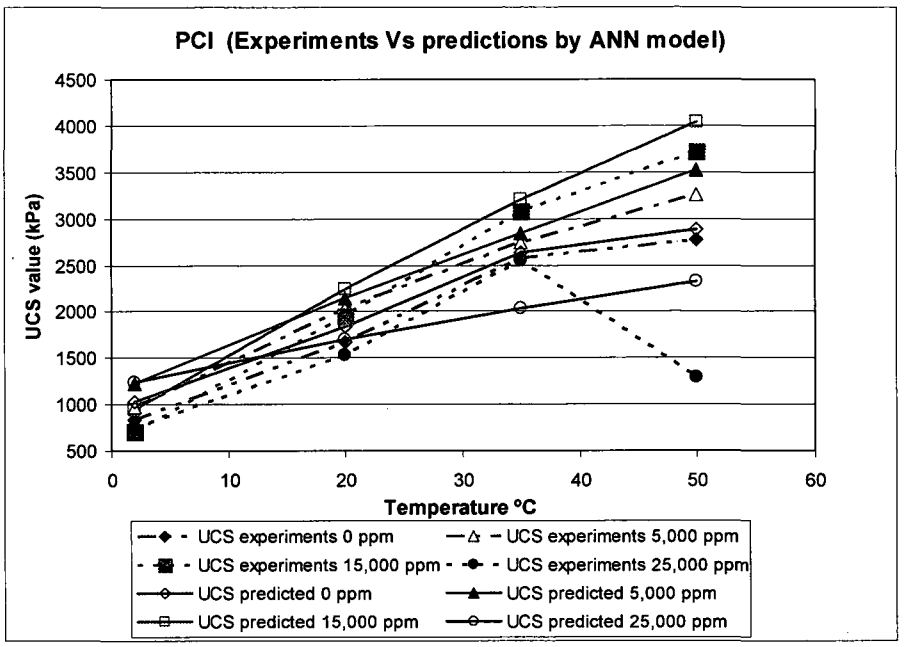

Figure 4.9 Coupled effects of sulphate and curing temperature on the 150 day strength of a CPB containing Slag (4.5% binder content; PCI/Slag:50/50; W/C = 7.6)

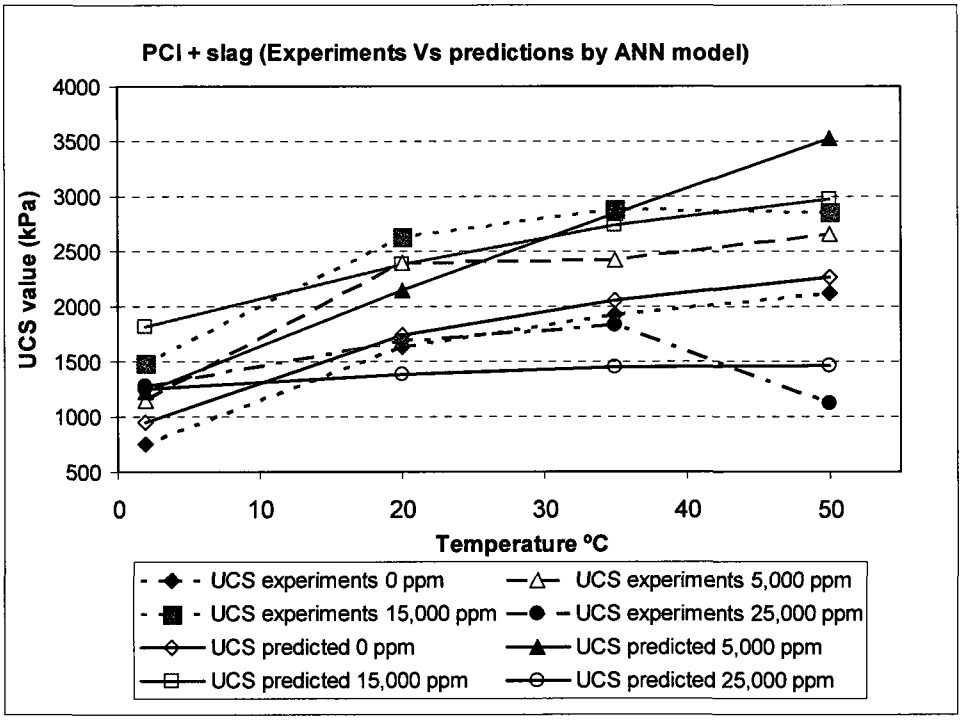

Figure 4.10 Coupled effects of sulphate and curing temperature on 150 day strength of Portland cement CPB (4.5% Portland cement content; W/C = 7.6)

4.6. Conclusions

The present study reaffirms that ANN methodology can be used to model complicated phenomena in engineering where the lack of a theoretical basis is not able to explain the behavior of the variables involved. A detailed description of how to carry out the model definition and development is provided. During such a process, the stage of the database selection and preprocessing is especially important in order to ensure the convergence of the model. The study also provides detailed results on how to assess model accuracy and determine the magnitude of the error involved in the estimation of the output variable as it can be useful for the reader to understand such concepts.

On the other hand, the model is tested against the results of an experimental study and it is found that the model predictions are in line with the findings. The coupled effect of sulphate and curing temperature has a beneficial outcome in the UCS value of a CPB until a certain value of sulphate concentration (15,000 ppm). Once the sulphate concentration goes beyond this threshold value, strength development is compromised and therefore, the UCS value is lower than expected for lower sulphate concentrations.

4.7 Acknowledgements

The authors would like to acknowledge the dedicated work of the graduate students at the Geotechnical Laboratory of the University of Ottawa who provided the source database of experiments used in the model development for the present study.

4.8 REFERENCES

1. Muldoon Paul, CELA and Mark Winfield, CIELAP. Brief to the House of Commons standing committee on Natural Resources regarding Mining and the Environment. 1996. Included in report: "The Boreal Below". Mining Watch Canada. 2001.

2. Fall M., Samb S.S., Influence of curing temperature on strength, deformation behavior and pore structure of cemented paste backfill at early ages. Construction and Building Materials (2006), doi:10.1016/j.conbuildmat.2006.08.010

3. Fall M., Benzaazoua M., Ouellet S. 2005 Experimental characterization of the effect of tailings fineness and density on the quality of cemented paste backfill. Journal Minerals Engineering 18 (1): 41-44.

4. Ilgner H. (2002) from Paste and Thickened Tailings – A guide. 2nd Edition. Australian Centre for Geomechanics, R.J. Jewell Ilgner and A.B. Fourie Editors., Natural Resources and the Environment Unit, South Africa.

5. Hassani F., Archibald J., 1998. Mine Backfill, CD-Rom, Canadian Institute of Mine, Metallurgy and Petroleum, Montreal, Que., 1998.

6. Fall M., Geotechnical Hazards, Notes from lecture given by Dr. Fall to Graduate Students registered at the course Geotechnical Hazards. University of Ottawa, ON. Canada. 2007.

7. Simms P., Mine Waste Management, Notes from lecture given by Dr. Simms to Graduate Students registered at the course Mine Waste Management. Carleton University, Ottawa, ON. Canada. 2008

8. Yilmaz E., Kesimal A., Erçikdi B., Evaluation of acid producing sulphidic mine tailings as a paste backfill.
Karadeniz Technical University, Department of Mining Engineering, 61080 Trabzon, Turkey. İstanbul Üniv. Müh. Fak. Yerbilimleri Dergisi, C. 17, S. 1, SS. 11-19, Y. 2004. From the Website:
http://www.istanbul.edu.tr/eng/jeoloji/library/dergi/cilt_18_s_1/cilt17-s1-syf(11-20).pdf

9. Huynh L. et al., Effect of polyphosphate and naphthalene sulfonate formaldehyde condensate on the rheological properties of dewatered tailings and cemented paste backfill. Minerals Engineering 19 (2006) 28–36

10. Fall M. , Benzaazoua M., Saa E.G., Mix proportioning of underground cemented tailings backfill, Tunnelling and Underground Space Technology 23 (2008) p. 80–90

11. Benzaazoua M., Fall M., Belem T., A contribution to understanding the hardening process of cemented pastefill, Minerals Engineering 17 (2004) 141–152

12. Pokharel, M. (2008). Geotechnical and environmental response of paste tailings systems to coupled thermo-chemical loadings. Master Thesis (M.A.Sc.), University of Ottawa, 248 p.

13. Fall M., Pokharel M. (2009). Coupled thermo-chemical effects on the strength development of Portland cement CPB. Journal of Composite and Concrete Materials (submitted).

14. Payne T., Mitra R. A review of heat issues in underground metalliferous mines, 12th U.S./North American Mine Ventilation Symposium 2008 – Wallace (ed), p. 197-201

15. Rawlins C.A., Phillips H.R., 2001. Reduction of mine heat loads. Proceedings of the 7th International Mine Ventilation Congress, 200, p.381-389.

16. Udd J.E., 2006. A bibliography on deep mining, Proceedings of the Core Project on Deep Mining, June 2006, 10p.

17. Fall M., Nasir O., Numerical Modeling of the Coupled Thermo-Chemo-Mechanical Response of Cemented Paste Backfill Structures in Deep Mine temperature Conditions. 3rd Canada-US Rock Mechanical Symposium and 20th Canadian Rock Mechanics Symposium, 2009 CD-Rom

18. Nasir O., Fall M., Modeling the heat development in hydrating CPB structures. Computer & Geotechnics 36(7) (2009), 1207-1218.

19. Bernier L.R., Li M., High Temperature Oxidation (Heating) of Sulfidic Paste Backfill: A Mineralogical and Chemical Perspective. Proceedings from the 2003 Mining & the Environment Conference, Sudbury. Canada.

20. Orejarena L., Fall M., Mechanical response of a mine composite material to extreme heat, Bull Eng Geol Environ, DOI 10.1007/s10064-008-0148-z, Received: 24 January 2008 / Accepted: 28 March 2008, Springer-Verlag 2008.

21. Fall, M., Célestin J.C., Pokharel M., Touré, M. (2010). Fundamentals of the effect of temperatures on the mechanical properties of mine cemented tailings backfill: experimental results. Engineering Geology (submitted).

22. Fall M., Nasir O., Celestin J.C., Paste backfill responses in deep mine temperature conditions, 9th International Symposium of mining with backfill. Montreal, Canada, June 2007

23. Yilmaz, E., Kesimal, A. Deveci H. and Ercikdi, B., The Factors Affecting the Performance of Paste Backfill; Physical, Chemical and Mineralogical Characterization. First Engineering Sciences Congress for Young Researcher (MBGAK'03), Istanbul (2003).

24. R.L. Bernier, M.G. Li, A. Moerman, Effects of tailings and geochemistry on the physical strength of paste backfill, Proceedings of Sudbury '99, Mining and the Environment II, in: D. Goldsack, Belzile, P. Yearwood, G. Hall (Eds.), Laurentian University, Sudbury, Canada, 1999, pp. 1113–1122.

25. Fall M., Benzaazoua M., Modeling the effect of sulphate on strength development of paste backfill and binder mixture optimization, Cement and Concrete Research 35 (2005) 301–314.

26. Orejarena L., The use of artificial neural networks to predict the effect of sulphate attack on the strength of cemented paste backfill, Technical paper, M.A.Sc. thesis in development, University of Ottawa, 2008.

27. Escalante-García J.I., Sharp J.H., Effect of temperature on the hydration of the main clinker phases in Portland Cements: Part II, blended cements, Cement and Concrete Research, Vol 28, No.9, pp.1259-1274, 1998.

28. Lothenbach B. et al., Effect of temperature on the pore solution, microstructure and hydration products of Portland cement pastes, Cement and Concrete Research 37 (2007) pp. 483–491

29. J.-K., Moon Y.-H., Eo S.-H., Compressive Strength development of Concrete with different curing time and temperature, Cement and Concrete Research, Vol. 28, No. 12, pp. 1761–1773, 1998

30. Neville, A.M., Properties of Concrete, Second Edition, 1973, Pitman Publishing Ltd., p.276.

31. Husem, M., Gozutok, S., The effects of low temperature curing on the compressive strength of ordinary and high performance concrete, Construction and Building Materials 19 (2005) 49–53.

32. Fall, M., Pokharel, M., Coupled effects of sulphate and temperature on cemented tailings materials. Conference for GeoEdmonton'08. Department of Civil Engineering – University of Ottawa, Ottawa, Ontario, Canada.

33. McIntosh, JD., The effects of low-temperature curing on the compressive strength of concrete, Gen. Report of session BII. In: Proceedings of RILEM symposium Winter Concreting. Danish Institute for Building Research, Copenhagen, 1956.

34. Basheer, I.A., Hajmeer, M., Artificial neural networks: fundamentals, computing, design, and application, Journal of Microbiological Methods 43 (2000) p. 3–31

35. Amaratunga, L.M., Yaschyshyn, D.N. , Development of a high modulus paste fill using fine gold mill tailings, Geotechnical and Geological Engineering, 1997, 15 p. 205–219

36. T. Grice, Underground mining with backfill, Proceedings of 2nd Annual Summit, Mine Tailings Disposal Systems. Brisbane, Australian, Australasian Institute of Mining and Metallurgy, Carlton South, Australia, 1998, p. 14.

37. Benzaazoua M., Belem T., Bussiere B., 2002. Chemical factors that influence on the performance of mine sulphidic paste backfill. Cement and Concrete Research 32 (7), 1133–1144.

38. Glasser F., Marchand J., Samson E., Durability of concrete — Degradation phenomena involving detrimental chemical reactions, Cement and Concrete Research 38 (2008) 226–246

39. Kesimal A. et al., Effect of properties of tailings and binder on the short-and long-term strength and stability of cemented paste backfill. Materials Letters 59 (2005) 3703 – 3709

40. Yeh I.-C., Modeling of strength of high-performance concrete using artificial neural networks, Cement and Concrete Research, Vol. 28, No. 12, pp. 1797–1808, 1998.

41. Lai, S., Serra, M., Concrete strength prediction by means of neural network, Construction and Building Materials, Vol. 11, No.2, pp. 93-98, 1997.

42. Lee, S.-C., Prediction of concrete strength using artificial neural networks, Engineering Structures 25 (2003) 849–857.

43. Haykin, S., Neural Networks A Comprehensive Foundation, MacMillan College Publishing Company Inc, 1994, 696 pp. ISBN 0-02-352761-7.

44. Demuth, H., Beale, M., Hagan, M., Artificial Neural Network Toolbox™ 6, User's Guide, MATLAB, p 1-18, 2008

45. Vogl, T.P., J.K. Mangis, A.K. Rigler, W.T. Zink, and D.L. Alkon, "Accelerating the convergence of the backpropagation method," Biological Cybernetics, Vol. 59, 1988, pp. 257-263.

46. Pokharel, M. (2008). Geotechnical and environmental response of paste tailings systems to coupled thermo-chemical loadings. Master Thesis (M.A.Sc.), University of Ottawa, 248 p.

47. Pokharel M., Fall M., (2009). Coupled thermo-chemical effects on the strength development of Slag-paste backfill materials. Journal of Materials in Civil Engineering (submitted).

48. Fall M., Pokharel M. (2009). Coupled thermo-chemical effects on the strength development of Portland cement CPB. Journal of Composite and Concrete Materials (submitted).

49. Taylor H.F.W., Cement Chemistry, 3rd ed., Academic Press Publisher, New York, 1990, 475 pp.

50. Williams, T.J., Denton, D.K., Larson, M.K., Rains, R.L., Seymour, J.B., Tesarik, D.R., 2001. Geomechanics of Reinforced Cemented Backfill in an Underground Stope at the Lucky Friday Mine. Report of Investigations 9655, p.24.

5. Chapter 5 - Summary, Conclusions and Recommendations

The applicability of ANNs has been tested in a relatively new area; CPB technology. The results, with regard to strength behavior under various thermal and chemical loading conditions, are satisfactory. Thus, several major conclusions and recommendations can be outlined as follows.

- More important than the amount of data available for the model is the availability of a close to uniformly or normally distributed data for the ranges in the study. For instance, if the output variable ranges from 0 to 2000 kPa, obtaining data sets that produce a close to normal distribution of the output variable is more desirable than thousands of data sets that are perhaps not distributed properly in the data range. This observation is specifically noted in the development of the second ANN model.

- From an engineering perspective, another major observation in this study is the applicability of the simplest architecture possible as an effective way to model the effect of sulphate and temperature on the strength of CPBs. In this regard, it appears that there is no need to have more than one hidden layer, at least for

this kind of problem in CPBs, in order to obtain suitable results when using the BP algorithm.

- In terms of the simulation carried out in the ANN model developed for sulphate attacks on CPBs (Chapter 3), it is noted that the mixes with the highest UCS values have a binder composition of 50% PC, 50% Slag and a medium content of binder (4.5%). The explanation for these findings is given under the above mentioned chapter. Likewise, it is found through the simulation performed for the coupled effect of sulphate and temperature that an increase of temperature up to 50°C positively contributes to the long term strength (150 days) of the studied CPBs. Such an effect is more notorious in mixes with low to medium sulphate content (5,000 to 15,000 ppm). CPBs with high sulphate contents (25,000 ppm) show lower strength due to the damaging effect of sulphate attacks.

- On the other hand, the simulation of the coupled effect of sulphate and temperature (Model No.2) allows the corroboration of results from experimental studies and also identification of a concentration of sulphate at 15,000 ppm as the threshold where the effect of sulphate starts to jeopardize the strength of the UCS. This result can contribute to CPB facilities for the establishment of control parameters of the mixes in order to ensure that the CPB will meet the desired requirements of strength and durability.

It should be also understood that the results here presented are far from being irrefutable findings; for instance, some differences in the results were noted in the two models such as the slight increase in strength under the same conditions from the Model No.2 (sulphate+temperature) for the different sulphate concentrations against Model No.1 (sulphate only) where the strength is almost constant; however the other findings already explained in the corresponding chapters and in the present one outcast these differences.

It is acknowledged that the models obtained in this study may have some limitations in the same way as any other model, mainly due to the limitations on the input variables assumptions and database availability; for that reason, the author should not be held accountable for the improper use of this information. Thus, as in ANN methodology, any inferences from this present study should be corroborated on the field or by experimental means.

Finally, it is worthwhile to mention that the tailings variable is kept constant for the current study. Provided that there is enough data available, a more comprehensive model to simulate the long term strength of CPB mixes could be developed, which includes the tailings chemistry as another input variable.

Appendix No.1 – Additional simulation with constant W/C on sulphate model

In addition to the initial simulation carried out under the sulphate attack model, another simulation was carried out to illustrate the model results under a constant W/C for the first two scenarios stated in Chapter 3, Table 3.3. The simulation variables for these two new scenarios can be described as follows:

Table A.1 Additional two scenarios for ANN sulphate model

1- Binder percentage (%)				
PCI	Slag	% binder	w/c	Sul (ppm)
50	50	3	7.6	variable
50	50	4.5	7.6	variable
50	50	6	7.6	variable
2- Binder composition (PCI/slag)				
PCI	Slag	% binder	w/c	Sul (ppm)
25	75	4.5	7.6	variable
50	50	4.5	7.6	variable
75	25	4.5	7.6	variable

In the first scenario, the intention is to isolate the effect of the binder percentage from the other variables and the results obtained through the model simulation can be seen in Figure A.1

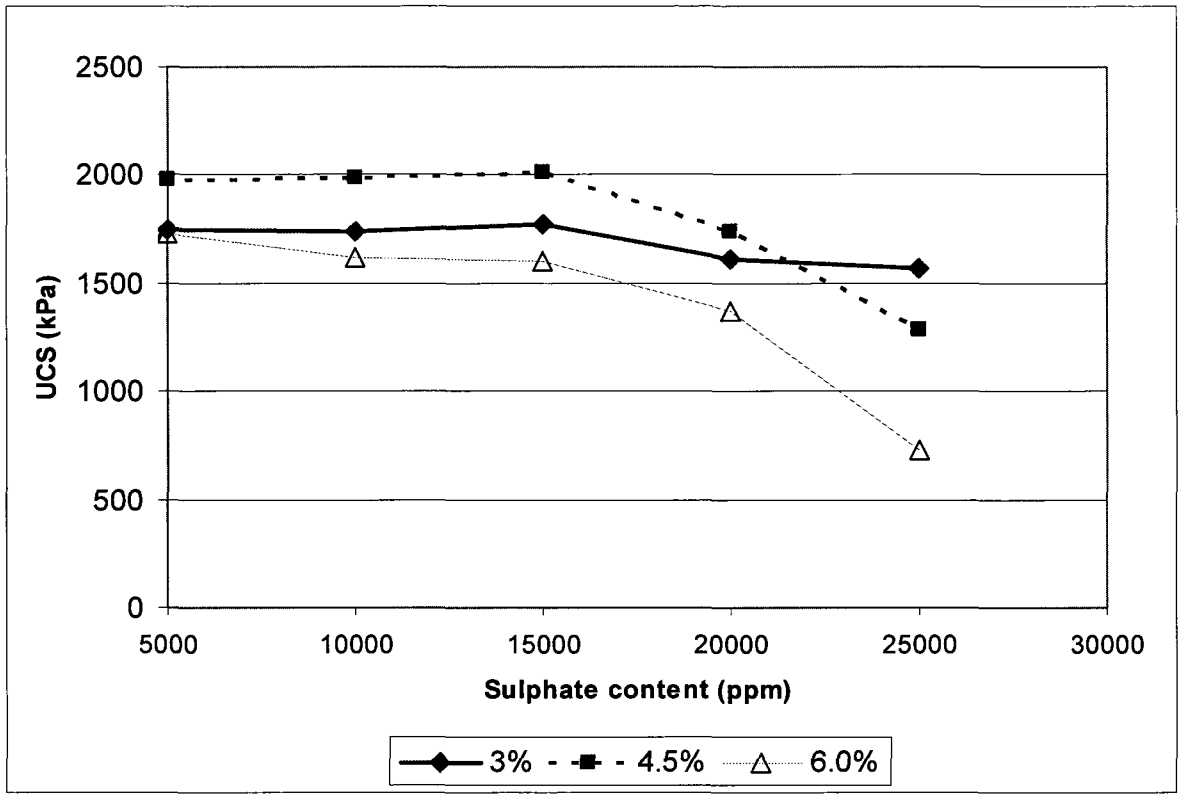

Figure A.1 Effect of binder content on the response of CPB to sulphate attack under constant W/C = 7.6

From Figure A.1 it can be noted the following similarities and differences with the previous scenario performed with variable W/C under Chapter 3:

- Mixes with binder content of 3% show the same relative stability under different sulphate contents. Whereas under constant W/C the UCS is around 1,700 to 1,500 kPa the UCS ranges between 900 to 490 kPa in the first simulation. This is somewhat expected due to the difference in W/C inputs; 7.6 for the higher UCS values and 11.09 for the lower ones.

  It is important to note that mixes with 6% of binder exhibit a consistent behavior when they are compared against the mixes with 4.5% since the trend is very similar in this simulation. However, it should be noted that in this case under the

same W/C, the mix with the highest binder percentage (6%) produces the lowest UCS value. This can be due to a greater sensitivity of the high binder content mix to sulphate attack as it was stated before. Thus, the simulation of constant W/C reaffirms the results of the simulation performed in Chapter 3 for binder content and it also exhibits the reasonable ability of ANN models to carry out different scenarios.

From the second scenario, concerning different binder composition between PCI and slag the only difference with the simulation performed in Chapter 3 is on the 75/25 (PCI/Slag) mix where the W/C is now 7.6 instead of 5.69 before. The results can be seen in Figure A.2

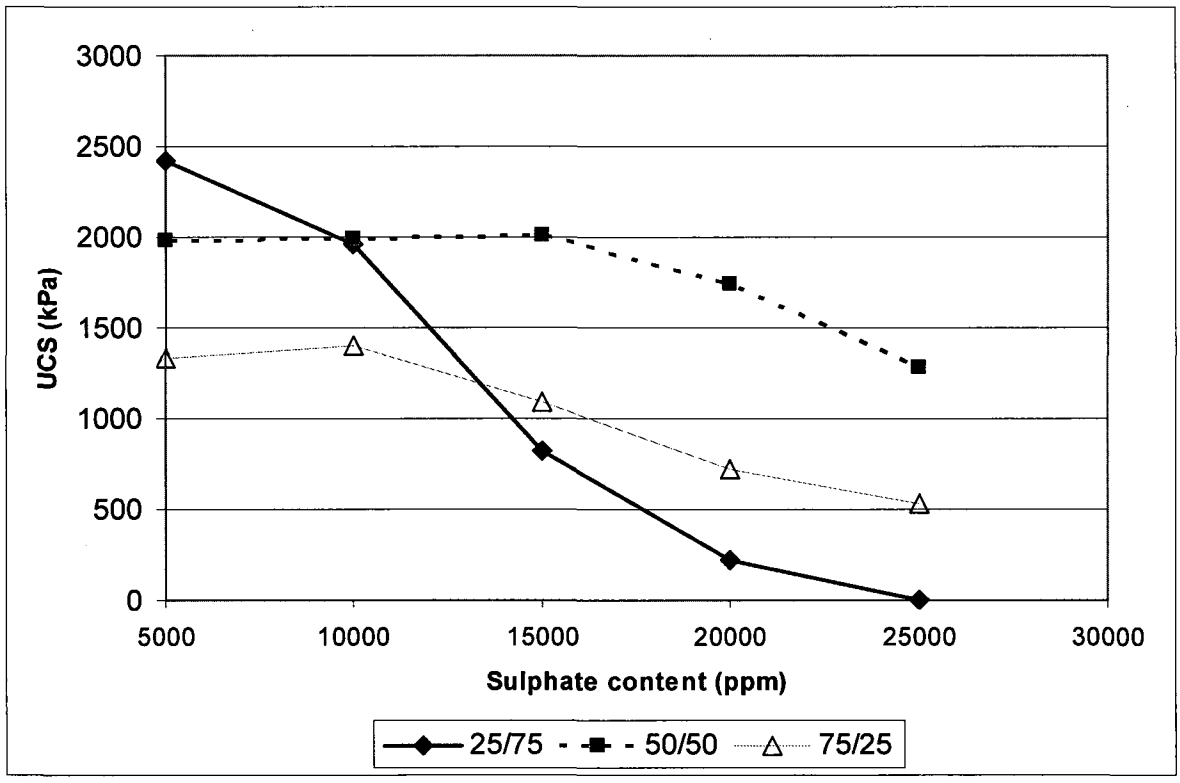

Figure A.2 Effect of binder type on the resistance of CPB to sulphate attack under constant W/C=7.6

In this case, the behavior of the UCS is very similar to the one obtained in the simulation performed in Chapter 3, except that now the strength values for the 75/25 mix are lower than those in Figure 3.10 due to a higher W/C which is somewhat expected.

Appendix No.2 – Data sets used in Model No.1 to predict the effect of sulphate attack on the strength of cemented paste backfill

#	PCI %	Slag %	%binder	W/C	Sulphate (ppm)	UCS (kPa - 150d)
1	25	75	6	9.2	25000	42.58
2	25	75	6	9.2	25000	82
3	25	75	6	9.2	25000	112.43
4	20	80	4.5	9.2	25000	189.59
5	20	80	4.5	9.2	25000	200.78
6	25	75	3	9.2	25000	205.52
7	25	75	3	9.2	25000	208
8	25	75	6	7.6	25000	222.96
9	25	75	3	9.2	25000	226.25
10	25	75	6	7.6	25000	368.09
11	50	50	4.5	7.6	35000	392.82
12	50	50	4.5	4.4	15000	469.71
13	50	50	4.5	7.6	35000	475
14	50	50	4.5	7.6	35000	528.35
15	75	25	6	9.2	25000	561.52
16	75	25	6	9.2	25000	573
17	75	25	6	9.2	25000	581.07
18	50	50	4.5	10.8	15000	603.7
19	100	0	4.5	9.2	25000	654.61
20	100	0	4.5	9.2	0	668.53
21	100	0	4.5	9.2	0	699.38
22	50	50	4.5	10.8	15000	765
23	100	0	4.5	9.2	25000	793.47
24	100	0	3	7.6	25000	794.92
25	100	0	3	7.6	15000	800.58
26	75	25	6	9.2	5000	863.04
27	100	0	3	7.6	0	870.48
28	75	25	6	9.2	5000	871
29	50	50	4.5	10.8	15000	890.02
30	100	0	4.5	9.2	15000	917.56
31	75	25	6	9.2	5000	923.09
32	100	0	3	7.6	5000	932.26
33	100	0	4.5	9.2	5000	967.22
34	75	25	6	7.6	25000	1014.26
35	0	100	4.5	7.6	15000	1015.41
36	75	25	6	6	25000	1024
37	100	0	4.5	9.2	15000	1027.3
38	75	25	6	7.6	5000	1029.58
39	100	0	3	7.6	0	1034.74
40	75	25	6	6	25000	1058.21
41	100	0	3	7.6	25000	1064.52
42	100	0	3	7.6	15000	1069.26

43	100	0	4.5	7.6	15000	1072
44	75	25	7	6	25000	1097.17
45	75	25	6	7.6	25000	1103.45
46	100	0	3	7.6	5000	1108.91
47	100	0	4.5	7.6	15000	1149.88
48	20	80	4.5	9.2	15000	1178.68
49	20	80	4.5	9.2	0	1217.35
50	50	50	7.5	7.6	15000	1299
51	50	50	7.5	7.6	15000	1304.55
52	100	0	4.5	9.2	5000	1313.88
53	100	0	6	7.6	0	1323.73
54	50	50	7.5	7.6	15000	1347.23
55	75	25	3	9.2	5000	1356.1
56	20	80	4.5	9.2	15000	1371.77
57	80	20	4.5	9.2	0	1379.41
58	100	0	6	7.6	0	1406.08
59	75	25	6	7.6	5000	1419.85
60	80	20	4.5	9.2	0	1427.98
61	75	25	3	7.6	5000	1437.09
62	75	25	3	6	25000	1457.5
63	75	25	3	9.2	25000	1465.7
64	75	25	3	9.2	25000	1494
65	75	25	3	9.2	5000	1515
66	75	25	3	9.2	25000	1519.85
67	100	0	4.5	7.5	25000	1530
68	50	50	4.5	7.5	25000	1531
69	80	20	4.5	9.2	15000	1547.89
70	80	20	4.5	9.2	25000	1553.02
71	75	25	3	6	25000	1573
72	100	0	4.5	7.5	25000	1582
73	80	20	4.5	9.2	15000	1593.63
74	100	0	4.5	7.5	0	1601
75	100	0	6	7.6	15000	1609.44
76	50	50	4.5	7.5	0	1612
77	75	25	3	6	25000	1613.22
78	20	80	4.5	9.2	0	1615.31
79	25	75	3	6	5000	1624.01
80	80	20	4.5	9.2	25000	1630.55
81	50	50	4.5	7.5	0	1632
82	100	0	4.5	7.5	0	1643
83	50	50	4.5	7.6	15000	1650.02
84	50	50	4.5	7.5	0	1653
85	50	50	4.5	7.6	0	1682.42
86	50	50	4.5	7.5	25000	1683
87	75	25	3	9.2	5000	1691.31
88	75	25	3	6	5000	1696.35
89	80	20	4.5	9.2	5000	1709.9
90	75	25	3	6	5000	1721
91	25	75	3	7.6	5000	1740.26

92	50	50	4.5	7.6	15000	1742
93	100	0	6	7.6	15000	1742.03
94	25	75	3	6	25000	1750
95	50	50	4.5	7.6	15000	1762.54
96	75	25	3	6	5000	1775.75
97	100	0	6	7.6	25000	1782.31
98	25	75	3	6	5000	1786
99	25	75	3	6	25000	1792.18
100	25	75	6	6	25000	1823.22
101	50	50	4.5	7.5	25000	1830
102	100	0	6	7.6	5000	1836.72
103	25	75	3	6	5000	1868.25
104	80	20	4.5	9.2	5000	1869.18
105	100	0	4.5	5	0	1888.94
106	25	75	6	6	25000	1912
107	100	0	4.5	7.5	15000	1920
108	100	0	4.5	7.5	15000	1943
109	25	75	6	6	25000	1992.61
110	100	0	4.5	7.5	5000	2030
111	100	0	4.5	7.5	5000	2045
112	100	0	6	7.6	25000	2056.35
113	25	75	3	7.5	5000	2062
114	25	75	3	7.6	5000	2062.47
115	100	0	6	7.6	5000	2094.52
116	75	25	6	6	5000	2114.24
117	25	75	3	9.2	5000	2239.44
118	75	25	6	6	5000	2295
119	25	75	3	9.2	5000	2300
120	25	75	3	9.2	5000	2339.13
121	25	75	6	7.6	5000	2369.97
122	25	75	6	9.2	5000	2371.77
123	50	50	4.5	7.5	5000	2388
124	50	50	4.5	7.5	5000	2397
125	25	75	6	9.2	5000	2405
126	100	0	4.5	5	25000	2407.31
127	50	50	4.5	7.5	5000	2408
128	100	0	4.5	5	0	2425.85
129	25	75	6	9.2	5000	2463.06
130	75	25	7	6	5000	2469.39
131	25	75	6	7.6	5000	2498.44
132	50	50	4.5	7.5	15000	2500
133	50	50	4.5	7.5	15000	2550
134	50	50	4.5	7.5	15000	2632
135	20	80	4.5	9.2	5000	2738.36
136	20	80	4.5	9.2	5000	2845.22
137	100	0	4.5	5	25000	2939.37
138	25	75	6	6	5000	3150.78
139	25	75	6	6	5000	3185

140	100	0	4.5	5	5000	3312.19
141	25	75	6	6	5000	3338.83
142	100	0	4.5	5	5000	3353.49
143	100	0	4.5	5	15000	3371.63

Appendix No.3 – Data sets used in Model No.2 to predict the coupled effect of sulphate attack and curing temperature on the strength of cemented paste backfill

#	PCI %	Slag %	% binder	W/C	Sulphate (ppm)	Temp °C	UCS kPa (150d)	Final ID (marker)
1	25	75	6	7.6	25000	50	60	II-bMF160370
2	25	75	6	7.6	25000	50	63.05	II-bI8
3	25	75	6	7.6	25000	50	63.91	II-bI8b
4	25	75	6	7.6	25000	20	222.96	II-bI6b
5	25	75	6	7.6	25000	20	300	II-bMF160368
6	50	50	4.5	7.6	35000	35	362.91	II-bL6
7	25	75	6	7.6	25000	20	368.09	II-bI6
8	50	50	4.5	7.6	35000	35	385.77	II-bL6b
9	25	75	6	7.6	5000	50	502.29	II-bI7
10	25	75	6	7.6	5000	50	521	II-bMF160369
11	50	50	4.5	7.6	35000	20	528.35	Ia109
12	25	75	6	7.6	5000	50	536.92	II-bI7b
13	100	0	4.5	9.2	0	20	668.53	Ia1
14	100	0	4.5	9.2	0	20	699.38	Ia2
15	100	0	4.5	7.6	15000	2	704	II-bMF160325
16	50	50	4.5	7.6	0	2	714	II-bMF160333
17	50	50	4.5	7.6	0	2	744	muk_01
18	100	0	4.5	7.6	25000	2	744.898	muk_29
19	50	50	4.5	7.6	0	2	745	II-bMF160301
20	100	0	4.5	7.6	25000	2	745	II-bMF160329
21	50	50	4.5	7.6	0	2	776	II-bMF160349
22	100	0	4.5	7.6	0	2	836	II-bMF160317
23	0	100	4.5	7.6	15000	35	862.69	II-bK5b
24	75	25	3	7.6	25000	20	912.22	II-bJ2b
25	100	0	4.5	7.6	5000	2	979	II-bMF160321
26	75	25	3	7.6	25000	20	999	II-bMF160372
27	75	25	6	7.6	25000	20	1014.26	II-bJ6b
28	75	25	6	7.6	25000	20	1014.26	Ia127
29	75	25	6	7.6	5000	20	1029.58	II-bJ5b
30	75	25	6	7.6	25000	20	1060	II-bMF160375
31	50	50	4.5	7.6	5000	2	1097	II-bMF160353
32	*100*	*0*	*4.5*	*7.6*	*25000*	*10*	*1100*	*muk_int_021*
33	25	75	3	7.6	25000	20	1102.48	II-bI2
34	75	25	6	7.6	25000	20	1103.45	II-bJ6
35	75	25	6	7.6	25000	50	1110.9	II-bJ8
36	75	25	3	7.6	25000	20	1111.7	II-bJ2
37	25	75	3	7.6	25000	20	1115	II-bMF160366
38	25	75	3	7.6	25000	20	1118.3	II-bI2b
39	50	50	4.5	7.6	25000	50	1122	II-bMF160316
40	0	100	4.5	7.6	15000	35	1127.55	II-bK5

41	50	50	4.5	7.6	5000	2	1150	II-bMF160305
42	50	50	4.5	7.6	5000	2	1150	muk_05
43	*50*	*50*	*4.5*	*7.6*	*0*	*10*	*1150*	*muk_int_001*
44	50	50	4.5	7.6	25000	50	1150	II-bMF160364
45	100	0	4.5	7.6	0	10	1200	muk_int_012
46	50	50	4.5	7.6	5000	2	1204	II-bMF160337
47	75	25	6	7.6	5000	20	1229	II-bMF160374
48	*100*	*0*	*4.5*	*7.6*	*15000*	*10*	*1250*	*muk_int_018*
49	50	50	4.5	7.6	25000	50	1263	II-bMF160348
50	50	50	4.5	7.6	25000	2	1265	II-bMF160345
51	50	50	4.5	7.6	25000	2	1275	II-bMF160313
52	50	50	4.5	7.6	25000	2	1286	II-bMF160361
53	100	0	4.5	9.2	5000	20	1313.88	Ia3
54	100	0	6	7.6	0	20	1323.73	Ia49
55	*50*	*50*	*4.5*	*7.6*	*25000*	*45*	*1350*	*muk_int_011*
56	80	20	4.5	9.2	0	20	1379.41	Ia25
57	100	0	6	7.6	0	20	1406.08	Ia50
58	75	25	6	7.6	5000	20	1419.85	II-bJ5
59	75	25	6	7.6	5000	20	1419.85	Ia124
60	75	25	3	7.6	5000	20	1437.09	II-bJ1b
61	75	25	3	7.6	5000	20	1441	II-bMF160371
62	75	25	3	7.6	5000	20	1448.23	II-bJ1
63	*50*	*50*	*4.5*	*7.6*	*25000*	*10*	*1450*	*muk_int_008*
64	*100*	*0*	*4.5*	*7.6*	*5000*	*10*	*1450*	*muk_int_015*
65	75	25	3	6	25000	20	1457.5	Ia83
66	50	50	4.5	7.6	0	20	1484	II-bMF160334
67	50	50	4.5	7.6	15000	2	1489	II-bMF160341
68	50	50	4.5	7.6	15000	2	1490	II-bMF160309
69	50	50	4.5	7.6	15000	2	1495	II-bMF160357
70	100	0	4.5	7.6	25000	20	1530	II-bMF160330
71	100	0	4.5	7.6	25000	20	1530	muk_30
72	*50*	*50*	*4.5*	*7.6*	*25000*	*40*	*1600*	*muk_int_010*
73	50	50	4.5	7.6	0	20	1632	II-bMF160302
74	50	50	4.5	7.6	0	20	1653	II-bMF160350
75	100	0	4.5	7.6	0	20	1673	II-bMF160318
76	100	0	4.5	7.6	0	20	1673	muk_18
77	50	50	4.5	7.6	25000	20	1683	II-bMF160314
78	50	50	4.5	7.6	25000	20	1683	muk_14
79	*50*	*50*	*4.5*	*7.6*	*25000*	*30*	*1775*	*muk_int_009*
80	100	0	6	7.6	25000	20	1782.31	Ia55
81	50	50	7.5	7.6	15000	35	1794.75	II-bL2
82	50	50	4.5	7.6	0	35	1816	II-bMF160351
83	*50*	*50*	*4.5*	*7.6*	*0*	*30*	*1825*	*muk_int_002*
84	50	50	4.5	7.6	25000	35	1826	muk_15
85	50	50	4.5	7.6	25000	20	1831	II-bMF160346
86	50	50	4.5	7.6	0	35	1856.84	II-bL5b
87	50	50	4.5	7.6	0	35	1875.6	II-bL5
88	25	75	3	7.6	5000	20	1897	II-bMF160365

89	50	50	4.5	7.6	0	35	1918	II-bMF160303
90	50	50	4.5	7.6	25000	35	1918	II-bMF160347
91	100	0	4.5	7.6	15000	20	1943	II-bMF160326
92	100	0	4.5	7.5	15000	20	1943	Ia130
93	100	0	4.5	7.6	15000	20	1943	muk_26
94	*50*	*50*	*4.5*	*7.6*	*0*	*40*	*1950*	*muk_int_003*
95	*50*	*50*	*4.5*	*7.6*	*15000*	*10*	*2000*	*muk_int_004*
96	50	50	4.5	7.6	0	35	2020	II-bMF160335
97	100	0	4.5	7.6	5000	20	2030	II-bMF160322
98	50	50	4.5	7.6	0	50	2040	II-bMF160352
99	100	0	4.5	7.5	5000	20	2045	Ia145
100	100	0	6	7.6	25000	20	2056.35	Ia56
101	25	75	3	7.5	5000	20	2062	Ia148
102	25	75	3	7.6	5000	20	2062.47	II-bI1b
103	100	0	6	7.6	5000	20	2094.52	Ia51
104	*100*	*0*	*4.5*	*7.6*	*25000*	*40*	*2100*	*muk_int_023*
105	50	50	4.5	7.6	0	50	2112	II-bMF160304
106	75	25	6	6	5000	20	2114.24	Ia88
107	50	50	4.5	7.6	0	50	2184	II-bMF160336
108	*100*	*0*	*4.5*	*7.6*	*25000*	*30*	*2200*	*muk_int_022*
109	50	50	4.5	7.6	15000	35	2201	II-bMF160377
110	50	50	4.5	7.6	15000	35	2262.35	II-bL8b
111	50	50	4.5	7.6	15000	35	2294.91	II-bKK17
112	75	25	6	6	5000	20	2295	Ia165
113	*100*	*0*	*4.5*	*7.6*	*0*	*30*	*2300*	*muk_int_013*
114	50	50	4.5	7.6	5000	35	2363	II-bMF160339
115	25	75	6	7.6	5000	20	2369.97	II-bI5
116	25	75	6	7.6	5000	20	2369.97	Ia116
117	50	50	4.5	7.6	5000	20	2388	II-bMF160354
118	50	50	4.5	7.6	5000	20	2397	II-bMF160306
119	50	50	4.5	7.5	5000	20	2397	Ia133
120	50	50	4.5	7.6	15000	35	2402.72	II-bKK20b
121	50	50	4.5	7.6	5000	20	2408	II-bMF160338
122	50	50	4.5	7.6	5000	35	2418	II-bMF160307
123	25	75	6	7.6	5000	20	2444	II-bMF160367
124	50	50	4.5	7.6	15000	35	2446.4	II-bKK19
125	50	50	4.5	7.6	15000	35	2477.32	II-bLL29
126	25	75	6	7.6	5000	20	2498.44	II-bI5b
127	*100*	*0*	*4.5*	*7.6*	*5000*	*30*	*2500*	*muk_int_016*
128	50	50	4.5	7.6	5000	50	2500	II-bMF160340
129	25	75	3	7.6	5000	50	2508.99	II-bI3
130	50	50	4.5	7.6	15000	35	2541	II-bMF160378
131	100	0	4.5	7.6	0	35	2571	II-bMF160319
132	50	50	4.5	7.6	5000	35	2573	II-bMF160355
133	50	50	4.5	7.6	15000	20	2632	II-bMF160310
134	50	50	4.5	7.6	15000	20	2632	muk_10
135	*100*	*0*	*4.5*	*7.6*	*0*	*40*	*2650*	*muk_int_014*
136	50	50	4.5	7.6	5000	50	2653	II-bMF160308

137	50	50	4.5	7.6	5000	50	2653	muk_08
138	50	50	4.5	7.6	5000	50	2657	II-bMF160356
139	*100*	*0*	*4.5*	*7.6*	*15000*	*30*	*2700*	*muk_int_019*
140	100	0	4.5	7.6	5000	35	2744	II-bMF160323
141	100	0	4.5	7.6	5000	35	2744	muk_23
142	100	0	4.5	7.6	0	50	2768	II-bMF160320
143	50	50	4.5	7.6	15000	50	2780	II-bMF160344
144	50	50	4.5	7.6	15000	30	2800	muk_int_005
145	75	25	6	7.6	5000	50	2846.45	II-bJ7
146	50	50	4.5	7.6	15000	50	2857	II-bMF160312
147	50	50	4.5	7.6	15000	50	2860	II-bMF160360
148	*50*	*50*	*4.5*	*7.6*	*15000*	*45*	*2865*	*muk_int_007*
149	75	25	6	7.6	5000	50	2865	II-bMF160376
150	*50*	*50*	*4.5*	*7.6*	*15000*	*40*	*2875*	*muk_int_006*
151	50	50	4.5	7.6	15000	35	2887	muk_11
152	75	25	6	7.6	5000	50	2899.35	II-bJ7b
153	*100*	*0*	*4.5*	*7.6*	*5000*	*40*	*2925*	*muk_int_017*
154	100	0	4.5	7.6	15000	35	3084	muk_27
155	25	75	6	6	5000	20	3150.78	Ia73
156	25	75	6	6	5000	20	3185	Ia157
157	100	0	4.5	7.6	5000	50	3255	II-bMF160324
158	*100*	*0*	*4.5*	*7.6*	*15000*	*40*	*3300*	*muk_int_020*
159	100	0	4.5	5	5000	20	3312.19	Ia12
160	25	75	6	6	5000	20	3338.83	Ia72
161	100	0	4.5	5	5000	20	3353.49	Ia11
162	100	0	4.5	5	15000	20	3371.63	Ia14
163	100	0	4.5	7.6	15000	50	3724	II-bMF160328
164	75	25	3	7.6	5000	50	3877.91	II-bJ3
165	75	25	3	7.6	5000	50	4215	II-bMF160373

Notes:

1- Underlined and *italic* fields mean UCS values obtained by interpolation on experimental study mentioned under section 4.3.5 Data enrichment in Chapter No.4

2- Last column is provided to facilitate future references.